

A MODEL FOR CASTING POLYESTERS

by

Selami Y. Pusatcioglu

Dissertation submitted to the Graduate Faculty of the
Virginia Polytechnic Institute and State University
in partial fulfillment of the requirements for the degree of

DOCTOR OF PHILOSOPHY

in

Chemical Engineering

APPROVED:

H. A. McGee, Jr., Chairman

A. L. Fricke

J. C. Hassler

J. E. McGrath

H. F. Brinson

November, 1977

Blacksburg, Virginia

ACKNOWLEDGMENTS

I am very grateful to Dr. H. A. McGee, Jr., for giving me the opportunity to work in this research project and for his care, encouragement, and helpful comments for the accomplishment of this work. I am indebted to Dr. A. L. Fricke for his guidance, advice, and friendship during this work and my entire graduate studies. I am also thankful to Dr. J. C. Hassler, Dr. J. McGrath and Dr. H. Brinson for their assistance and suggestions while serving as members of my advisory committee.

There are many other people to whom I am deeply appreciative for their help in the completion of this project. I wish to thank Mr. S. C. Reid for his assistance with the electronic components of this work and Mr. B. G. Williams and Mr. A. A. Lafon for their great job with the mechanical aspects of this project. Special thanks are also due my fellow students, Mr. Tom Mason and Mr. Russell Smith, for their help with the development of the computer interfacing and software to obtain my experimental data.

Thanks to my dearest friend, Hayrani, for sharing my hard days during the last four years.

In addition, I would like to thank the Department of Chemical Engineering for supporting both myself and this research project.

Last, but never least, I wish to express my gratitude to my parents for their desire and support that has permitted me to obtain a successful, professional education.

TABLE OF CONTENTS

	Page
ACKNOWLEDGMENTS	ii
LIST OF TABLES	vi
LIST OF FIGURES	vii
 Chapter	
I. INTRODUCTION	1
II. BACKGROUND INFORMATION AND LITERATURE	4
History of Thermoset Polyesters	4
Chemistry of Unsaturated Polyesters	6
Crosslinking Reaction and Curing	11
Description of the Crosslinking Reaction of Polyesters	11
Chemical Kinetics	15
Differential Scanning Calorimetry	18
Description of the Instrument	18
Analysis of DSC	18
Kinetics and Thermal Characterization of Thermoset Cure by DSC	21
Heat Transfer and Processing of Thermoset Plastics	24
Casting and Related Processes	24
III. EXPERIMENTAL	28
Materials	28
Casting and Temperature Measurements	30

Chapter	Page
Experimental Setup	31
Development of the Data Acquisition Technique	33
Measurement Procedure	33
Thermal Conductivity Measurements	36
Description of Colora Thermo- Conductometer	36
Calibration	39
Measurements	41
Calorimetric Measurements	43
Experimental Procedures for Heats of Reaction and Kinetics	44
Specific Heat Measurements	45
IV. MATHEMATICAL MODELLING	48
Problem Statement	48
Assumptions	49
Model	51
V. RESULTS AND DISCUSSIONS	54
Experimental Results	54
Experimental Temperature Profiles	54
Residual Stresses	56
Thermal Conductivity	60
Heats of Polymerization and Kinetic Model	70
Specific Heat	85
Thermomechanical Analysis	92
Application of Proposed Mathematical Model	93
Formulation	93
Method of Solution	96
Solution	99

Chapter	Page
VI. CONCLUSIONS AND RECOMMENDATIONS	112
VII. BIBLIOGRAPHY	116
APPENDICES	119
VITA	160
ABSTRACT	

LIST OF TABLES

Table		Page
1.	TECHNICAL DATA OF POLYESTER RESIN	29
2.	SELECTED LIQUID PAIRS FOR THERMAL CONDUCTIVITY MEASUREMENTS	40
3.	EXPERIMENTAL TEMPERATURE MEASUREMENTS	57
4.	THERMAL CONDUCTIVITY DATA	69
5.	ISOTHERMAL HEATS OF REACTION	72
6.	RESULTS OF THE CURING STUDIES REPORTED BY SEVERAL INVESTIGATORS	81
7.	PREDICTED KINETIC PARAMETERS	83
8.	LIST OF VARIABLES USED IN MODEL	95
9.	LIST OF VARIABLES USED IN DSC CALCULATIONS	157

LIST OF FIGURES

Figure		Page
1.	Formation of a polyester chain	9
2.	Crosslinking Reaction of Polyesters	10
3.	180°F standard exotherm curve for polyester resins containing 1% BPO catalyst	14
4.	DSC cell	19
5.	Experimental set-up for temperature measurements	32
6.	Analog data link	34
7.	Principle of Colora Thermoconductometer	38
8.	Modified sample system for thermal conductivity measurements	42
9.	Determination of specific heat using DSC	47
10.	Temperature profiles	55
11.	Experimentally determined temperatures at different locations in curing polymer	58
12.	Experimentally determined temperature profiles	59
13.	Birefringent patterns of a cured specimen	61
14.	Birefringent patterns of a cured specimen	62
15.	Birefringent patterns of a cured specimen	63
16.	Birefringent patterns of a cured specimen	64
17.	Thermal conductivity of cured polyester	66
18.	Total heat generation vs. curing temperature	73

Figure		Page
19.	Cumulative heat evolution during isothermal cure	74
20.	Rate of heat generation for isothermal cure	76
21.	Rate of heat generation for isothermal cure at 122°C	77
22.	Experimental rate of heat generation during scanning	78
23.	Extent of reaction during isothermal cure	79
24.	Extent of reaction during isothermal cure at 122°C	80
25.	Arrhenius plot	84
26.	Comparison between experimental and predicted rate of cure at 82°C	86
27.	Comparison between experimental and predicted rate of cure at 93°C	87
28.	Comparison between experimental and predicted rate of cure at 105°C	88
29.	Comparison between experimental and predicted rate of cure at 122°C	89
30.	Specific heat of cured polyester	90
31.	Coordinate system of casting	97
32.	Flow diagram of the iteration procedure	100
33.	Calculated temperatures at different locations in curing polymer	102
34.	Calculated temperature profiles	103
35.	Comparison of experimental and calculated temperatures at the center of curing polymer	104
36.	Comparison of experimental and calculated temperatures at $X = 0.5$	105

Figure	Page
37. Comparison of experimental and calculated temperatures at the surface of curing polymer	106
38. Comparison of experimental and calculated temperature profiles	107
39. Calculated extent of polymerization at different locations as function of time in curing polymer	109
40. Calculated profiles of extent of polymerization	110
41. Isothermal curing at 82°C	143
42. Re-scanning of sample previously cured at 82°C	144
43. Isothermal curing at 93°C	145
44. Re-scanning of sample previously cured at 93°C	146
45. Isothermal curing at 105°C	147
46. Re-scanning of sample previously cured at 105°C	148
47. Isothermal curing at 122°C	149
48. Re-scanning of sample previously cured at 122°C	150
49. Scanning of a fresh sample	151
50. Determination of specific heat of polyester	152
51. DSC thermogram of cured polyester	153
52. TGA thermogram of cured polyester	154

I. INTRODUCTION

The physical, mechanical, and electrical properties of a thermosetting material depends upon the extent of the polymerization reaction during cure* or upon the degree of cure in the molded material. Determining such dependence is not only important for a better understanding of structure--property relationships, but it is also fundamental in optimizing the properties of the final product.

Recently, due to energy and resource problems, thermoset polyesters have captured many applications in automotive and appliance components as a substitute for other more traditional materials. As a result of these developments the processing of these materials has become very significant in those industries. Like processing of other plastics, the processing of thermosets involves exposure of these materials to varying levels of heat treatment. During such treatment, the thermal behavior of thermoset resins is complicated by the highly exothermic nature of the polymerization reaction. Thermosets are generally polymerized and processed in a single operation which transforms low molecular weight material into network polymer in an irreversible process.

Most of the polymer reaction molding processes like casting, potting, lamination, thermoset molding or reaction injection molding

*The overall transformation from liquid to gel to rubber to glass due to chemical reaction is termed cure.

are controlled by a balance of internal heat generation and heat transfer through the mold walls. In some cases, where the piece to be molded varies greatly in thickness, the exothermic temperature differences between the various sections of the piece generate stress gradients of considerable magnitude. These stresses may remain in the product practically indefinitely. This is usually a disadvantage, since such stresses may lead to eventual deficiencies, such as cracking, crazing and delamination of the piece. These stresses can only be relieved if the piece is post-baked or annealed at a temperature that is as high or higher than the maximum temperature attained in any part of the piece during the cure.

There are a number of reports in the literature concerning studies of the curing mechanism of the thermoset polyesters. The traditional approach to determine proper curing has been to mold samples at various cure times and temperatures and to measure physical properties of the cured samples. Thus, the cure time and temperature giving the maximum in the desired property were selected as the optimum cure conditions. Many of the electrical or mechanical properties selected as curing criteria suffer from the difficulty that relatively large changes in cure give small changes in the measured property. Therefore, there is an increasing demand for the development of a theoretical curing model in order to control the rate of heat generation and the temperature variations during the processing of these materials. Such a model can be readily developed from the conductive heat transfer rates and the chemical kinetics of the polymerization reaction.

Temperature and concentration profiles that can be obtained from such a model can be applied to determine the variations of the physical and mechanical properties with position and time in the mold so that the desired process conditions can be established.

The primary objective of this research was to develop a mathematical model which could be utilized in characterizing the curing process, predicting curing performance and establishing guidelines for better production and application of these polymers. The following types of theoretical and experimental studies were necessary for the achievement of this project: (1) development of a kinetic model of the polymerization reaction; (2) determination of the thermal properties and the heats of reaction as a function of both temperature and extent of reaction; (3) experimental measurements of the temperature variations with time and position in the mold during polymerization; and (4) development of a numerical simulation technique for the curing operation.

II. BACKGROUND INFORMATION AND LITERATURE

History of Thermoset Polyesters

The first attempt to make a polyester resin is attributed to the Swedish chemist, Jons Jacob Berzelius who, in 1847, reacted tartaric acid with glyceryl to obtain a resinous mass, poly (glyceryl tartrate) (1). As early as 1916, resinous compositions based on the combination of glycerin and phthalic anhydrides were used as finishes for wood and metal. Additional work in the late 1930's by Bradley (2) extended the theories of Carothers (3) and Kienle to clarify the so-called drying properties of unsaturated polyesters. Bradley discovered that the main requirement for this drying was not oxidation but the ability of molecules to unite to form very high molecular weight groups. In their experiments with maleic anhydride containing polyesters, Kropa, Bradley and Johnston (4) established that the formation of insoluble, infusible polyester compositions was based on the presence of unsaturated double bonds in the polyester chain. In 1937, Ellis (5) discovered that the addition of unsaturated monomers to polyesters containing unsaturated groups increased their setting speed by more than a factor of thirty.

The commercial development of unsaturated polyester resins began in the United States in 1941, when an allyl casting-resin was introduced for use as a glass substitute (1). Here unsaturation was obtained by using an unsaturated alcohol, allyl alcohol, instead of following

the more usual practice of using an unsaturated acid such as maleic or fumaric. This was followed in 1942 by an allyl low-pressure laminating resin, allyl diglycol carbonate, which was used for the manufacture of some of the first glass cloth reinforced resin radomes for aircraft (1). This development has led to entirely new processing techniques in molding and laminating large and often complex structural products. Products made in the early stages of development included serving trays, tote boxes, lamp shades, flat sheets for the electrical industry and corrugated sheets for the building industry.

The earliest polyester resins were cured only at a temperature of about 100°C. The introduction of polyesters that could polymerize quickly at room temperature without external pressure brought about wholly new industries and opened new markets for these plastic products. Development of cold-curing catalyst systems permitted the production of boats, reinforced translucent sheets and other articles requiring no or low pressures and low temperatures in their fabrication.

Recently, polyester-based low-profile sheet and bulk molding compounds (SMC and BMC) have captured many applications in automotive and appliance components as an attractive replacement for metal and other traditional materials especially with the entrance of glass-fiber reinforced plastics into a position of supremacy in terms of the strength-to-weight ratio and other properties.

The large demand of these thermosetting resins has caused extensive research and development studies on these materials. Following are the present areas of study on these polymers:

1. Synthesis studies to develop new resins which can produce better ultimate properties of the final product.
2. Studies of the polymerization mechanism which is an important consideration in processing of these plastics.
3. Studies of new processing techniques and methods.

Chemistry of Unsaturated Polyesters

In inorganic chemistry the reaction between an acid and a base--referred to as a neutralization reaction--produces a salt. An analogous reaction involving organic molecules is the reaction of an organic acid with an alcohol (an "organic base") to yield an ester. A water molecule is also produced during the esterification reaction.

The resins commonly referred to as unsaturated polyesters are mixtures of the long-chain polymer which results from the esterification reaction dissolved in a polymerizable monomer which can subsequently be reacted to unite the chains into three-dimensional cross-linked network. The two components co-react or copolymerize at room temperature or higher temperatures upon introduction of a peroxide catalyst to form a rigid, infusible thermoset. The terminology, "unsaturated," indicates that unbroken double bonds are carried over from the original (acid) ingredients into the finished resin to provide points of reactivity; the double bonds (unsaturation) are opened up by the free radical catalyst and unite with similar reactive chemical groups or units of the monomer. The final curing reaction is

classed as "addition" polymerization because no by-products result, as opposed to condensation polymerization as occurs, for example, with phenolics.

Unsaturated polyesters are of major interest as reinforceable plastics due to the wide variety of ultimate end properties which may be obtained by varying the many potentially usable raw materials. These raw materials fall into four classes:

1. Unsaturated polybasic acids, e.g., maleic acid or maleic anhydride, are so termed because of the doubly bonded carbon atoms that appear in the aliphatic molecular structure which also contains two or more carboxyl (COOH) groups. These double bonds introduce high reactivity and ultimate rigidity into the crosslinked polyester.

2. Saturated aromatic polybasic acids, when included as a polyester resin ingredient, modify to some extent the rigidity introduced by the unsaturated polybasic acids. These materials behave like saturated acids, but do not provide complete flexibility because of their rigid ring structure, e.g., phthalic acid, which is unlike the loose aliphatic structure of the saturated acids.

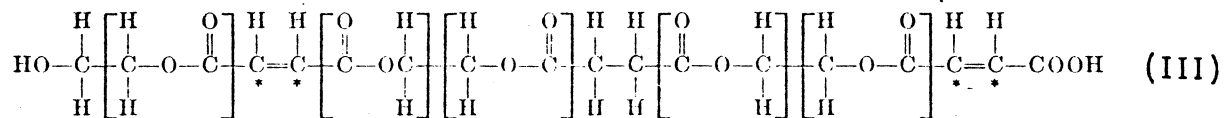
3. Saturated dibasic acids, e.g., adipic acid, in which carboxyl groups again exist in an aliphatic structure, but in which no unsaturation exists, are used to modify the resin reactivity by introducing longer chain lengths between the crosslinking junctures, resulting generally in the more resilient or flexible, higher molecular weight resins.

4. Polyhydric alcohols (polyol), so termed because two or more

hydroxyl (OH) groups exist on each aliphatic glycol chain, and each may react with either type of dibasic acid to form ester linkages.

The fundamental dibasic acid (I) plus dihydric alcohol (II) to form the polyester chain (III) may be represented as shown in Figure 1 with maleic acid and ethylene glycol. Such a polyester is capable of subsequent crosslinking (or thermosetting) either directly to similar unsaturated double bonds in adjacent polyester chains of the same structure by direct reaction or, as occurs more frequently, through an unsaturated double bond in a monomer such as styrene. The monomers such as styrene are generally used are liquids and serve as a solvent to dissolve the highly viscous-to-solid polyesters and thus give them a consistency ideal for various fabricating operations.

When the base resin-monomer mixture is catalyzed and cure is under way, the unsaturated reactive groups of the monomer readily combine or copolymerize with the reactive groups of the base resin after the latter have been attacked and opened by the free radicals resulting from dissociation of the peroxide catalyst. The resulting three-dimensional, crosslinked thermoset structure may be made to yield many and varied properties depending upon the type and amount of both base-resin ester and monomer and the extent of the cross-linking reaction that is allowed to occur. Between one and two moles of styrene are required for each mole of unsaturated acid in the original ester (26). The formula in Figure 2 schematically represents this chain-joining and network growth.

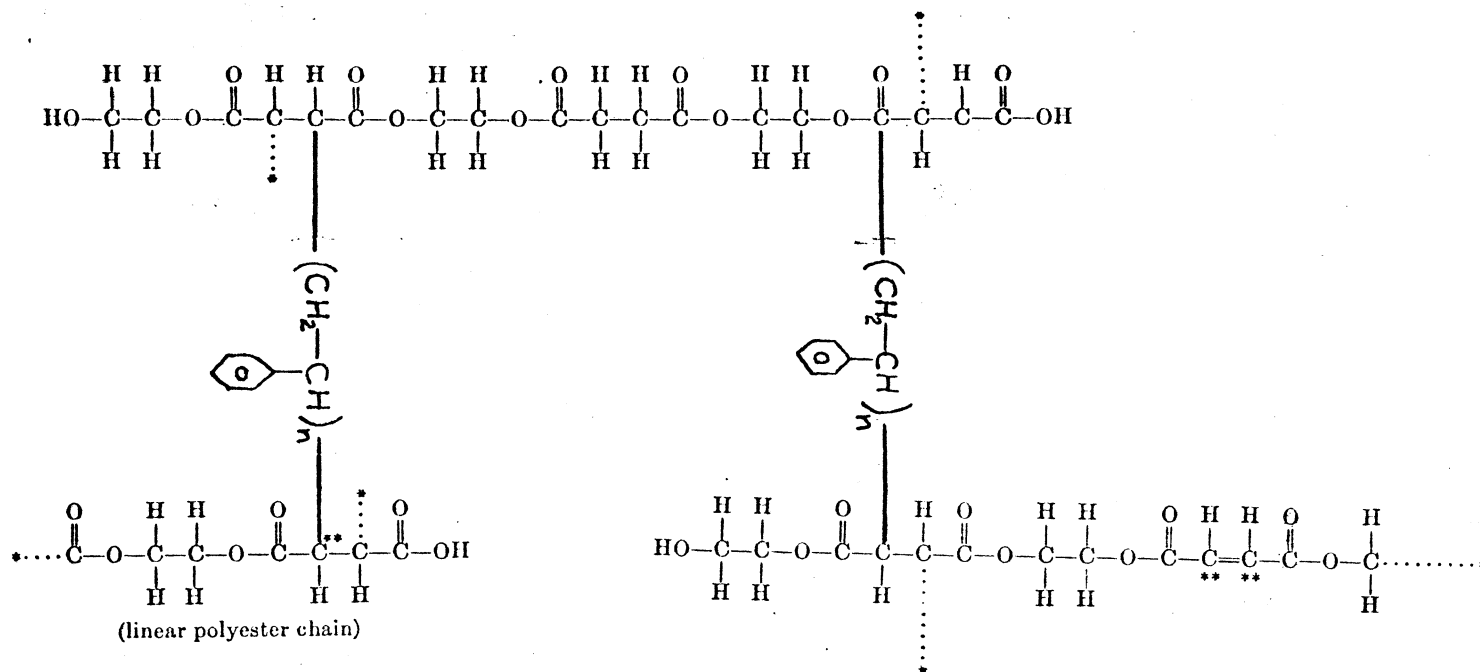


Polyester chain: ester groups linking the carbon chains of alcohols and acids.

* Represents active sites for further reactions.

Figure 1. Formation of a polyester chain.

(linear polyester chain)



- * Linear chain continues.
- ** Active sites (unsaturation) for further reactions.

$n \cong 1-3$

Figure 2. Crosslinking reaction of polyesters.

Hamann and coworkers (7) concluded that crosslinking is initiated and propagated through the styrene and that neither the styrene nor the double bonds of the fumaric or maleic acids would normally homopolymerize. They also reported that the amount of crosslinking depended upon the ratio of styrene to polyester.

The formation of an infinite network structure was considered in the classical papers of Carothers, Flory, and Stockmayer (8), and additional theoretical considerations affecting the conditions of formation of a polyester network have been stated by Gordon and Grievson (9).

There are at least five specific types of polyester resins (10) which have been developed that possess different properties to satisfy the performance requirements of the fields in which they are used:

1. General Purpose Polyesters
2. Light-Stable and Weather-Resistant Resins
3. Chemically-Resistant Polyester Resins
4. Resins with High Heat Distortion Temperature
5. Flame-Resistant Resins.

Crosslinking Reaction and Curing

Description of the Crosslinking Reaction of Polyesters (10)

Although polyesterification takes place as a "condensation" or step-growth polymerization reaction, the ultimate thermoset cure of a polyester essentially takes place due to "addition" polymerization as we have seen. This signifies that polyester and monomer units are

successively and systematically linked due to a chain-joining network-forming mechanism (Figure 2).

The unsaturated double bond becomes the locus or point of development of an "active center" (11) from which polymer growth may propagate. There are several ways of initiating or triggering addition polymerization: these include thermal and photochemical means, for which no chemical catalyst is required; and free radical or ionic means, which involves catalysts (10).

Free radicals are generally produced from either thermal decomposition or by the action of a promoter on an organic peroxide. The peroxides are referred to as catalysts, though they are not so in the truest sense, because they are consumed in the polymerization reaction. There is evidence that residual portions of the free radical sources exist in the final product (10).

Assuming that a dibasic acid-dihydric alcohol-monomer polyester is activated with an organic peroxide, the following mechanism is set into motion (10):

1. The organic peroxide, represented as $R-O-O-R'$, where R and R' may be an alkyl or acyl group or hydrogen, decomposes by either a promoter or thermally to homolytically cleave the O-O bond which then releases the $R-O\cdot$ and $R'-O\cdot$ free radicals.

2. The free radicals first react with the chemical inhibitor ^{*} so that the inhibitor material is consumed prior to the onset of the polymerization reaction.

^{*}Inhibitors such as ortho substituted phenols are previously added to the resin in order to maintain its stability during storage.

3. Apparently, the free radicals serve to open the double bonds in the polyester linear chain. This portion of the polymerization is designated as initiation.

4. The addition reactions then occur and the processes which are descriptive of continuation of this polymerization are termed "propagation" (or chain growth). The final step is the combination of two free radicals so that each terminates the growth of the other. This latter step is then called the "termination" step.

Theoretically, the reaction of polyesters should go to completion with all double bonds reacted upon by free radicals, and complete crosslinking established under the most favorable conditions. However, 92 to 95% conversion of the total unsaturation can be considered as an optimum cure (12). The remaining unreacted double bonds can cause the discoloration of polyesters upon weathering and long-term aging.

The crosslinking reaction of a typical polyester generates as much as 150 calories of heat per gram of resin, which results in peak-exotherm temperatures of up to 500°F (12).

The physical and chemical changes occurring in polyesters during polymerization may be shown in a graphical representation by noting the rate of variation of resin temperature with time immediately after catalyzing and initiation of cure (Figure 3). The exotherm curve is of substantial value in indicating the effect of changes in concentration of catalysts, promoters, fillers and temperature on a specific resin.

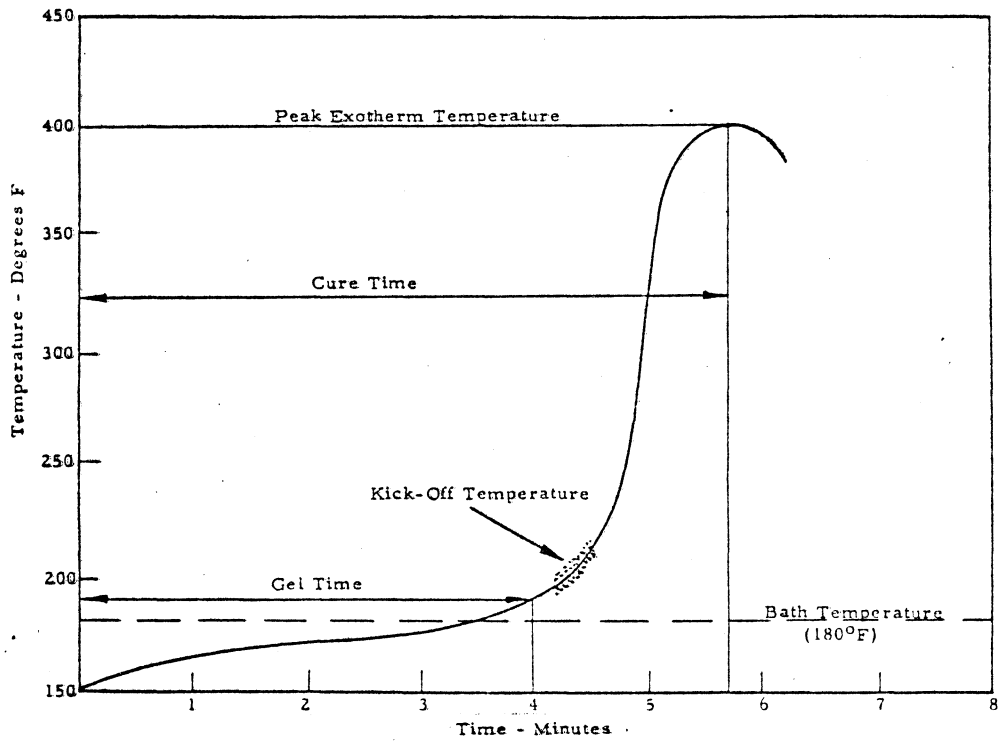


Figure 3. 180°F standard exotherm curve for polyester resins containing 1% BPO catalyst.

Chemical Kinetics

Actually, the kinetic mechanism in almost all thermosetting polymerizations are very similar in nature. Autoacceleration which is also known as the "gel effect" is the term used to describe a unique situation which develops in the curing of polyester and other thermoset resin systems (13). As the initial crosslinking occurs, the mobility of the system and the frequency of collisions are rapidly decreased as the gel forms. Since the frequency of termination reactions is a function of the rate of their meeting other growing chains, the proportion of termination reactions gradually decreases and the number of addition reactions to other double bonds becomes greater (2). Since more heat is liberated by the addition reaction (2), the system automatically heats more rapidly as the gel structure becomes tighter and the mobility decreases. This heat, or exotherm, increases the activity of the growing radicals and also speeds the release of more radicals from decomposing catalyst, both of which add to the increased frequency of the addition reactions.

The "gel effect" in free radical polymerization has been studied by many investigators since the studies of Schultz (14, 15) and Trommsdorff (16). They observed a sudden increase in the rate of polymerization of these systems and showed that it was due to the diffusion control of the termination process. It was also reported that when the material is rubbery, the propagation reaction itself becomes diffusion controlled (17).

The kinetic scheme of the polymerization reaction of polyesters has been described in many publications. While some of them include the analysis of the results in terms of the possible mechanisms of polymerization, only physical interpretation of the results were made. Therefore, more studies are necessary if one is to develop a single kinetic model which can fit the entire curing process.

Determination of the kinetics, particularly beyond the gel point, is difficult. Indirect methods must be used, since the polymers formed are usually three-dimensional and insoluble. Calorimetry, infrared and other spectrographic methods, electrical conductivity, dilatometric techniques, dynamic mechanical and dielectric methods have all been applied, and examples of each are discussed below.

Chemical tests of the extent of crosslinking reaction were definitive to some degree, and bromine absorption (18) and styrene determination (19) have been used by some investigators. However, these methods gave variable results due to the immobilization of the system at an early stage (20).

Lewis and Gillham (21) developed an interesting technique in which a nylon braid was impregnated with resin and the changes in stiffness followed during the full curing process. There were some difficulties in interpretation of results, but this was a distinct improvement on the empirical methods.

Dynamic mechanical testing such as the torsional pendulum was recently used successfully in the study of the later stages of curing of novolacs, resoles, epoxy resins and polyesters (22).

Henson and coworkers (23) applied the techniques of a Farol-Weissenberg rheogoniometer to investigate the early stages of a polyester cure. By using the oscillatory facility of the rheogoniometer it was possible to follow the response of the resin system to torsional shear from the time of gelation into the early region of the gel state. They measured the torsional forces to determine the modulus of elasticity at intervals of time during the cure, and they showed that this parameter increased with increasing degree of crosslinking.

Rubens and Stochdopole (24) used a new type dilatometer which automatically recorded volume changes to determine the rate curves during the entire course of polymerization.

From experimentally determined gel fractions, rates of disappearance of styrene and ester unsaturation, and the degree of polymerization of the growing chains, Burland and Hinsch (25) suggested a kinetic model based on a free radical copolymerization, assuming a single effective propagation and termination rate constant.

Recently, application of thermal analysis and calorimetric techniques have seemed to be the most effective method to get complete qualitative and quantitative information on the curing process of thermosets. For this purpose, the differential scanning calorimeter (DSC) has been used by a number of workers to study the exothermic heat of cure and the kinetics of curing.

Differential Scanning Calorimetry

Description of the Instrument

Differential scanning calorimetry is a technique of non-equilibrium calorimetry in which the heat flow into or from an unknown sample and a reference is measured as some function of time or temperature (26).

Since a DuPont DSC instrument has been used in the kinetics and thermal analysis studies of this project, more of the information in this dissertation will be based on the techniques and theories developed for such instruments.

A DuPont DSC cell is a plug-in module for the DuPont Thermal Analyzer. It is simply a heated constantan disc incorporating two raised platforms upon which the sample and reference pans are placed. The disc acts as the primary means of heat transfer to the sample and reference pans. The two platforms are connected with a differential thermocouple which measures their temperature difference. The temperature of the sample is measured with a thermocouple which is embedded in the sample platform. The sample and reference platforms are calorimeters themselves which are programmed against each other in order to reduce or eliminate the heat loss factors which are inherent in all calorimeters. A DuPont DSC cell is shown in Figure 4.

Analysis of DSC

The underlying theory of the DuPont DSC has been discussed by Baxter (27), David (28), and Gillham and Mentzer (29). The following is a summary of those analyses:

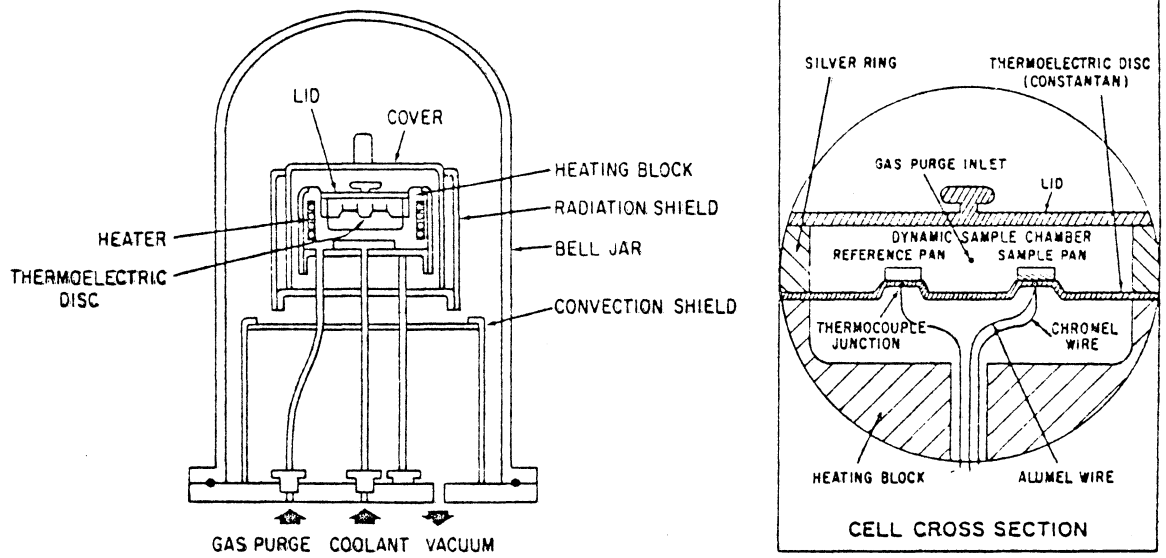


Figure 4. DSC cell.

The recorded ΔT can be due to several factors. One is the heat capacity mismatch between the sample and reference. Another contributing factor occurs when the sample is undergoing a thermal event. The basic equation for this instrument (complete derivation and development of this equation was given in (29)) is

$$\Delta T = (T_{RP} - T_{SP}) = R_C (C_S - C_R) \frac{dT_R}{dt} + R_C \frac{dh}{dt} - (R_C + R_S) C_S d \frac{d(\Delta T)}{dt} \quad [1]$$

where T_{RP} and T_{SP} = reference and sample platform temperatures; C_S and C_R = sample and reference heat capacities; $\frac{dT_R}{dt}$ = programmed heating rate; R_C = average thermal resistance of the constantan disc ($^{\circ}\text{C}\text{-sec/cal}$); R_S = thermal resistance between the sample pan and the sample platform; $\frac{dh}{dt}$ = rate of heat generation during a thermal event in the sample (- if exothermic, + if endothermic). The first term on the right-hand side of the above equation is associated with the heat capacity mismatch, and the second term is associated with the thermal event occurring in the sample. The last term is due to the thermal lag which is inherent in all programmed calorimeters. It can be quite large during a rapid thermal event.

Measurement of the area under the ΔT - versus - T_{SP} curve for a thermal event is equivalent to integration of the above equation. The heat capacity term is either neglected or subtracted out (29). The thermal lag term can also be neglected since the response of the instrument (ΔT) before and after the thermal event is approximately the same (the limits of integration for the thermal lag term are the same). This means that the area under the curve ($\int \Delta T dt$) is directly

proportional to the heat generated during the thermal event (ΔH), and the proportionality constant is R_C , and it usually varies with temperature. It can be determined as a function of temperature using the known heat capacity or heats of fusion of some calorimetric standards. Since sample size, heating rate, and shape of the sample pan also affect the calibration, calorimetric measurements and calibration should be performed at the same experimental conditions. Curves of ΔT versus T are converted to heat flux versus temperature by multiplying the ΔT by the calibration coefficient at the same temperature.

Kinetics and Thermal Characterization of Thermoset Cure by DSC

Almost all of the kinetic methods used in DTA and DSC are based on the equation

$$\frac{dP}{dt} = f(P, T) \quad [2]$$

where $\frac{dP}{dt}$ is the rate of polymerization reaction, $f(P, T)$ is a function of the amount reacted, and temperature at time t .

An early description of the application of differential thermal analysis to the study of reaction kinetics was reported by Borchardt and Daniels (30). Assuming that the heat evolved in a small time interval is directly proportional to the number of moles reacting during that time they showed that

$$\frac{dP}{dt} = \frac{1}{\Delta H} \left[C_P \frac{d(\Delta T)}{dt} + K\Delta T \right] \quad [3]$$

where P was the extent of the reaction, ΔH was the heat of the reaction (equal to KA where K was the average heat transfer coefficient (cal/°C-sec) and A the area under the DTA curve), C_p was the average heat capacity and ΔT was the temperature differential between sample and reference. They assumed that C_p , K and ΔH did not change in the temperature interval where the reaction occurred.

For DSC the expression equivalent to the above equation has been shown by the same workers to be

$$\frac{dp}{dt} = \frac{1}{\Delta H} \frac{dH}{dt} \quad [4]$$

where $\frac{dH}{dt}$ was the rate of heat generation and p was the fraction of total heat evolved at time t . ΔH was determined from the total area under the DSC curve.

For a first-order reaction the rate constant was simply

$$k(t) = \frac{dH/dt}{\Delta H - \Delta h(t)} \quad [5]$$

where $\Delta h(t)$ was the heat generated up to time t and the difference $\Delta H - \Delta h(t)$ was the fraction of unreacted material at time t .

Dynamic DSC studies of the epoxy cure reaction have been reported by Fava (31), Abolafia (32), and Prime (33). Fava described an extensive investigation of the isothermal and dynamic cure of an amine-catalyzed epoxy anhydride.

Choi (34) studied the effect of time and temperature on the cure of diallyl phthalate molding compounds using isothermal techniques of DSC. He assumed that the amount of exothermic heat measured was

proportional to the number of double bonds reacted in the system. Then, he showed that determination of the exothermic areas as a function of time and temperature could provide the necessary data for polymerization rate studies.

M. R. Kamal and Sourour (17) argued that the exothermic heat of cure and kinetics of cure of thermosetting materials could be determined more accurately using the isothermal techniques rather than the dynamic techniques. The dynamic techniques are performed by scanning samples at a linear rate to obtain cure thermograms. The utilization of these thermograms to generate kinetic data usually involved the assumption of a constant specific heat while both the temperature and degree of cure varied simultaneously (31, 34).

Few attempts have been made to study the curing reaction of polyesters by using DSC. Horie and his group (35) investigated the curing reaction of a polyester fumarate with styrene, and they applied the isothermal techniques. They observed a large autoacceleration in rate of cure and a strong dependency of final conversion on the curing temperature.

Recently, Kamal and coworkers (36) used DSC and proposed the following empirical curve-fit model to describe the cure kinetics of both epoxy and unsaturated polyester systems:

$$\frac{dP}{dt} = (k_1 + k_2 P^m) (1 - P)^n \quad [6]$$

where k_1 and k_2 were rate constants and m and n were constants independent of temperature. The relative degree of cure, P , was defined as

$$P = \frac{Q_R}{Q_m} \quad [7]$$

where Q_R = the total amount of heat evolved isothermally as the result of reaction between the beginning of reaction and time t , and Q_m = an adjustable reducing parameter which may depend on temperature.

Heat Transfer and Processing of Thermoset Plastics

Thermoplastics soften and flow on heating and, when cooled, return to the solid state. The methods used for processing these materials depends on this reversible behavior. Synthesis and processing of thermoplastic materials are generally distinct operations. On the other hand, thermosets are generally polymerized and processed in a single operation which transforms low molecular weight material to network polymer in an irreversible process. Examples include polymer reaction molding operations like casting, potting, lamination, thermoset molding, and reaction injection molding.

Casting and Related Processes

The process of casting consists of pouring a liquid substance into an open mold to harden without benefit of an external pressure. There are variations of casting in which some form of light pressure is applied, or by which a casting is built up to final size in multiple steps (12). Casting processes are used to produce a wide variety of products ranging in weight from a few grams to several tons. Embedding is the process whereby sales display items and mineral, botanical, or

biological samples are preserved for ease of handling and observation. Encapsulation involves surrounding a component (usually electronic) with resin for protection against shock, moisture, or chemicals. A variation of encapsulation called potting generally involves vacuum impregnation of porous or internal sections of an object in addition to forming the protective outer shell. Controlling the exothermic reaction is the most important factor for a successful casting operation. Unless controlled, undesirable results occur: (1) castings are brittle or discolored; (2) castings are cracked or contain voids; (3) castings froth and foam; (4) castings ignite. Exothermic heat is always concentrated in the center of any mass, with the result that the center of the casting is expanding rapidly because of this thermal influence, while at the same time, it is trying to contract as molecules join under chemical reaction. Control of this exotherm is still a challenging problem in this field. At the present time it is controlled unsystematically as: (1) reducing promoter and catalyst concentrations in proportion to other conditions of time and temperature; (2) completing the casting in a series of successive pours, rather than as a mass casting; (3) incorporating heat-conductive fillers, and using heat-conductive molds.

Lamination: Combining layers of fabric, paper, or mat with thermoplastic or thermosetting resins is called lamination. Laminates may take the form of flat sheets, molded tubes, or wrapped rods.

Reaction Injection Molding (RIM): Reaction injection molding is a new processing method which has grown at a substantial rate during

recent years with the development of a number of fast thermoset systems. RIM is distinguished from standard liquid casting techniques or automated reactive liquid molding systems by its utilization of high-pressure impingement mixing, a technique developed in Europe (37).

There are a number of descriptive reports in the literature concerning the theory of these processes, but there are only a few analytical studies on the problems of nonuniform reaction due to both heat transfer and the reaction exotherm during these processes. Since the rate of heat transfer is generally slow compared to the rate of reaction (38), a distribution of temperatures significantly in excess of the curing temperature develops within the mold. The rate of the curing reaction is dependent on the temperature and the composition of the resin-catalyst mixture. The temperature in the mold is a function of time and position, and it is determined by a balance between heat conduction, heat exchange with the environment, and internal heat generation from the curing reaction. Convection and molecular diffusion can be generally neglected (39).

In 1966 Stonecypher et al. (38) applied transient heat transfer concepts in curing highly exothermic solid propellants, and developed a mathematical model for the curing process so that the curing performance could be simulated. Later in 1971 Hills (40) reported some transient heat transfer calculations to predict cure development in thick sections in rubber molding. Engelmaier and Roller (41) also used transient heat transfer and a time and temperature dependent viscosity to model thickness changes in epoxy electrical laminates.

Very recently, Broyer and Macosko (39) have proposed a theoretical model for curing in polymer reaction molding operations, and they have also presented the variations of some physical properties with position and time in the mold for a typical urethane system.

So far, there has been no systematic study reported in the literature concerning an application of heat transfer concepts to curing unsaturated polyesters.

III. EXPERIMENTAL

This section describes the primary experiments that were performed in this research.

Materials

Polyester Resin

A general purpose polyester resin was selected and used in this investigation. It was supplied by Ashland Chemical Co., Columbus, Ohio. In preparing the base polyester resin, the following monomers were employed in the ratios indicated:

2 moles phthalic anhydride

1 mole maleic anhydride

3 moles propylene glycol

As a crosslinking agent styrene monomer was added to the resin mixture by the manufacturer. The styrene content has been determined as 28% by weight with an accuracy of $\pm 2\%$ by heating a 5 g sample of fresh resin in an oven at 110°C until a constant weight was attained.

The technical data on the resin which was provided by the manufacturer are presented in Table 1.

Catalyst (or initiator)

A 60% solution of methyl ethyl ketone peroxide in dimethyl phthalate (Lupersol DDM) was used to initiate the crosslinking reaction. It was obtained from Pennwalt Co., Lucidol Division.

TABLE 1

TECHNICAL DATA OF POLYESTER RESIN

DESCRIPTION: AROPOL 8310--a medium-viscosity polyester resin designed for general purpose matched-die molding

PERFORMANCE: Cures fast
Has high gloss
Exhibits good hot strength for fast demoldability
Has excellent color

SUGGESTED USES: Preform molded chairs
Tote bins
Trays and boxes
Outboard motor cowlings
Pultrusion applications

SPECIFICATIONS

Percent styrene	28-30
Viscosity--Brookfield at 77°F #3 spindle at 30 rpm, cps	2,000-2,400
Color, Gardner ('63)	1 max
Acid number (solids)	18-24
Pounds per gallon	9.7

TYPICAL PERFORMANCE DATA

TYPICAL CURING CHARACTERISTICS:

Standard 180°F bath--1% benzoyl peroxide	
SPI gel time, minutes (150-190°F)	5
Total time to peak exotherm, minutes (150 to peak °F)	7
Peak exotherm, °F	400

TYPICAL PHYSICAL PROPERTIES OF CURED CASTINGS:

Barcol hardness	50
Tensile strength, psi	10,000
Elongation, percent	1.9
Flexural strength, psi	17,000
Flexural modulus, psi x 10 ⁶	0.61
Heat distortion temperature, °C	73

Promoter

For room temperature reactions, it was necessary to use a promoter to activate the peroxide catalyst. For this purpose cobalt naphthenate (6%), supplied by Troy Chemical Co., was used.

Silicone Rubber

Due to its excellent properties, silicone rubber was selected as the most proper compound from which to prepare molds for the casting operations. All the molds were prepared using General Electric's RTV700 compound with a Beta 5 curing agent. Its high elongation and excellent tear resistance insured easy release of the molded article (no release agent was necessary). It had also the ability to withstand the high exothermic temperatures of polyester that was to be cured in the mold. The master pattern for the silicone rubber molds was prepared from stainless steel.

In all the experimental work requiring polyester samples in this investigation, the same mixture of resin and catalyst has been prepared and used. Necessary precautions had been taken in all the experiments to prevent the loss of any styrene monomer due to its high volatility.

Casting and Temperature Measurements

The following Section describes the techniques developed and used for the experimental measurements of time-temperature-position data in the curing polymer mass. Basically, it involved a typical room temperature casting operation.

Experimental Setup

The experimental set-up for the temperature measurements consisted of a silicone rubber mold, thermocouples, and a PDP-11 digital computer for data acquisition.

A silicone rubber mold was prepared using a stainless steel mold pattern. Its inner dimensions were designed as 6"x6"x1-1/2". Also a top cover with the same thickness (1") as the mold bottom was prepared.

After reviewing the properties and performance of different thermocouple systems, 30 AWG Iron/Constantan thermocouple wires were selected to prepare the temperature sensing assemblies. Each sensing assembly had its own measuring and reference junctions, and more than thirty thermocouples were prepared in this way. Experimental set-up is shown in Figure 5.

Required number of thermocouples to be placed inside the mold and the proper spacing between the measuring junctions was carefully determined from a study of several approximate solutions of the temperature profiles that could be created inside the polymer mass as a result of the presumed unidirectional heat flow during casting. The measuring junction of each thermocouple was then placed at its previously determined location along the depth of the mold. The wires were stretched firmly at the mold edges to hold the position of junction against the contraction and expansion forces during casting. The positions of the measuring junctions were also checked after casting operations to make sure that they had not been disturbed during the measurements.

ThermocoupleDistance, cm

1	0.00
2	0.38
3	0.95
4	1.80
5	2.35
6	2.85

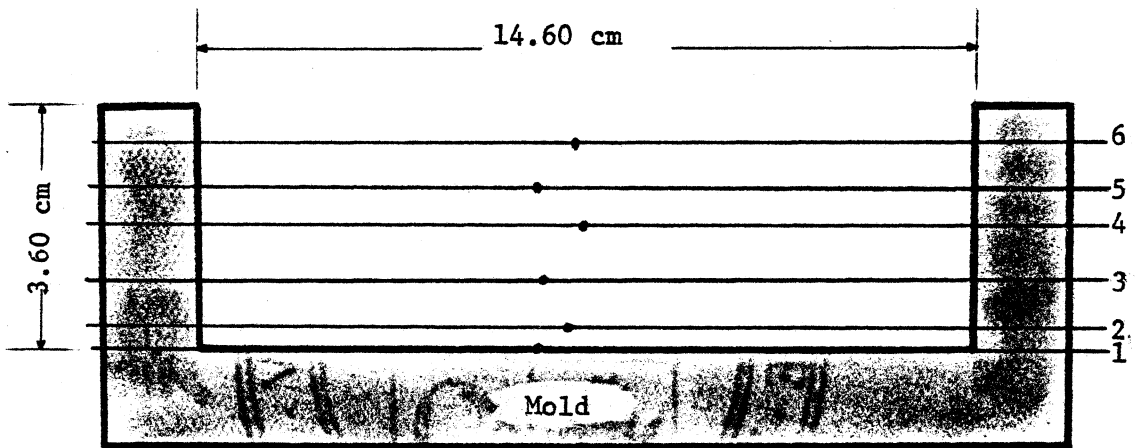


Figure 5. Experimental set up for temperature measurements.

Development of the Data Acquisition Technique

Handling of the emf output from the thermocouples was facilitated through use of a computer program. For this purpose, an interfacing unit was designed, and a software package was developed.

To convert a voltage signal from the thermocouples to a current signal, an electronic circuit was built which consisted of signal conditioning amplifiers. These analog signals were read by a PDP 11/40 digital computer with an A/D converter (Figure 6).

The program called SEL2 was used to display the data on a computer screen at the desired time intervals. The data format on the screen showed numbers equivalent to the analog signals received from the thermocouples. The system was built for a maximum of eight channels, but in most of the measurements only six were used. The program had a limit of 10,000 sets of data. The time interval between the acquisitions was selected as either 3 or 5 seconds. In each time interval the program took eleven points at the same channel, averaged them, and gave the output. The SEL2 program also had the option of storing the data on a disk for later analysis. The program SELREP was used to call the data from disk to be sent either to a printer or onto the screen.

Measurement Procedure

In order to convert the computer massaged output from a thermocouple to a temperature, a calibration procedure had been followed before any measurements. Calibration curves for each thermocouple

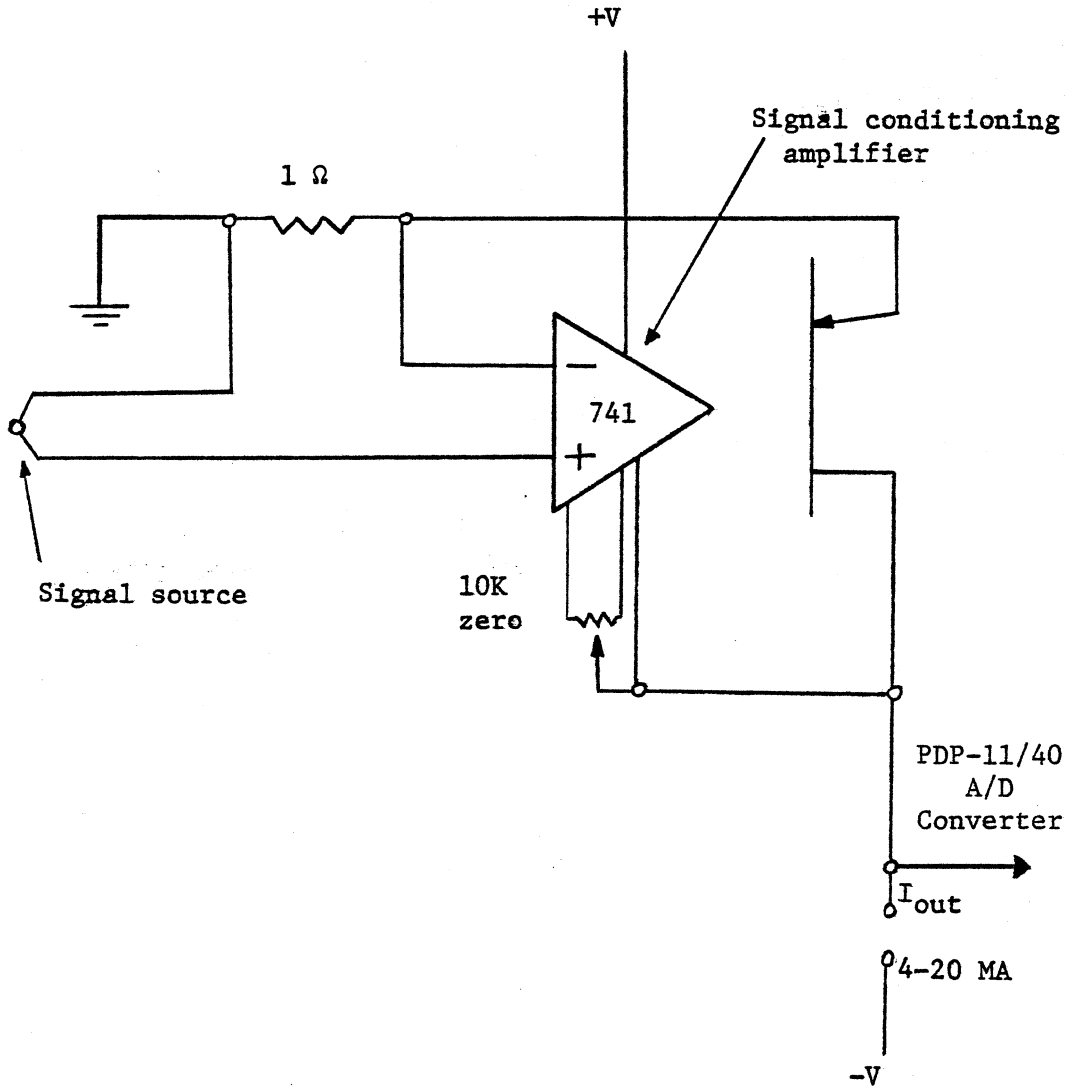


Figure 6. Analog data link.

were obtained over the temperature range of interest by using a constant temperature bath. An ice bath was maintained for the reference junctions. Before each measurement, at least 10 thermocouples were calibrated, and the ones which had the most reproducible calibration curves were employed.

The measuring junction of each thermocouple was placed in the mold as described above, and their vertical distances from the bottom surface of the mold were carefully measured.

Required amounts of the resin mixture, catalyst, and promoter were weighed separately, and they were mixed thoroughly in a large glass beaker for about a minute. The system employed in this investigation contained 100, 0.70 and 0.25 parts by weight polyester, catalyst solution and promoter, respectively. The catalyzed mixture was poured into the mold and the surface was covered with the mold top. At the same time, the computer program was initiated for temperature logging. It was also necessary to note the time for mixing and filling stages to keep their records for later data analysis. The total time for mixing and filling was about 150 seconds which was negligible compared to the reaction time.

The polymerization process was observed by watching the thermocouple outputs on the CRT screen. The exothermic reaction proceeded for about 20 minutes. Temperatures during cooling of the polymer mass were measured until a uniform temperature was observed in all sections of the polymer. The polymer block was removed from the mold, and the

positions of thermocouple junctions were checked to compare with their initial positions. These thermocouples were discarded, and a new set of thermocouples were prepared for the next measurement.

Casting operations were performed at room temperature.

Thermal Conductivity Measurements

There were relatively few reports in the literature concerning studies of thermal conductivity of crosslinked systems. The reactive nature of thermosets and the combination of physical and chemical changes that accompany the curing process all contribute to the experimental difficulties in measuring this thermal property.

Several experimental alternatives were considered as a means to measure the variation of thermal conductivity during polymerization. One alternative was to design and build a new thermal conductivity apparatus for this purpose. However, because of the well-known difficulties and time requirements in construction of such an apparatus, such a task was not encouraging in view of the other primary objectives of this investigation. Therefore, utilization of an existing instrument (a Colora Thermoconductometer) with the necessary modifications was selected as the best alternative at this time.

Description of Colora Thermoconductometer

The Colora Thermoconductometer, based upon a method developed by Schröder (42), is a new measuring device for making quick

determinations of the thermal conductivity of solids. It requires time measurements only and does not involve any calorimetric measurements.

A cylindrical sample of the material to be tested is brought into contact with two boiling liquids having a suitable boiling point difference (10-20°C). The time is measured for a given quantity of heat, determined by the volume of liquid which evaporates from the "cold" side of the sample, to flow through the sample. If a reference sample with a known conductivity is measured with the same selected pair of liquids, the conductivity of the test sample can be obtained directly from a calibration curve.

The principle of the method is illustrated in Figure 7. A pure liquid is boiled in A, heating a silver plate S_1 , and returned to A after being condensed in a condenser K_1 . The temperature of the silver plate S_1 is kept at the boiling temperature of this liquid. An upper vessel, B, contains another pure liquid boiling 10-20°C lower than the liquid in A. There is a second silver plate, S_2 , which forms the bottom of B and the test sample, P, is fitted between the two silver plates. After the liquid in lower vessel A is made to boil, the heat flowing through the sample from S_1 to S_2 causes the liquid in B to boil, thereby keeping the temperature of the silver plate S_2 at the boiling point of the upper liquid. The vapor from the upper liquid is condensed in a condenser K_2 , and the condensate is collected in a graduated container, M.

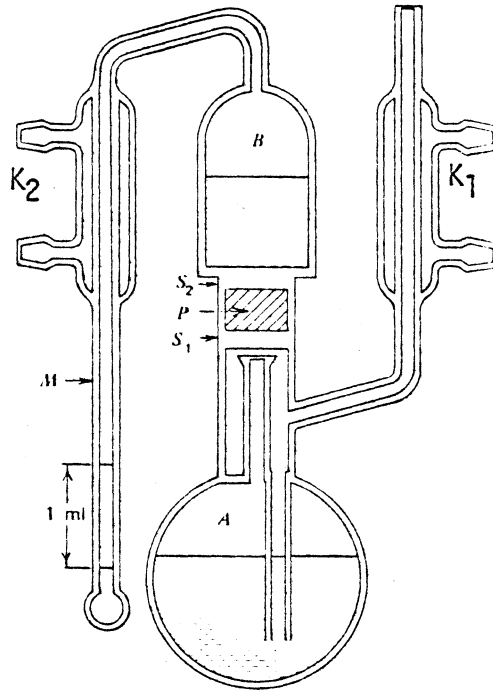


Figure 7. Principle of color thermoconductometer.

After steady state is reached, the time t necessary to distill a fixed amount (1 ml) of the liquid in B into M is measured. If the heat of vaporization of this amount of liquid is Q , the thermal conductivity k_T is then given by

$$k_T = \frac{Qh}{At(T_A - T_B)} \quad [8]$$

where h and A are the thickness and cross-section area of the sample, respectively. If several samples of known conductivity are available, k_T can be determined by a comparative measurement without the necessity of knowing the exact values of the heat of vaporization, and the boiling temperatures of the two liquids.

According to the above equation the thermal resistance of the sample R is given by

$$R = t(T_A - T_B)/Q \quad [9]$$

whence

$$k_T = \frac{h}{RA} \quad [10]$$

Calibration

In this investigation three different pairs of liquids were selected (Table 2) to measure the thermal conductivity of samples at different temperatures. Calibration diagrams (R vs. t) for each liquid pair were obtained using three glass samples which had different thicknesses.

TABLE 2
 SELECTED LIQUID PAIRS FOR THERMAL CONDUCTIVITY MEASUREMENTS

Liquid A	Liquid B	T _A (°C)	T _B (°C)	T _M (°C)
Carbon Disulphide	Ether	46.3	34.6	40.5
Ethyl Acetate	Methanol	77.0	64.2	70.6
Water	Trichloroethylene	100.0	87.0	93.5

NOTES:

T_A = Boiling temperature of liquid A.

T_B = Boiling temperature of liquid B.

T_M = Measuring temperature $\left(\frac{T_A + T_B}{2}\right)$

Measurements

Thermal conductivity measurements with polyesters involved the following type of samples:

- (a) Uncured resin
- (b) Partially polymerized resin
- (c) Cured product

The purpose of those measurements was to determine the variation of thermal conductivity with temperature and degree of cure.

The most important step prior to the measurements was the preparation and handling of the samples. Since the apparatus was basically designed for thermal conductivity measurements with solid samples, a new method was developed for samples of uncured and partially cured resins which were highly viscous liquids (Figure 8). Uncured and partially cured samples were embedded in cylindrical rings that were prepared from a cured polyester product. In order to maintain the samples inside the rings and in good contact with the silver plates, the top and bottom of the rings were covered with very thin teflon sheets. (Such a sample system required the development of a new method of calculation. It will be discussed later in this dissertation.)

Partially polymerized samples were obtained by inhibiting the polymerization reaction just before gelation. As an inhibitor, a small amount of hydroquinone solution was used. Partially polymerized

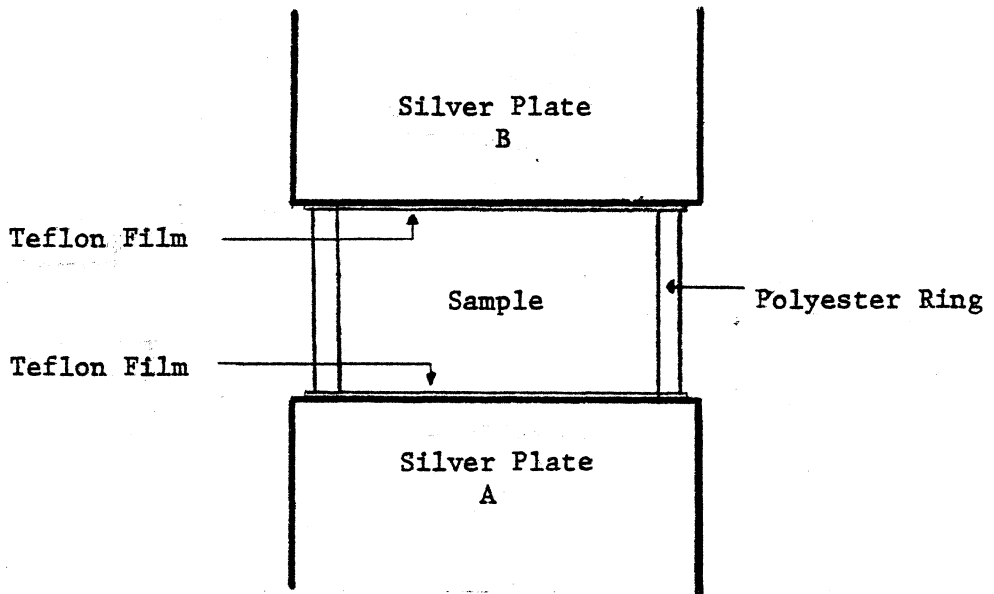


Figure 8. Modified sample system for thermal conductivity measurements.

samples maintain their form for 2 to 3 hr and up to 70 to 80°C. Table 2 presents the selected liquid pairs, and measuring temperatures.

Calorimetric Measurements

The calorimetric measurements were conducted in a DuPont Thermal Analyzer, Model 900, equipped with a DSC cell. The primary objectives of these measurements were to determine (1) heats of polymerization, (2) kinetics of cure, and (3) specific heat.

A continuous calibration curve was obtained using known values of heat capacities of tin and sapphire in order to convert the output of the instrument in ΔT into useable calorimetric quantities. The calibration curve thus obtained was again checked with the values predicted using the heats of fusion of tin, indium, and benzoic acid. The temperature range of the calibration curve was 80-200°C.

In all measurements, samples were sealed into previously weighed hermetic containers. Aluminum hermetic cups and lids that were coated by the manufacturer to be inert were used to minimize any reactivity between the sample and the container. Hermetic sealing was accomplished using the sample encapsulating press which was part of the DSC accessory kit. This was also necessary to prevent the evolution of styrene monomer during the measurements. Measurements were conducted in an air atmosphere. Empty sample containers were used for the reference system. The weight of the containers with the sample was measured

before and also after the runs to determine whether there was any loss of sample during the measurements.

Calibration and scanning experiments were performed using a constant heating rate of 10°C/min.

Areas under peaks were measured by using a polar planimeter.

Experimental Procedures for Heats of Reaction and Kinetics

Exothermic heats of reaction were measured by isothermally carrying the crosslinking reaction to completion at a series of different curing temperatures.

Resin samples were catalyzed by mixing with a MEK peroxide solution (0.7%) for about half a minute, and no promoter solution was added. The resulting stock solutions were kept in a refrigerator and the required amount of sample was weighed into a previously weighed sample pan (after encapsulation) for each isothermal run. Sample weights were between 15 and 25 mg.

After the instrument was prepared for isothermal operation at desired temperature, the sample and reference containers were introduced into the DSC cell, and the recording of the ΔT output was immediately started. It took about one minute for the sample and reference containers to reach equilibrium as was determined from the time required for the recorder pen to return to or override the original baseline. A record of the time or ΔT output was taken until the exotherm curve leveled off to a baseline which was not far from the

original baseline. The total area under the exotherm curve based on the extrapolated baseline at the end of the reaction was referred to later as Q_T which was the total heat generated isothermally at temperature T.

At the end of each isothermal run, samples were cooled rapidly and re-scanned using a $10^\circ\text{C}/\text{min}$ heating rate until no exotherm was observed. Scanning of samples above the temperature of their isothermal polymerization was necessary to determine their residual reactivity. Areas under the scanning exotherms are referred to later as Q_S .

Isothermal operations were performed at 82, 93, 105 and 122°C . At higher temperatures the cure time was of the order of minutes so that the heat absorbed as the sample equilibrated at the cure temperature partially cancelled out the exotherm. Therefore, no reaction was conducted isothermally at higher than 122°C .

The maximum heat of cure was measured by scanning a freshly catalyzed but unpromoted sample with a $10^\circ\text{C}/\text{min}$ heating rate starting at room temperature until no further reaction was evident.

Specific Heat Measurements

Variation of the specific heats of uncured resin and cured samples with temperature was measured using the same procedure as was described by DuPont in the DSC Manual (43).

First the heat lag for a blank run in which both sample and reference containers were empty was measured. The system was heated starting from an established equilibrium position (a zero differential temperature point), and heating was stopped at a desired temperature to allow the instrument to equilibrate in the "Hold" mode. Thus, a second zero differential temperature point was established after scanning the system. The temperature difference between the line joining the zero differential temperature points and the heating curve at temperature T was referred to as ΔT_{BLANK} . The same procedure was repeated with the samples, and the temperature lag between the sample and reference systems under "blank" and "sample" conditions was determined to determine the specific heat at temperature T (Figure 9).

Many investigators (29) have shown that the above temperature lag was due to the heat capacity of sample.

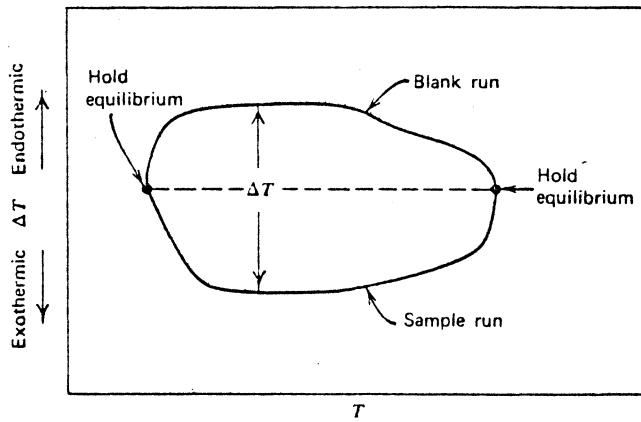


Figure 9. Determination of specific heat using DSC.

IV. MATHEMATICAL MODELLING

This section describes the theoretical studies that were undertaken to develop a mathematical model of the curing process.

Problem Statement

Thermoset products are formed into their final shape by polymerization in situ. That is, the final stage of polymerization and processing of these materials is a single operation. Examples include processes like casting, potting, lamination, thermoset molding, or reaction injection molding (RIM).

The crosslinking reaction of thermosets is a highly exothermic process, and heat thus liberated tends to raise the mold temperature and accelerate the curing reaction. Therefore, the processing of these materials involves a heat conduction problem in the transient state with a coupled, exothermic chemical reaction.

The rate of heat transfer is generally slow compared to the rate of reaction (38). As a result of this behavior a distribution of temperatures significantly in excess of the curing temperature develops within the curing mass.

The rate of the polymerization reaction is dependent on the temperature and the concentrations of monomer and initiator. On the other hand, the temperature in the curing mass is a function of time and position; it is determined by a balance between heat conduction,

heat exchange with the environment, and internal heat generation from the curing reaction. Because of the different local thermal histories developed within the curing mass, the extent of reaction or the degree of cure is also a function of time and position.

Curing performance can be changed by changing the initiator concentration or by changing the temperature of the curing environment. It is difficult to predict the effect of initiator concentration, since free radical initiation is a complex process with many interacting and competing chemical reactions. Increasing the initiator concentration increases the rate of polymerization at a particular temperature. However, it does not provide a direct means for controlling the reaction, since its concentration is established prior to the curing operation. On the other hand, the curing reaction may be easily controlled by means of controlling the curing environment and cure time. Curing environment can be controlled with a knowledge of heat transfer during the process, and the optimum cure time can be selected based on the kinetics of the polymerization reaction. Clearly both heat transfer and reaction kinetics must be considered together to obtain a complete process model.

Assumptions

Following are the basic assumptions in developing a model for the curing process.

No Flow

In reaction molding processes, the filling time (flow time) is significantly less than the cure time; therefore, convection effects have been neglected.

No Mixing

The system was assumed to be well-mixed and homogenous at $t = 0$.

No Molecular Diffusion

The equation of continuity in terms of the concentration of the reacting group of type A can be written (44) as

$$-\frac{\partial C_A}{\partial t} + (V \cdot \nabla C_A) = D\nabla^2 C_A + R_A \quad [11]$$

D = average diffusion coefficient of molecules in the polymerizing mixture

and

R_A = molar rate of disappearance of A.

If flow is neglected, Equation [11] becomes

$$-\frac{\partial C_A}{\partial t} = D\nabla^2 C_A + R_A \quad [12]$$

Crank and Park (45) calculated D for diffusion of hydrocarbons into rubber as 10^{-9} cm²/sec. Using 10^{-9} for D , the order of magnitude of diffusion and generation terms on the right-hand side of Equation [12] was compared and shown as

$$-\frac{\partial C_A}{\partial t} = R_A \quad [13]$$

which is just the kinetic expression for the rate of disappearance of A.

One-Dimensional Heat Conduction

Most molded parts are thin in one dimension, so heat transfer could be reduced to that for a slab.

Model

The most general treatment of the problem of transient heat conduction, including nonuniform and variable heat generation in the conducting body can be represented (46) as

$$\rho C \frac{\partial T}{\partial t} = \nabla \cdot k_T \nabla T + G(x, y, z, t) \quad [14]$$

where G is a function representing that part of the temperature change with time which is due to the generation of heat within that element of the curing mass.

In this work, only temperature gradients perpendicular to the mold walls, i.e., the y -direction, were considered to be significant. Thus, the energy equation reduces to

$$\rho C \frac{\partial T}{\partial t} = \frac{\partial}{\partial y} \left(k_T \frac{\partial T}{\partial y} \right) + G(y, t) \quad [15]$$

where ρ is resin density, C is specific heat, and k_T is thermal conductivity.

The volumetric internal heat generation rate, $G(y,t)$, was assumed to be proportional to the curing reaction rate. That is,

$$G(y,t) = \rho \Delta H_R \frac{\partial P(y,t)}{\partial t} \quad [16]$$

where ΔH_R is the total heat release per unit mass of resin and P is the fraction polymerized.

The rate of polymerization can be represented as

$$\frac{\partial P}{\partial t} = kf(P) \quad [17]$$

where k is the rate constant and $f(P)$ is a function to be determined to represent the amount reacted and order of reaction.

It was assumed that the reaction followed the Arrhenius relationship:

$$k = Ae^{-Ea/RT} \quad [18]$$

Thus, a mathematical model of the curing process was defined as

$$\rho C \frac{\partial T}{\partial t} = \frac{\partial}{\partial y} (k_T \frac{\partial T}{\partial y}) + \rho \Delta H_R Ae^{-Ea/RT} f(P) \quad [19]$$

$$\frac{\partial P}{\partial t} = Ae^{-Ea/RT} f(P) \quad [20]$$

The solution (temperature and concentration profiles) of the above differential equations can be obtained by applying numerical techniques and methods, and by using the necessary initial and boundary conditions.

The thermal properties, density, heat of reaction, and the constants of the kinetic expression are the major input parameters for a computer calculation.

Initial and boundary conditions can be defined as:

Homogeneous initial conditions

$$T(y,0) = T_0$$

$$P(y,0) = 0$$

Boundary Condition: 1 (Symmetry about $y = 0$)

$$\frac{\partial T}{\partial y} (0,t) = 0$$

$$\frac{\partial P}{\partial y} (0,t) = 0$$

A second boundary condition can be defined according to the specified processing conditions.

Boundary Condition: 2

(a) For the case of an isothermal wall case

$$T(L,t) = T_W$$

(b) For the case of a constant wall heat flux

$$\frac{\partial T}{\partial y} (L,t) = q$$

(c) For the case of an adiabatic process

$$\frac{\partial T}{\partial y} (L,t) = 0$$

V. RESULTS AND DISCUSSIONS

In the first part of this section, the experimental results are presented and discussed. In the second part, an application of the proposed mathematical model to a typical polyester casting process is shown with the comparison of experimental and simulated results.

Experimental Results

Experimental Temperature Profiles

A fast and accurate analysis of the temperature variations in the polymer mass during the curing process have been successfully achieved with the aid of PDP-11 computer routines.

For preliminary studies, the temperature changes have been measured by locating the thermocouples at different positions along the polymer thickness. Thus, the optimum number of thermocouples and the most appropriate spacing between them were selected to obtain the most informative data on the temperature profile. Figure 5 shows the best location for the thermocouples in polymerizing mass.

The geometry and the heat flow characteristics of the bottom and top sections of the mold were identical. A check of the conduction effects from those boundaries was made by placing thermocouples along both sides of the center plane. The temperature profiles thus obtained from those measurements verified the assumption of symmetry about the central plane (Figure 10).

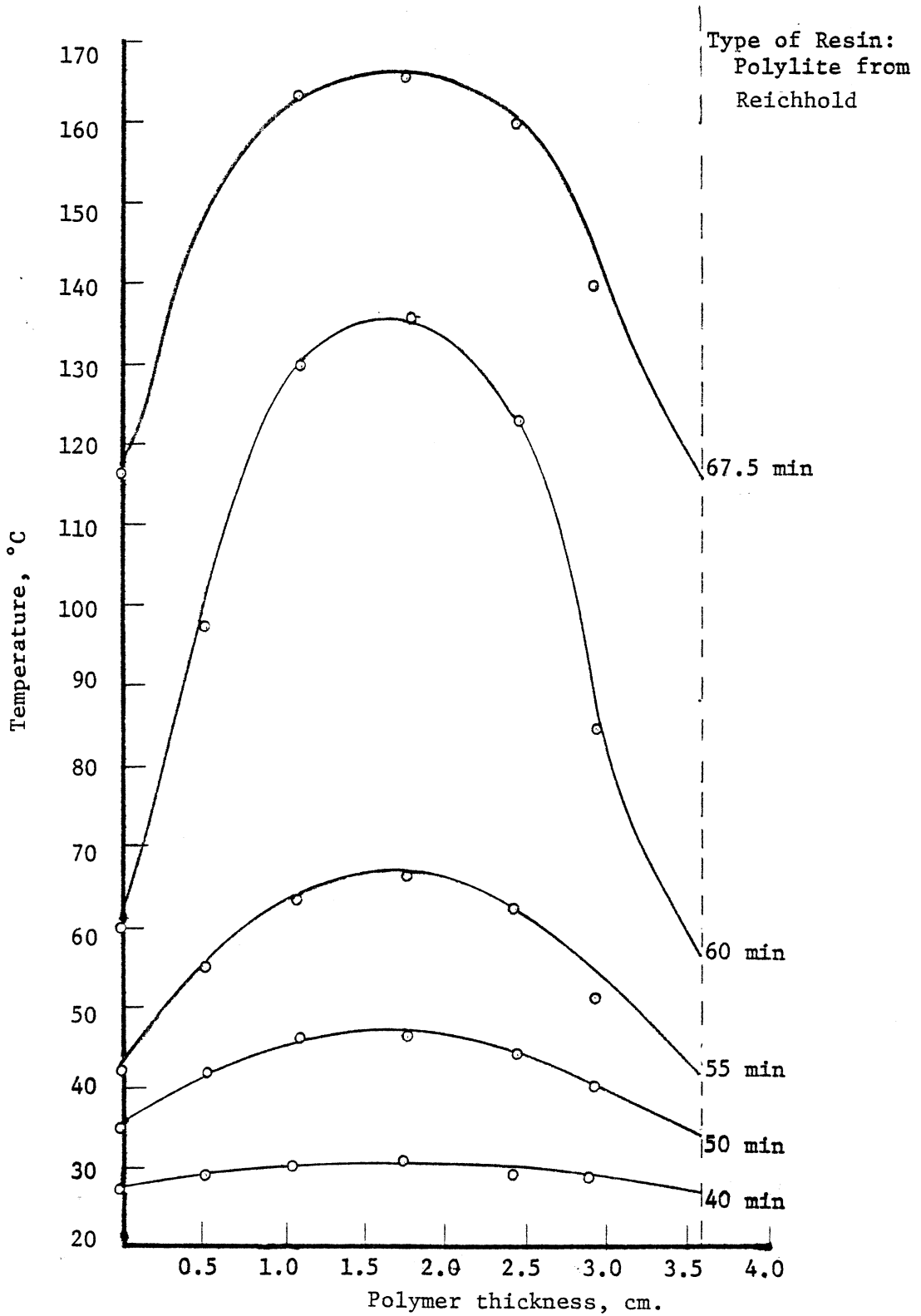


Figure 10. Temperature profiles.

In the first measurements, output values of the thermocouples were read at time intervals of 3 seconds. Later the speed of the data acquisition was increased and the program took eleven points on the same channel at smaller time intervals, averaged them, and presented this averaged value at the end of each 5 seconds (Table 3).

As expected, the polymerization reaction was faster at the center of the curing mass, and it slowed toward the surfaces as the result of the heat flow from the mold walls. Because of the low conductance of silicone rubber mold, larger temperature gradients were observed near these surfaces.

Reaction began about 150 seconds after the data acquisition was started as was observed by merely watching the change of the computer output on the screen.

Figure 11 shows the exotherm curves that have been obtained at different positions in the curing polymer mass. The polymer at the center reached its maximum temperature, 177°C, in 21.7 min. The surface temperature at this time was recorded as 90°C, and it reached its peak temperature, 136°C, with a 100 to 120 second time delay. The polymer started to cool after the heat generation due to reaction was complete. The observed cooling curves are also included in Figure 11.

The experimental temperature profiles as a function of polymer thickness at different stages of curing are presented in Figure 12.

Residual Stresses

The temperature variation at different locations within the polymer during the cure cycle is very significant in view of the

TABLE 3
EXPERIMENTAL TEMPERATURE MEASUREMENTS

$T_i = \text{Thermocouple}_i \text{ (}^\circ\text{C)}$

Time, sec.	T_1	T_2	T_3	T_4	T_5
100	29	29	29	29	29
150	29	29	29	30	29
250	29	30	30	30	30
350	29	30	31	31	31
450	30	30	32	32	32
550	31	32	34	33	33
650	32	33	36	36	36
750	33	36	39	39	39
850	36	39	44	44	43
950	38	44	50	52	50
1050	42	51	60	64	60
1150	48	61	79	86	80
1250	58	82	123	151	129
1350	88	155	176	177	174
1450	135	162	175	176	174
1550	129	155	174	176	174
1650	124	148	170	175	171
1750	121	144	167	173	168
1850	120	140	163	171	165
2450	116	130	148	155	149

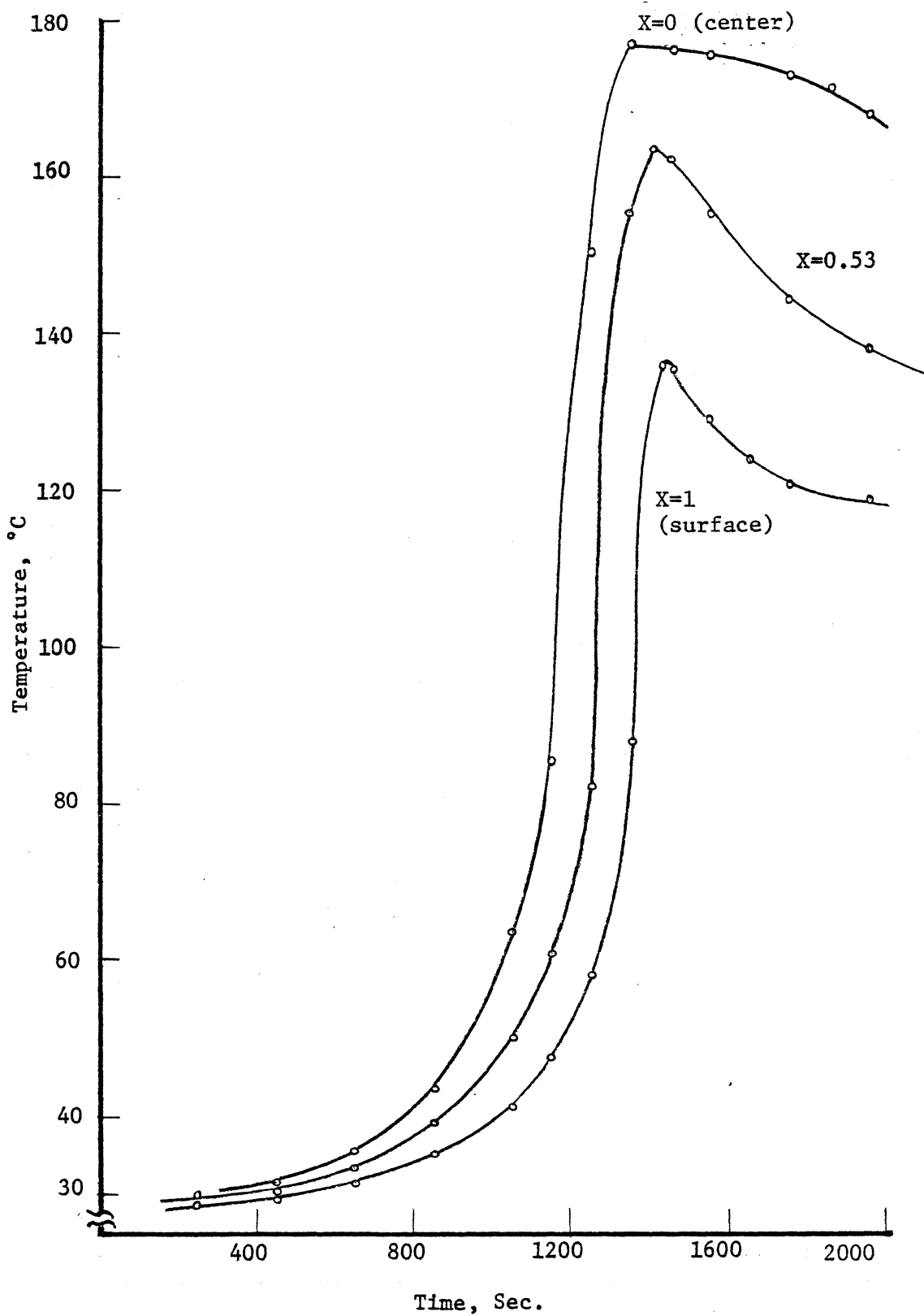


Figure 11. Experimentally determined temperatures at different locations in curing polymer.

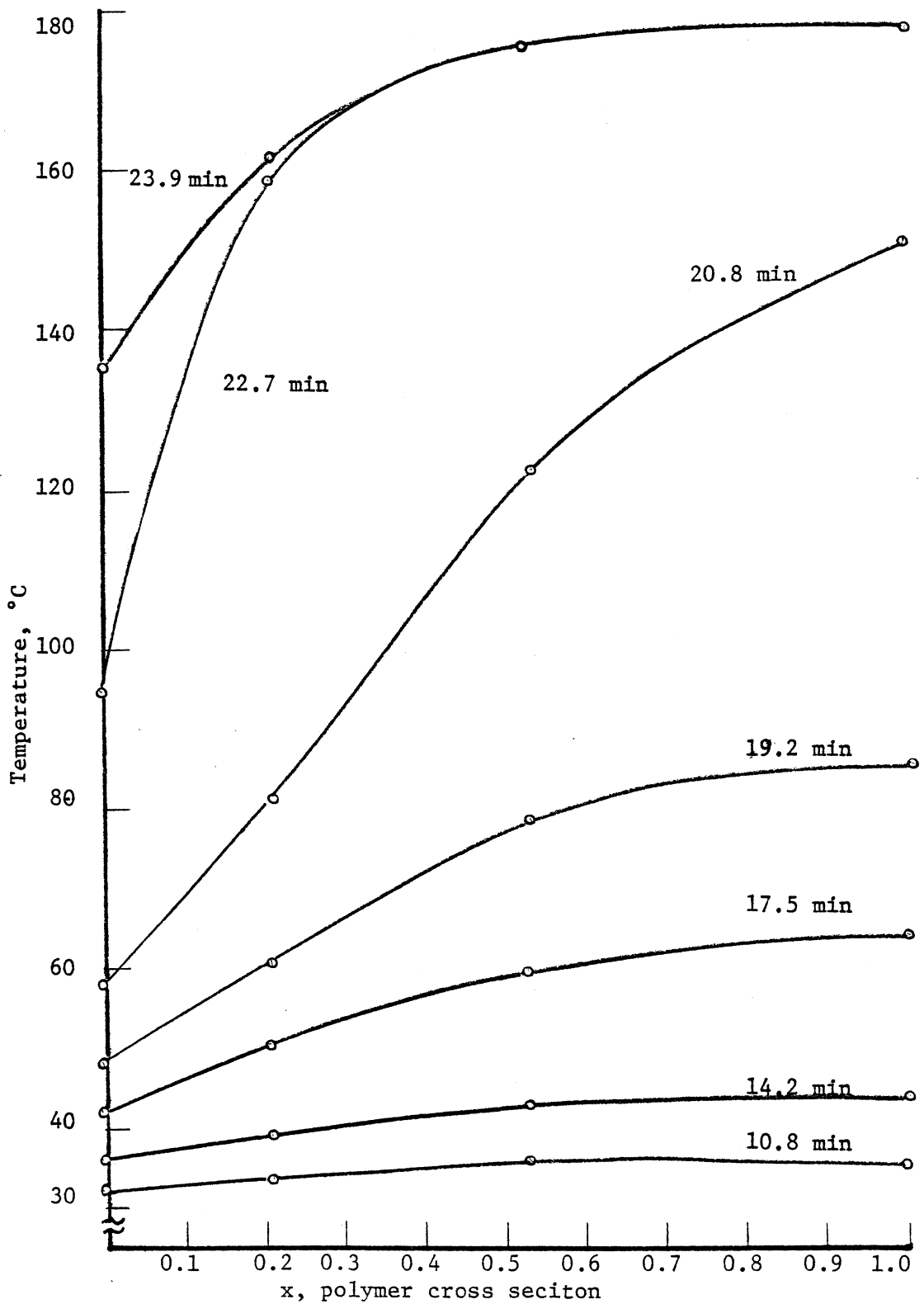


Figure 12. Experimentally determined temperature profiles (Here $x=1.0$ represents center of curing polymer).

process design and the desired applications of these polymers. The exothermic temperature differences between the various sections of the piece generate stress gradients of considerable magnitude. These stresses depend largely upon the highest temperature reached during the cure in any given section of the piece. As the result of the thermal contraction due to cooling and the shrinkage due to curing, thermal residual stresses are developed in molded article which may remain in the product indefinitely. This is usually a disadvantage since such stresses may lead to eventual deficiencies, such as cracking, crazing and delamination of the article.

In order to show that some residual stresses could exist in a molded piece, birefringent patterns in those pieces were visually observed using a polariscope. Typical pictures are presented in Figures 13-16. Each band (black and white) in those photographs corresponds to the locus of points with a constant principal stress difference. As it is seen, the number of birefringences increases near the surfaces which indicates the existence of residual stresses that were developed at those sections as a result of the polymerization reaction.

Thermal Conductivity

Thermal conductivity measurements of cured polyester samples were determined after they had been post-cured at 90°C for 3 hours. This was necessary to prevent any further post-curing during the measurements themselves. Measurements at different temperatures were

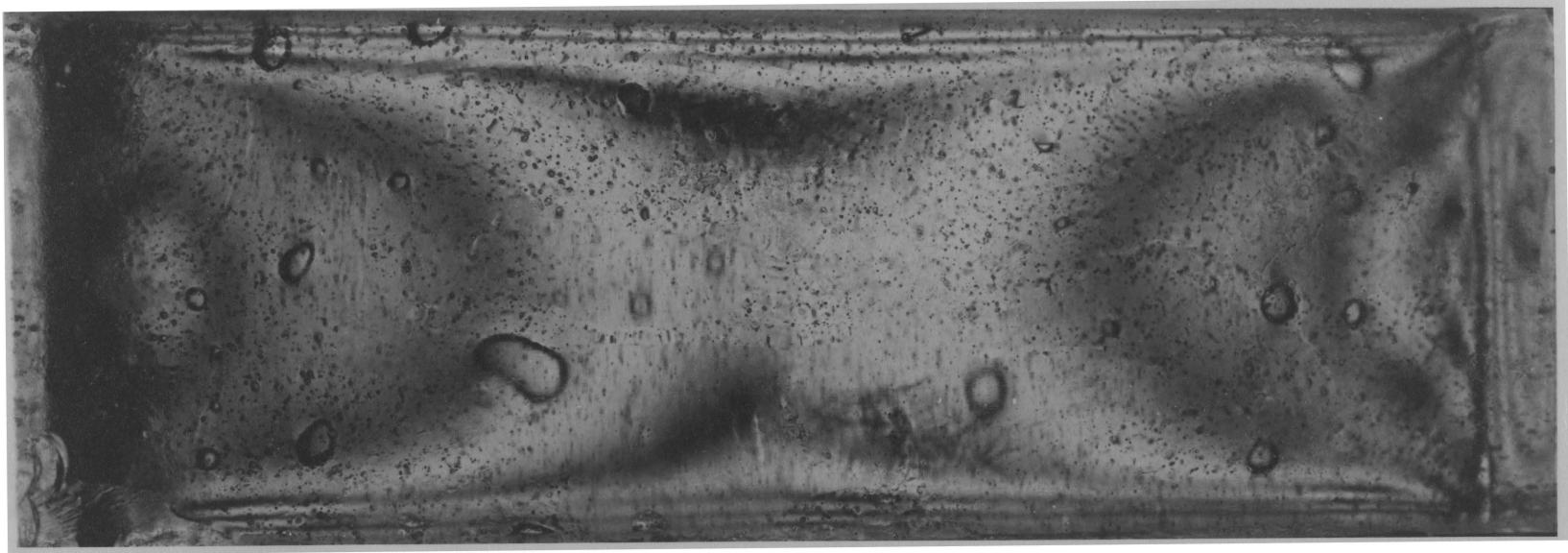


Figure 13. Birefringent patterns of a cured specimen (top view).

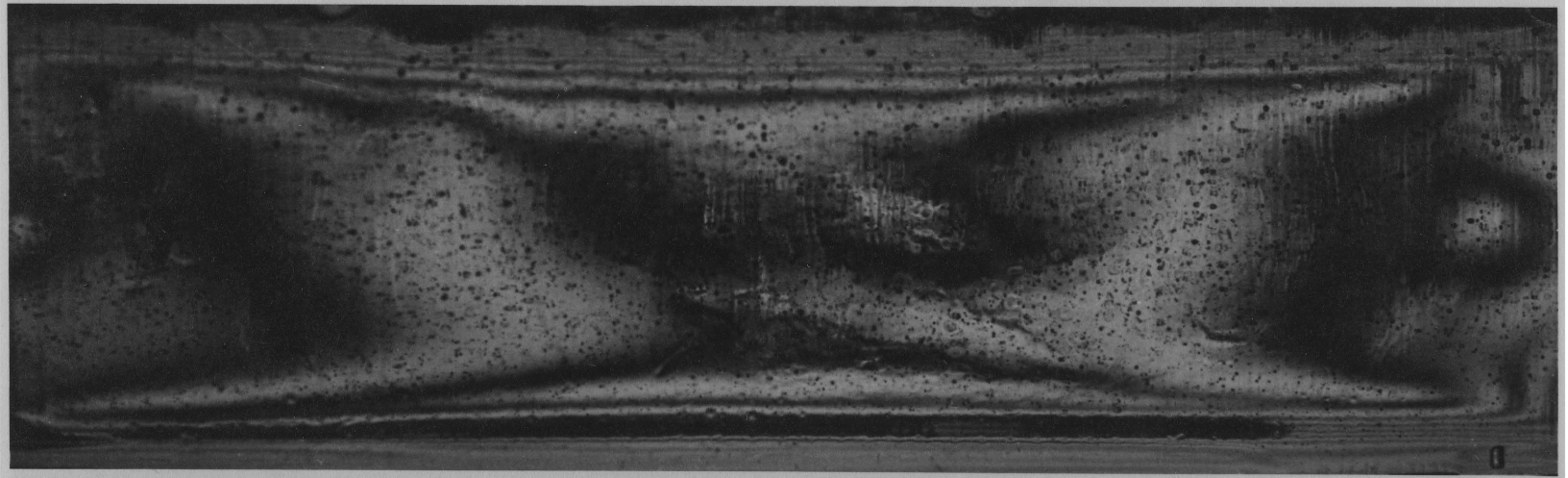


Figure 14. Birefringent patterns of a cured specimen (side view).

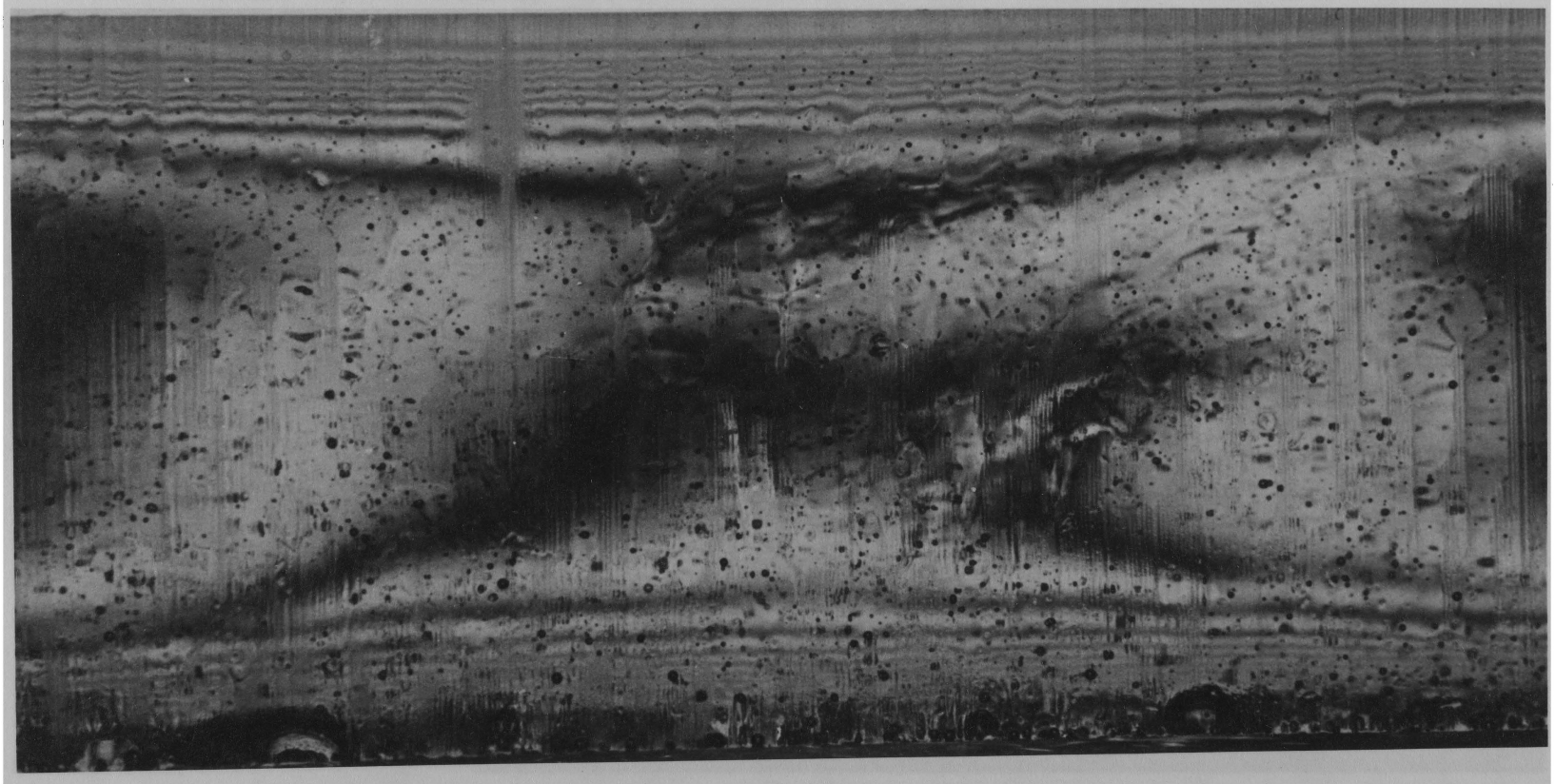


Figure 15. Birefringent patterns of a cured specimen (side view).

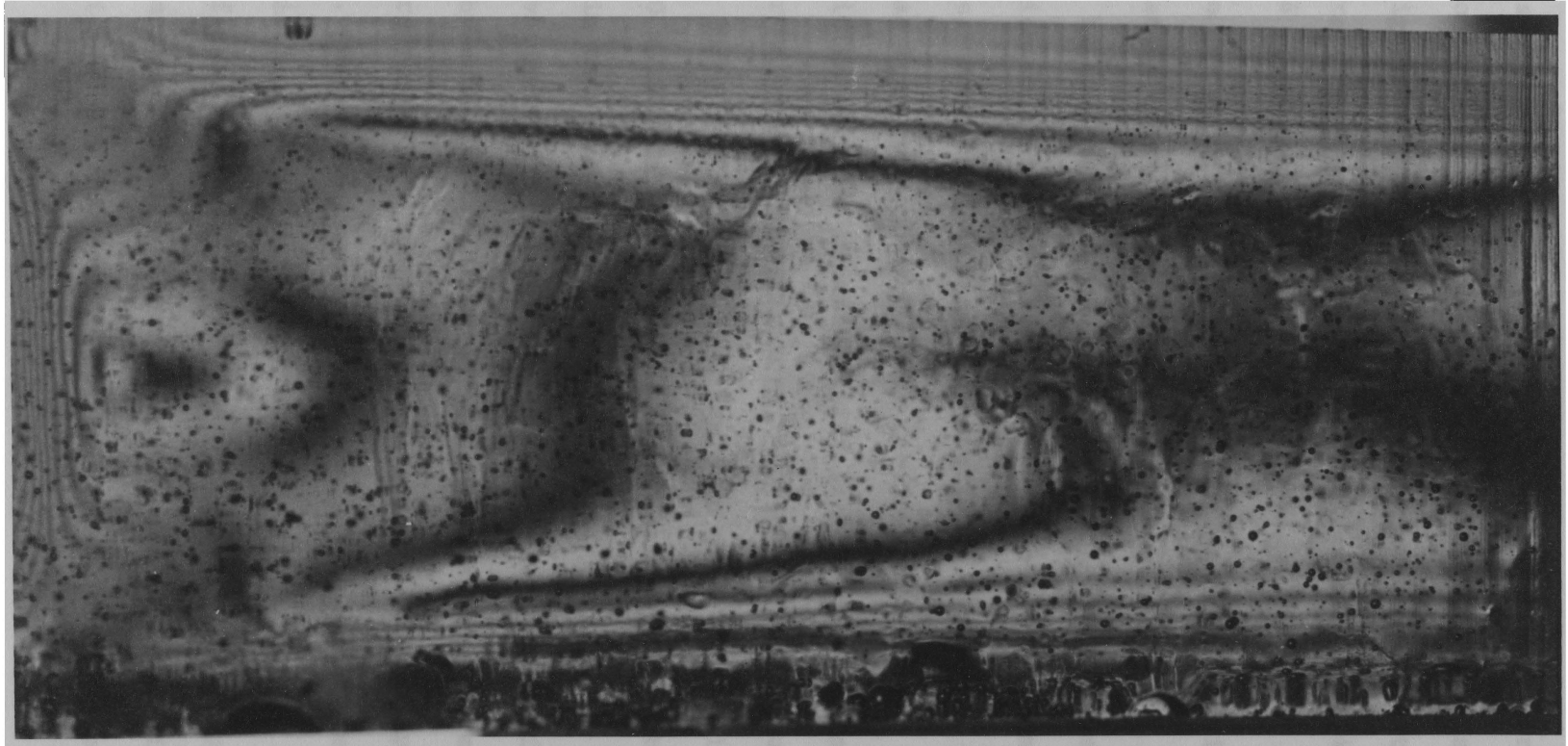


Figure 16. Birefringent patterns of a cured specimen (side view).

repeated at least twice in order to obtain reproducible results. Thermal conductivity of cured polyester is plotted against temperature in Figure 17. A linear increase in conductivity with increasing temperature from a value of 4.5×10^{-4} cal/cm-sec-°C at 40°C to 5.0×10^{-4} cal/cm-sec-°C at 94°C was observed.

There are no previous data on the thermal conductivity of thermoset polyesters over a large temperature range, and hence these results could not be compared with other conductivity data. However, the values which were presented as a result of this work seemed to be reasonable. Most of the thermal conductivity studies on crosslinked systems has been conducted on epoxy resins, and a linear increase in conductivities of these materials with increasing temperature have been observed by most investigators (47, 48). Thermal conductivity of a typical cured polyester at 25°C has been given in the literature as $4.0-5.0 \times 10^{-4}$ cal/cm-sec-°C (1) which agreed well with the values obtained in this work.

The variation of thermal conductivity with degree of cure was observed by studying fresh and partially cured resins over the temperature range in which the measurements on cured samples were performed. For those measurements a new sample system was developed for an existing instrument as has already been explained in a previous section of this thesis. It was also necessary to develop a new method of calculation for these measurements because of the additional complication of the new sample system. The Colora Thermoconductometer

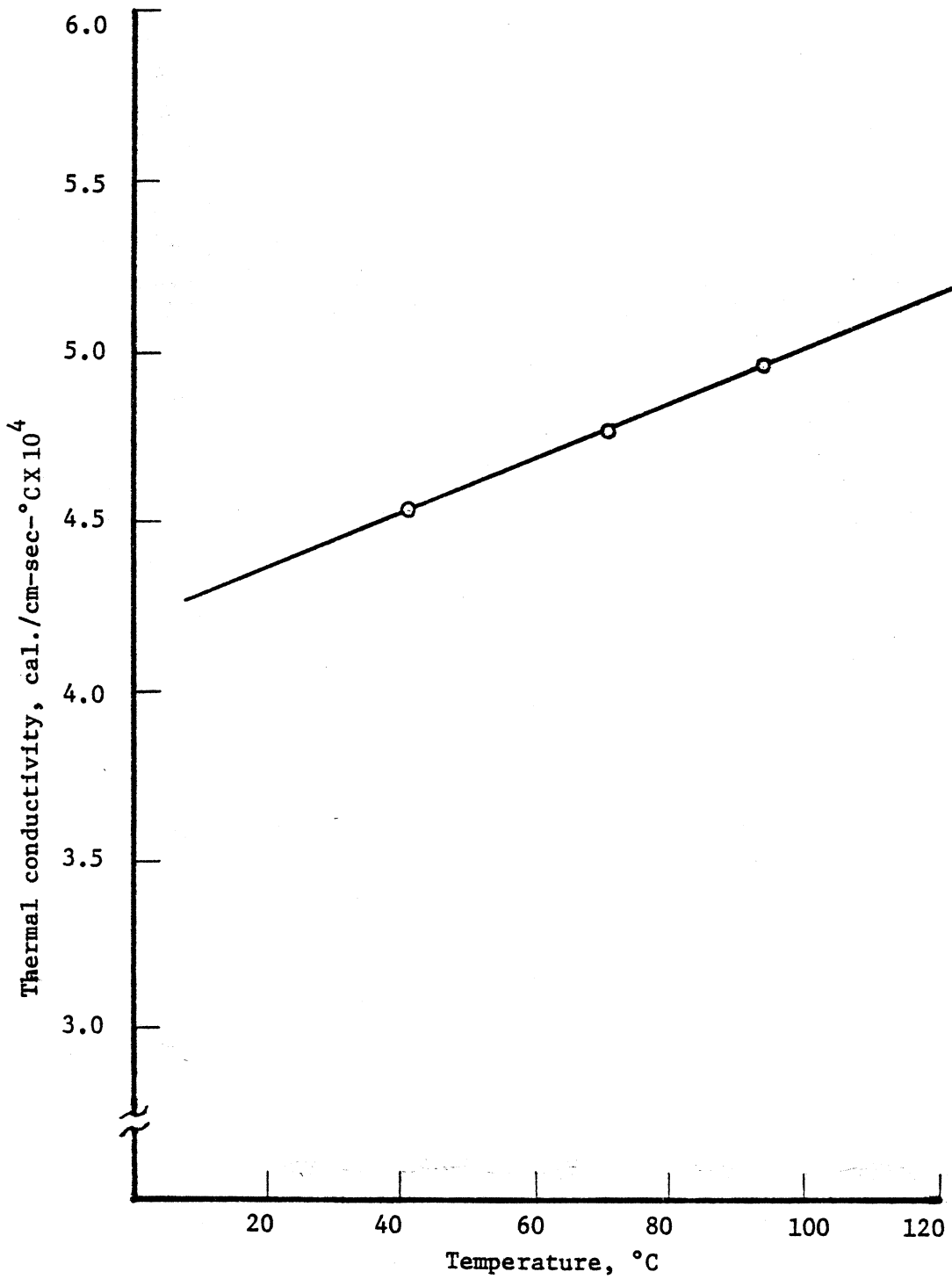


Figure 17. Thermal conductivity of cured polyester.

was basically designed for measurements on solids, and its original sample system contained only the test material. However, in the new system developed in this work, the conducting sample system contained two different materials. In order to hold the uncured and partially cured resins between the two silver plates (Figure 8) and to prevent their flow, the samples were embedded into cylindrical rings which were prepared from a cured polyester product. Therefore, the measured resistance of the total sample system, R_S , involved the thermal resistances of the embedded material, R_M , and the ring, R_K . Since the surfaces of the sample were most effectively kept at constant temperature through heats of evaporation of liquids, the entire cylindrical surface was maintained at a fixed temperature, the radial heat losses were considered to be negligible, and then each surface plane of the sample was isothermal. Since the embedded materials were highly viscous, it was also assumed that the convective effects were negligible.

Consequently, the conductances, $1/R_M$ and $1/R_K$, of the two materials were additive, and then

$$\frac{1}{R_S} = \frac{1}{R_M} + \frac{1}{R_K} \quad [21]$$

With the known values of thermal conductivity, cross sectional area and height of the ring, the resistance of the ring, R_K , was calculated from

$$R_K = \frac{h}{k_T \cdot A} \quad [22]$$

From the measured resistance of the total sample system, R_S , and the calculated resistance of the ring, R_K , the thermal resistance, R_M , of the embedded material was predicted using Equation [21]. That is,

$$R_M = \frac{R_S \cdot R_K}{R_K - R_S} \quad [23]$$

The results of these measurements were given in Table 4. For the purpose of comparison, the values of the cured samples were also included in that Table.

Although the results obtained in this work were not sufficient at this time to show a complete relationship of thermal conductivity to both temperature and degree of cure, they suggest that the conductivity increased with increasing temperature and presumably with degree of cure.

The reactive nature of these materials and the combination of physical and chemical changes that accompany the curing process contributes to the experimental difficulties in measuring conductivity. Actually, the commonly used steady-state techniques are not particularly suited to measuring the thermal conductivity of thermosetting polymers during their polymerization. The prolonged maintenance of a significant temperature gradient in the test sample during the crosslinking reaction creates several problems, and all of these competing effects make it very difficult to correlate the results. Therefore, it is necessary to develop some new techniques and methods for these

TABLE 4
THERMAL CONDUCTIVITY DATA

Sample	Thermal Conductivity, 10^{-4} cal/sec-cm- $^{\circ}$ C		
	40.5 $^{\circ}$ C	70.6 $^{\circ}$ C	93.5 $^{\circ}$ C
Uncured	2.5-3.0	4.9	4.5
Partially cured	4.5	4.6	3.7
Cured	4.5	4.8	5.0

measurements. Very recently, some preliminary work in developing a unique apparatus for those measurements has been reported by Sourour and Kamal (49).

Heats of Polymerization and Kinetic Model

Heats of Polymerization: Polymerization can be defined simply as the process of joining together small molecules by covalent bonds. During a vinyl addition polymerization process the conversion of a double bond to a single bond is accompanied by an exothermic heat of polymerization. Removal of this heat often limits the rate at which the reaction can be carried out. Measurement of the heat of polymerization as a function of time and temperature by using a differential scanning calorimeter has been seemed to be the most useful technique for purposes of this study.

It was assumed that the exothermic heat of curing of the polyester came from the following reactions: (1) the propagation reaction of free-radical crosslinking of the styrene monomer with a reactive double bond of the unsaturated polyester; and (2) the decomposition reaction of the peroxide initiator, the heat of which was negligible as compared to the heat from the crosslinking reaction.

It was also reasonably assumed that the exothermic heat generated per unit mass or volume during an isothermal cure was proportional to the number of double bonds reacted in that unit mass or volume. Thus,

the measurement of the heat evolved at any time was a direct indication of the degree of cure (extent of reaction) of the sample at that instant.

The fraction of double bonds reacted during the cure reaction, or the relative degree of cure, P , was defined as

$$P = \frac{Q_t}{Q_T + Q_S} \quad [24]$$

where Q_t was the cumulative heat of reaction which was evolved isothermally when the sample was taken from its initial unreacted state to that at time, t ; Q_T was the total heat of reaction that was measured at the end of an isothermal run and Q_S was the heat evolved due to the residual isothermal reactivity of the sample at temperature T . Q_S was determined by heating the sample above its isothermal cure temperature until no exotherm was observed. $(Q_T + Q_S)$ represented the maximum possible heat of cure at an initial isothermal cure temperature. This quantity could not be easily measured by a single isothermal run, because the reaction became highly diffusion controlled at advanced stages of cure and a very long time was required to reach completion under isothermal conditions.

Table 5 presents the calculated isothermal heats of reaction at different temperatures. They were also plotted against cure temperature and shown in Figure 18. Isothermal heat generation as a function of time at different temperatures is shown in Figure 19.

TABLE 5
ISOTHERMAL HEATS OF REACTION

T (°C)	Q _T (Cal/gm)	Q _S (Cal/gm)	[Q _T + Q _S]
82	42.1	10.2	52.3
93	47.9	6.6	54.5
105	51.4	4.6	56.0
122	63.5	1.6	65.1

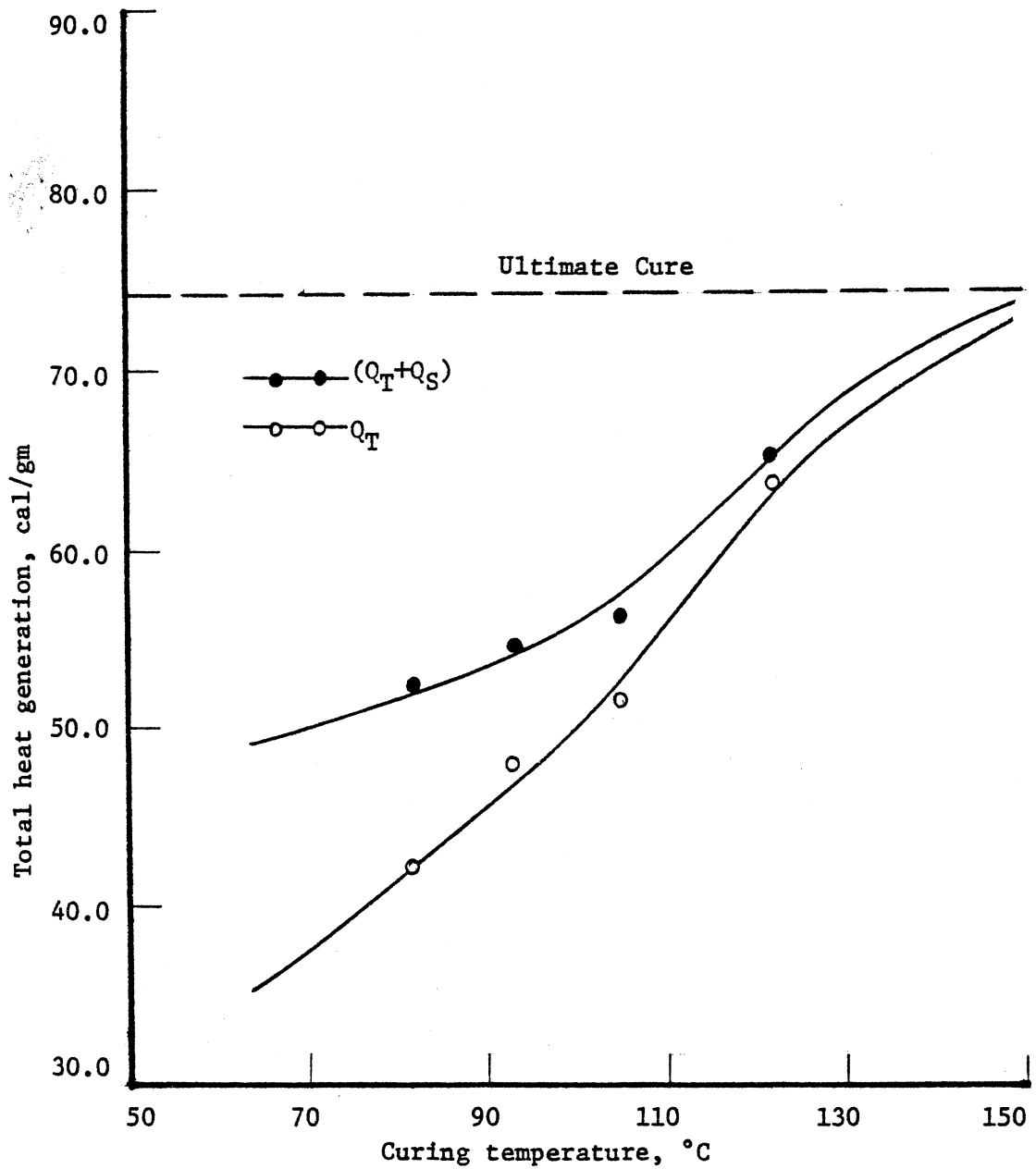


Figure 18. Total heat generation vs. curing temperature.

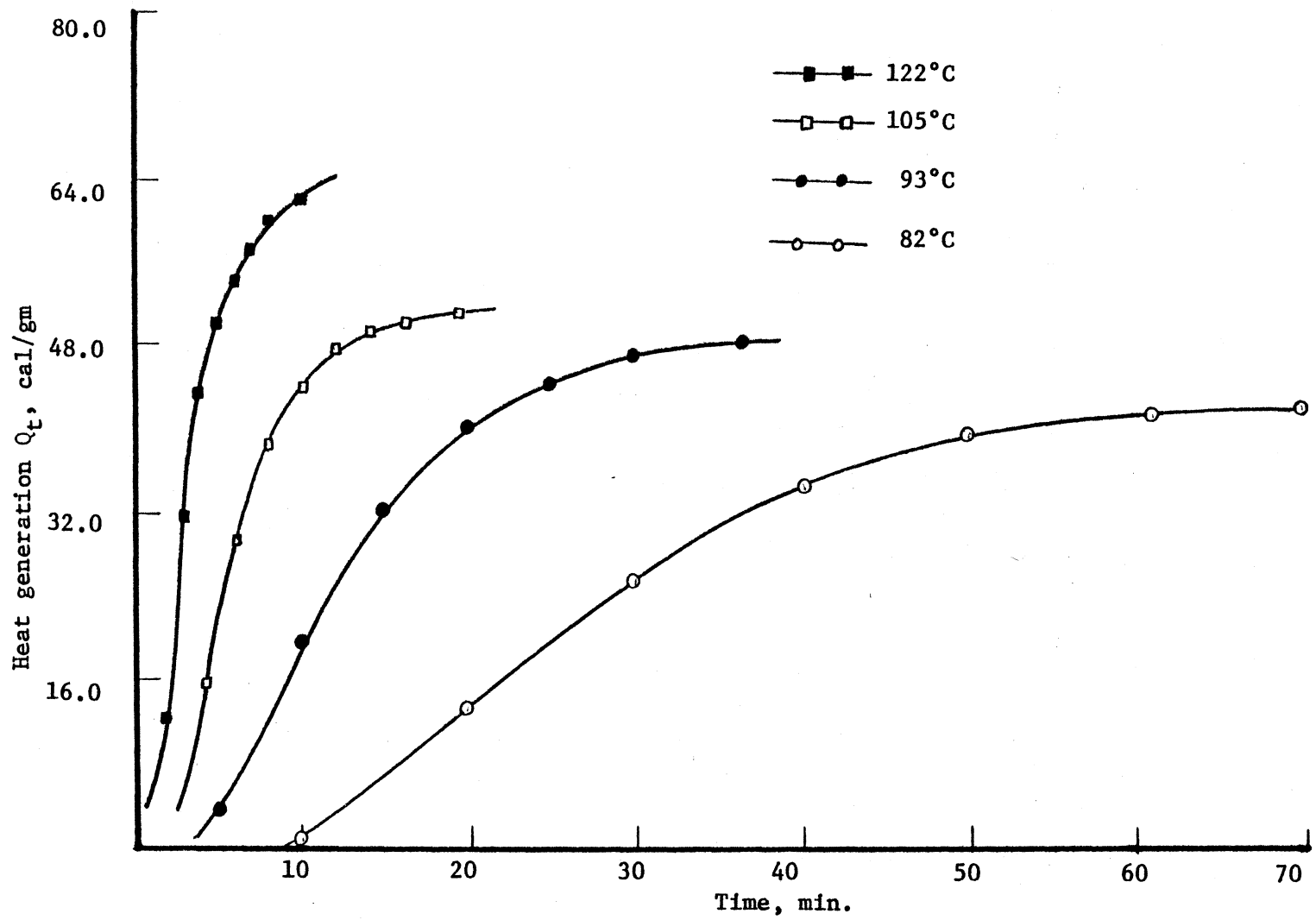


Figure 19. Cumulative heat evolution during isothermal cure.

It was concluded from the isothermal data that the reaction became faster (Figures 20 and 21) and the rate of heat generation increased with increasing temperature.

Ultimate Heat of Cure: In addition to these isothermal studies, the ultimate or maximum heat of cure was measured by scanning a sample at a constant heating rate from room temperature until no further reaction was evident. The final exotherm temperature of the sample at the end of such a measurement was 175-180°C (Figure 22), and the ultimate heat of cure was predicted as 73.90 ± 0.60 cal/g (Figure 18). This value agreed well with the values reported by the previous investigators (Table 6).

Kinetic Model: Figures 23 and 24 show the extent of reaction, P, as a function of time at different temperatures. Experimental curves of rate of reaction as a function of time have been obtained by using the relation

$$\frac{dP}{dt} = \frac{1}{Q} \left(\frac{dQ}{dt} \right)_T \quad [25]$$

where $\frac{dP}{dt}$ is the rate of reaction, and $\frac{dQ}{dt}$ and Q represent the rate of heat evolution and total heat of reaction at temperature T, respectively.

A mathematical expression for the polymerization reaction which could fit all of the experimental data has been developed from studies of different proposed kinetic models (17, 34, 35). In previous studies, it was difficult to predict the kinetics beyond the gel

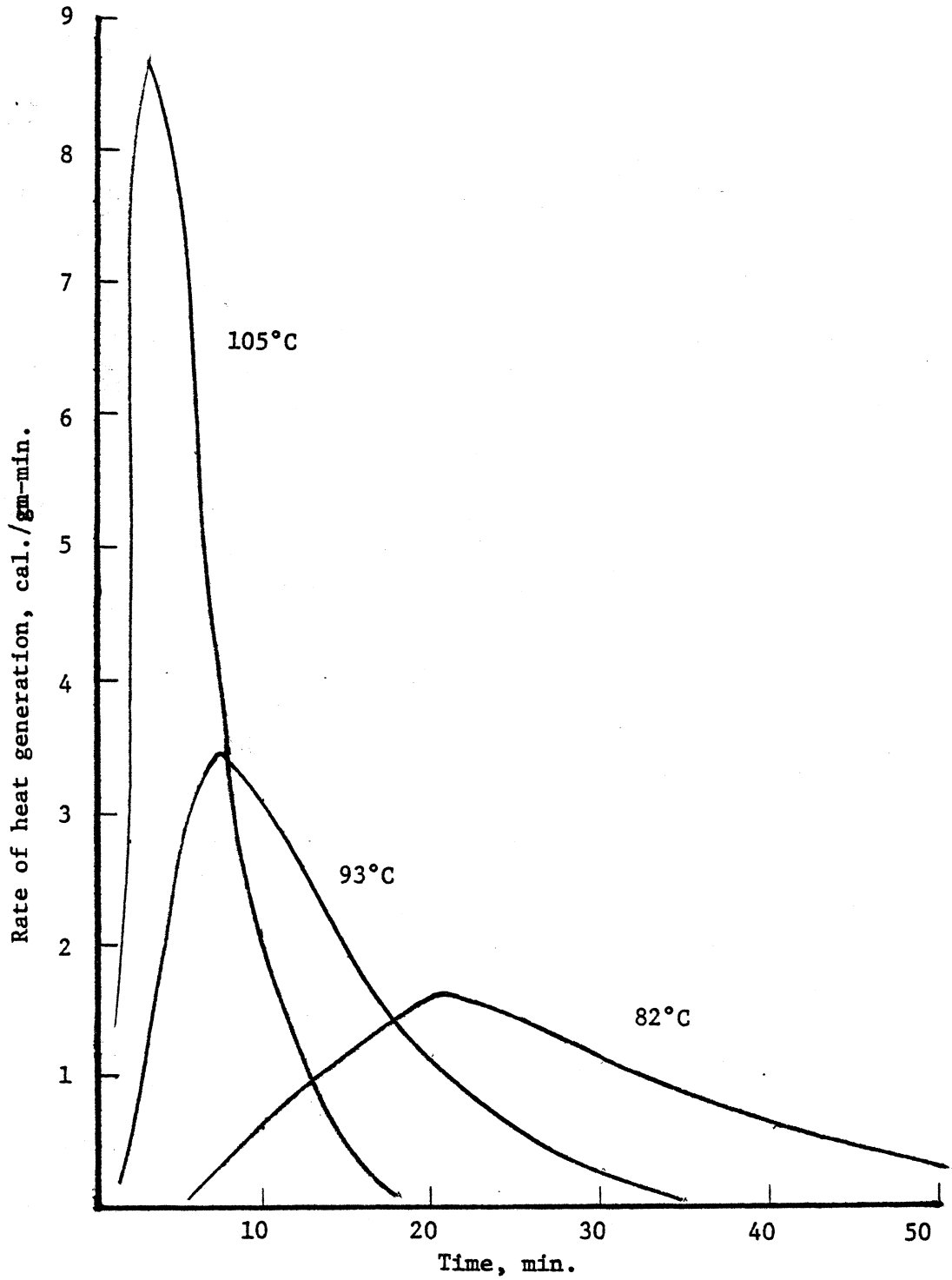


Figure 20. Rate of heat generation for isothermal cure.

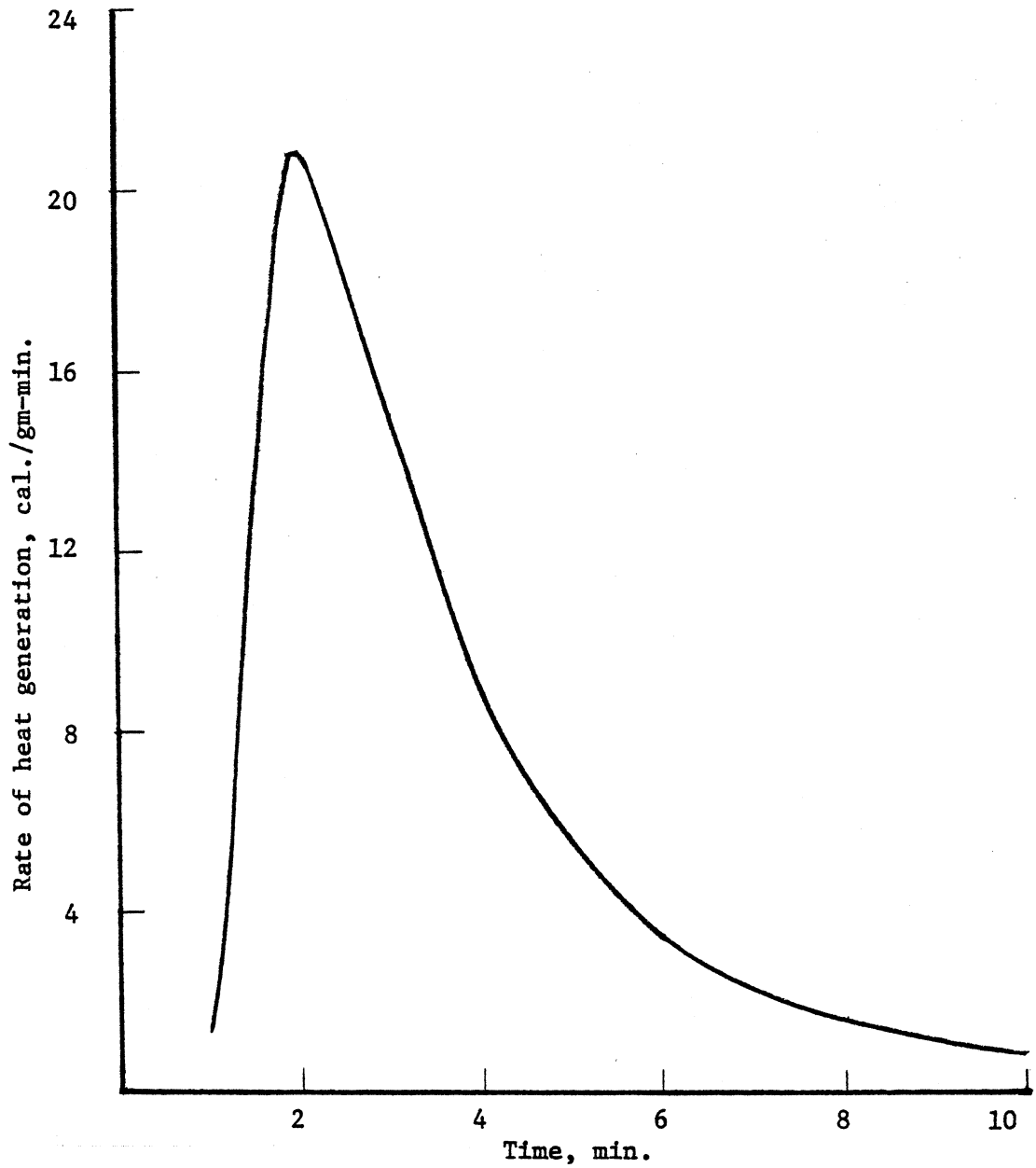


Figure 21. Rate of heat generation for isothermal cure at 122°C.

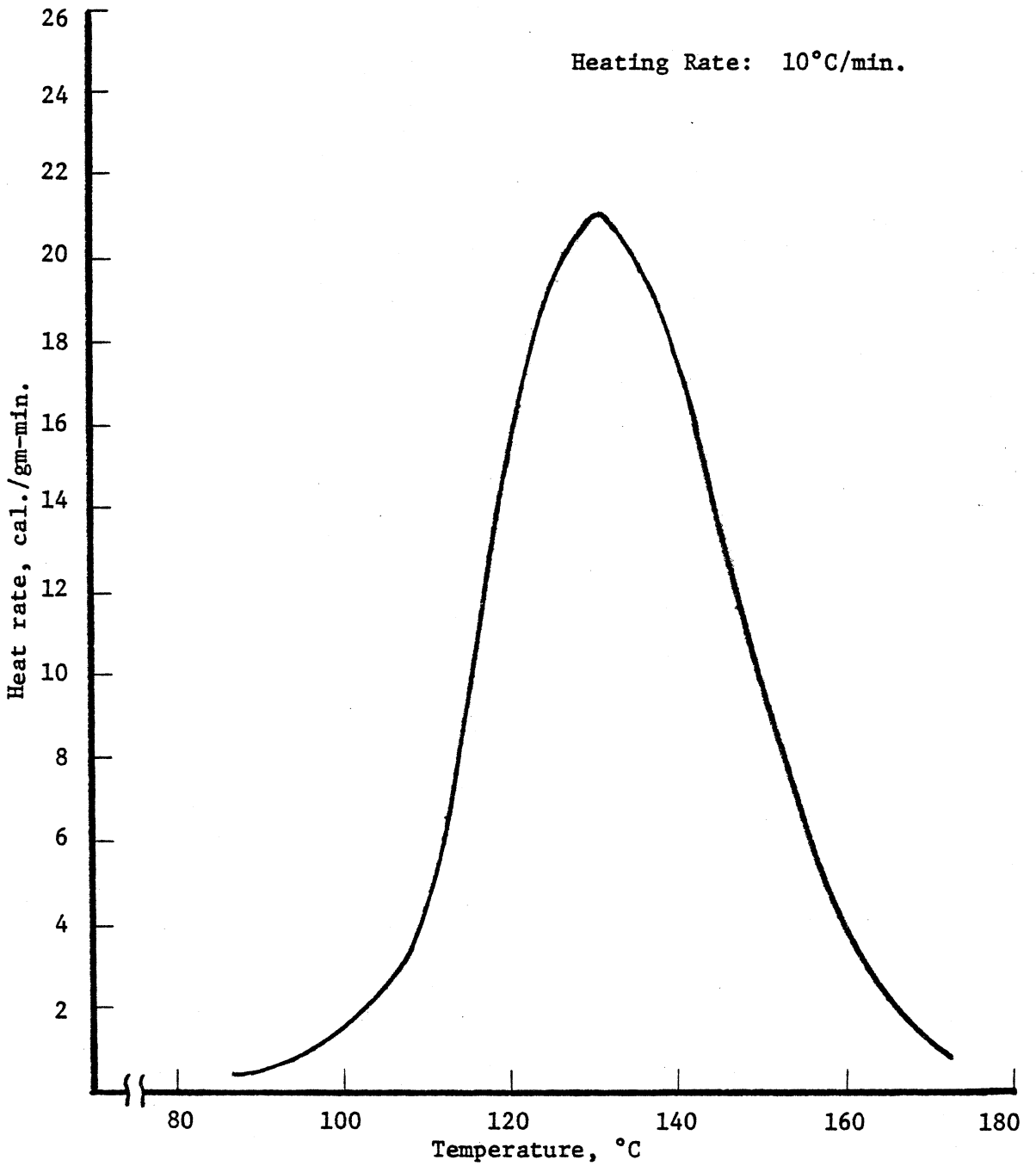


Figure 22. Experimental rate of heat generation during scanning.

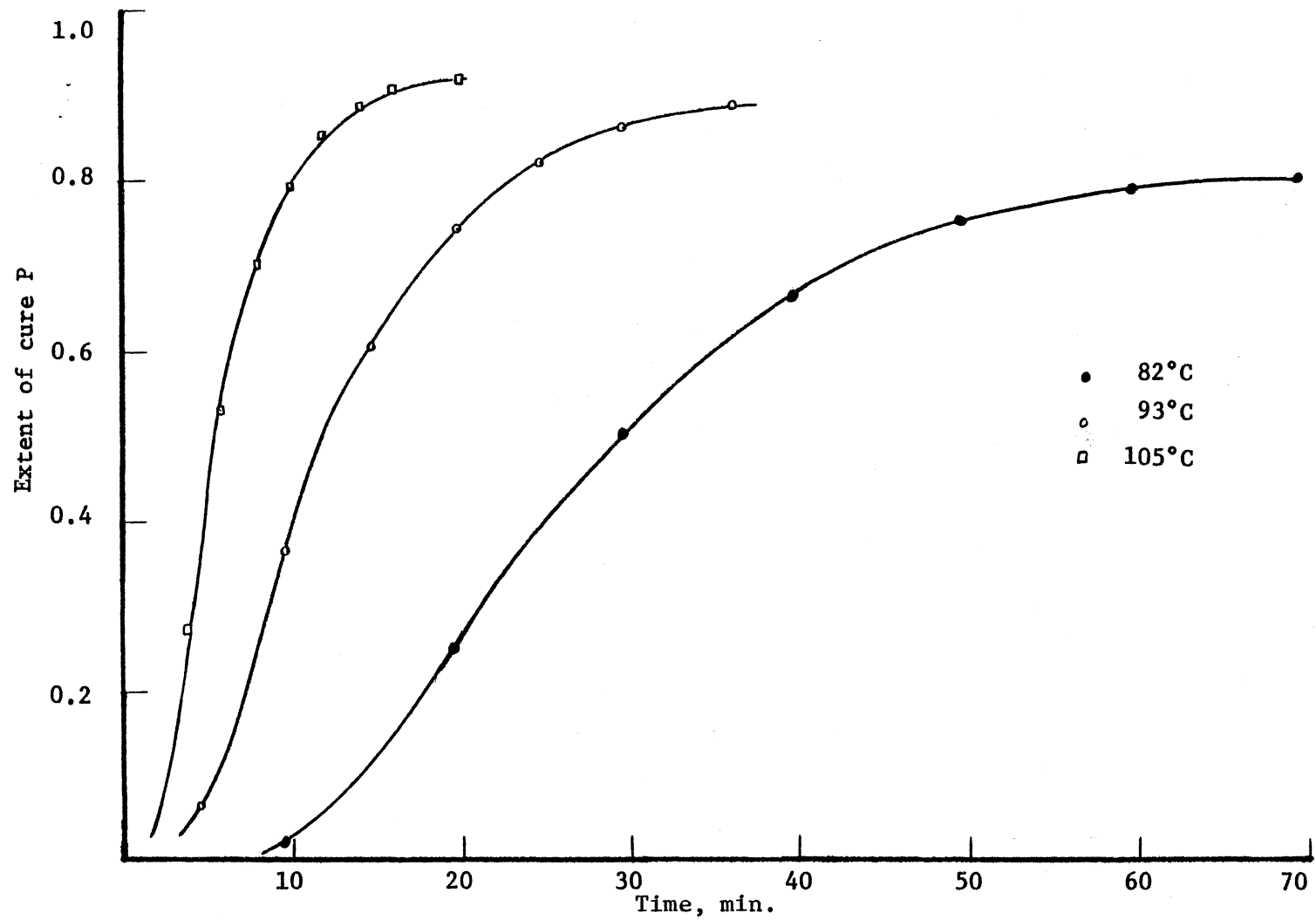


Figure 23. Extent of reaction during isothermal cure.

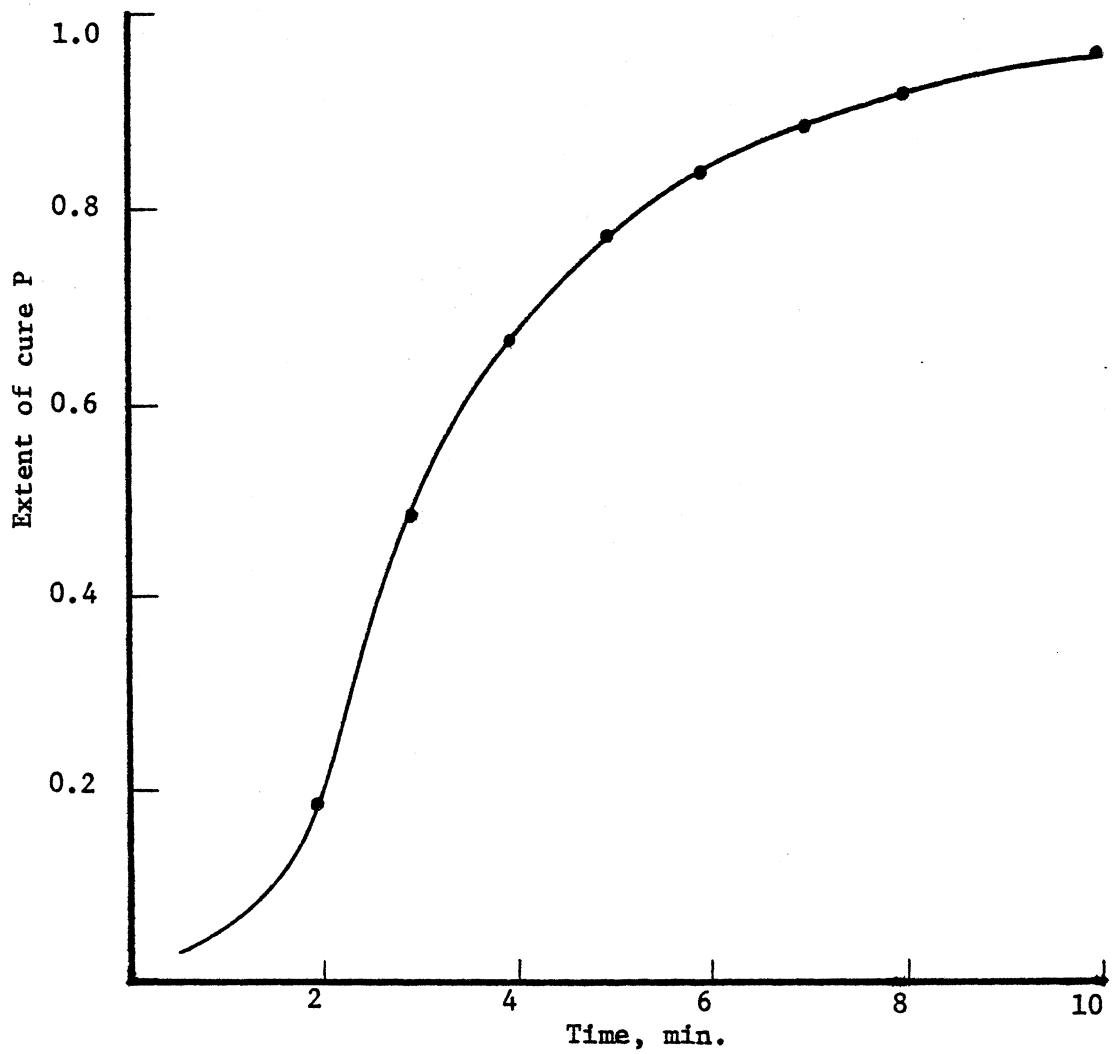


Figure 24. Extent of reaction during isothermal cure at 122°C.

TABLE 6

RESULTS OF THE CURING STUDIES REPORTED BY SEVERAL INVESTIGATORS

	M. R. Kamal and S. Sourour (17)	M. R. Kamal S. Sourour and M. Ryan (36)	H. Kubota (52)	K. Hori I. Mita and H. Kambe (35)	Present Study
Total heat of cure (cal/gm)	73 ± 2	83.0	99.5 (630 psi)	----	73.9
Rate constant (min ⁻¹)	2.39x10 ¹⁰ exp(-18,700/RT)	2.72x10 ⁹ (-17,400/RT)	----	----	2.60x10 ⁹ exp(-17,040/RT)
Activation energy (KCal/gmole)	18.7	17.4	----	18.5	17.0

point because of the lack of experimental data. Those studies included only a qualitative analysis of the results or suggested some models based on n^{th} order kinetics. Such models were not satisfactory, because they could not predict the maximum observed in the isothermal rate of reaction. Also, they did not satisfy the zero initial rate of reaction that was particularly evident at low temperatures. Therefore, a kinetic equation of the following form was used to fit these experimental data:

$$\frac{dP}{dt} = kP^a(1 - P)^b \quad [26]$$

where the parameters a and b were constants independent of temperature, and k was the rate constant. Dependency of the rate constant upon temperature was represented with an Arrhenius relationship

$$k = Ae^{-Ea/RT}$$

This proposed kinetic model was fitted to the experimental rate data using the computer and a multiple linear regression technique. The results are summarized in Table 7.

The Arrhenius plot for the predicted rate constants is shown in Figure 25 over a temperature range of 82-122°C.

The activation energy of 17.0 kcal/mole that was calculated from the model was very similar to earlier values reported for those systems (Table 6).

TABLE 7
PREDICTED KINETIC PARAMETERS

MODEL

$$\frac{dP}{dt} = A \exp(-E_a/RT) P^a (1-P)^b$$

a = 0.445

b = 1.500

$E_a = 17.04$ Kcal/gmole

$A = 2.60 \times 10^9$ min⁻¹

Multiple Correlation Coefficient: 0.9895

Number of Data Points: 38

Standard Error of Estimate: 0.0670

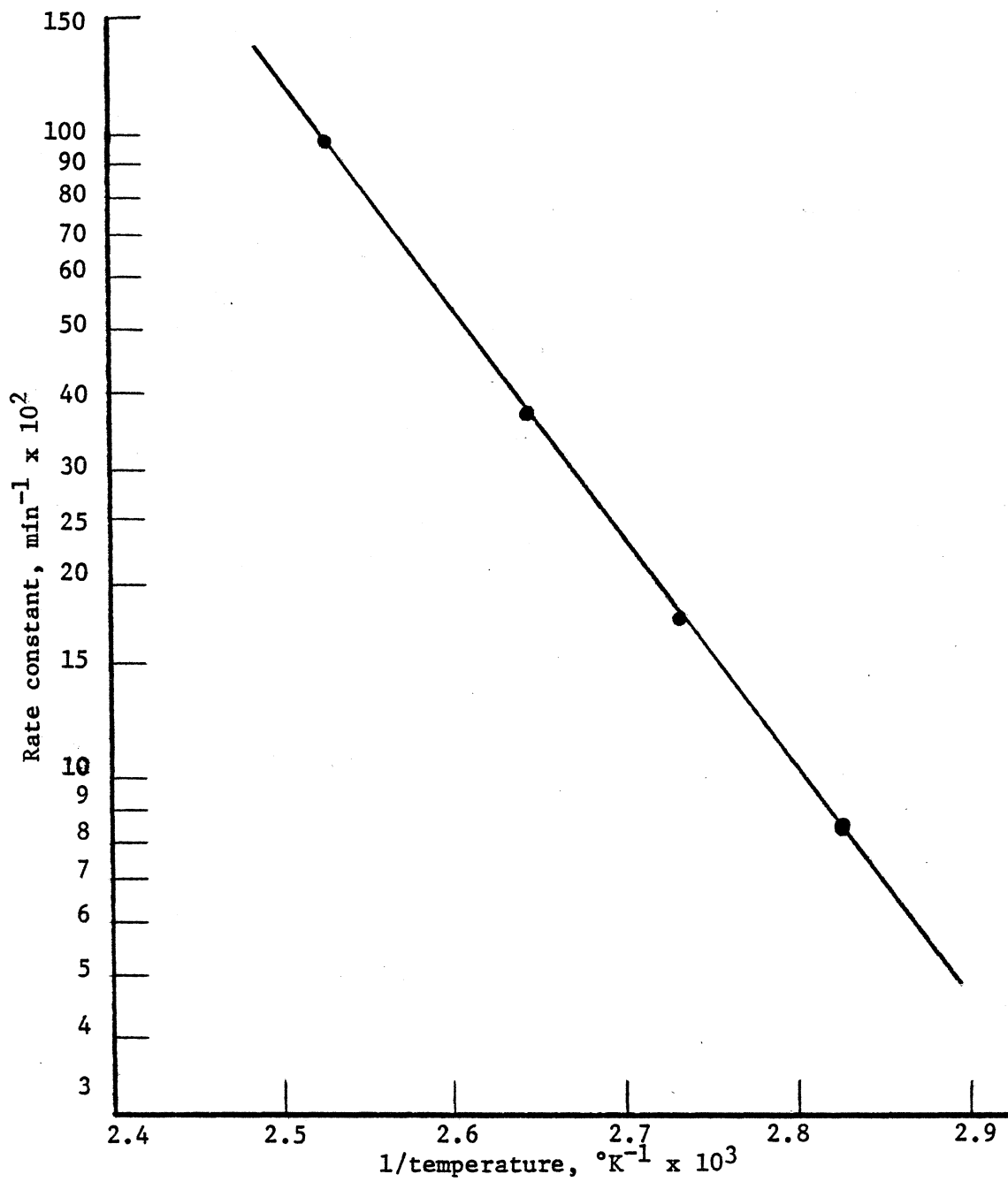


Figure 25. Arrhenius plot.

A comparison of the model-predicted and experimental rate data is shown in Figures 26-29. The agreement between those results was very satisfactory.

Specific Heat

The specific heat of cured polyester samples has been determined over the temperature range 60-180°C with an accuracy of about 1%, and the results are shown in Figure 30. A more or less linear increase in specific heat with increasing temperature between 60° and 120°C was observed, and the values of above 120°C did not change significantly.

Warfield and co-workers (50) have noted the existence of a possible glass transition at 126°C upon heating these materials. Only a limited amount of data are available in the literature concerning these transitions in thermosetting polymers, although these transitions are particularly significant because of their relationship to the mechanical and electrical properties of the polymer.

Studies to determine the existence of such transitions were then undertaken in this investigation, too. A slight change of slope near 120°C on the DSC heating curves suggested the probable existence of a second-order transition in this range. In the thermomechanical analysis (TMA) of the cured samples, one of the samples showed a definite transition with the point of inflection at 116°C. However, an abrupt increase in specific heat at this presumed transition has not been observed. Therefore, it was reasonably concluded that these polymers did not undergo a sharp transition upon heating over the

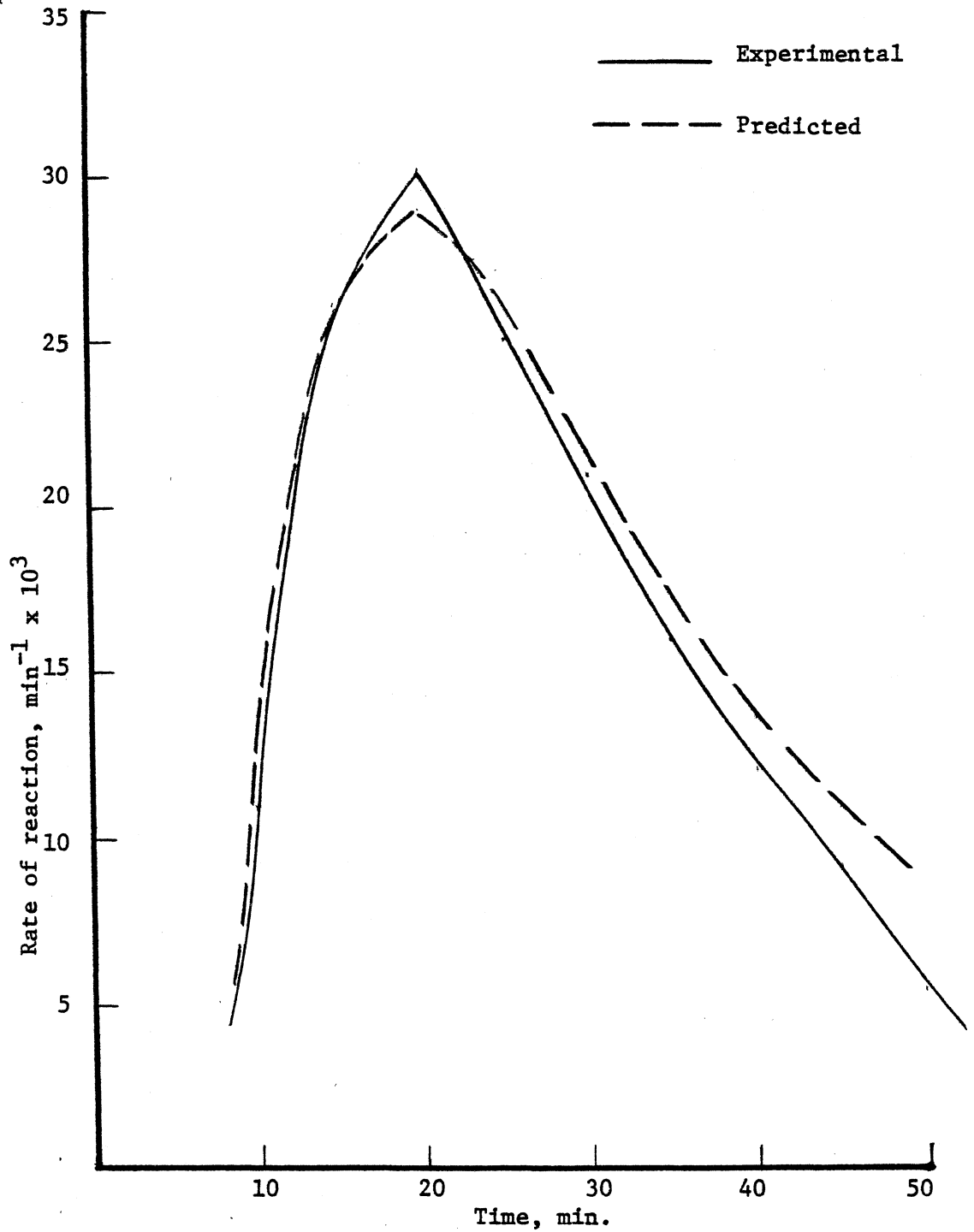


Figure 26. Comparison between experimental and predicted rate of cure at 82°C.

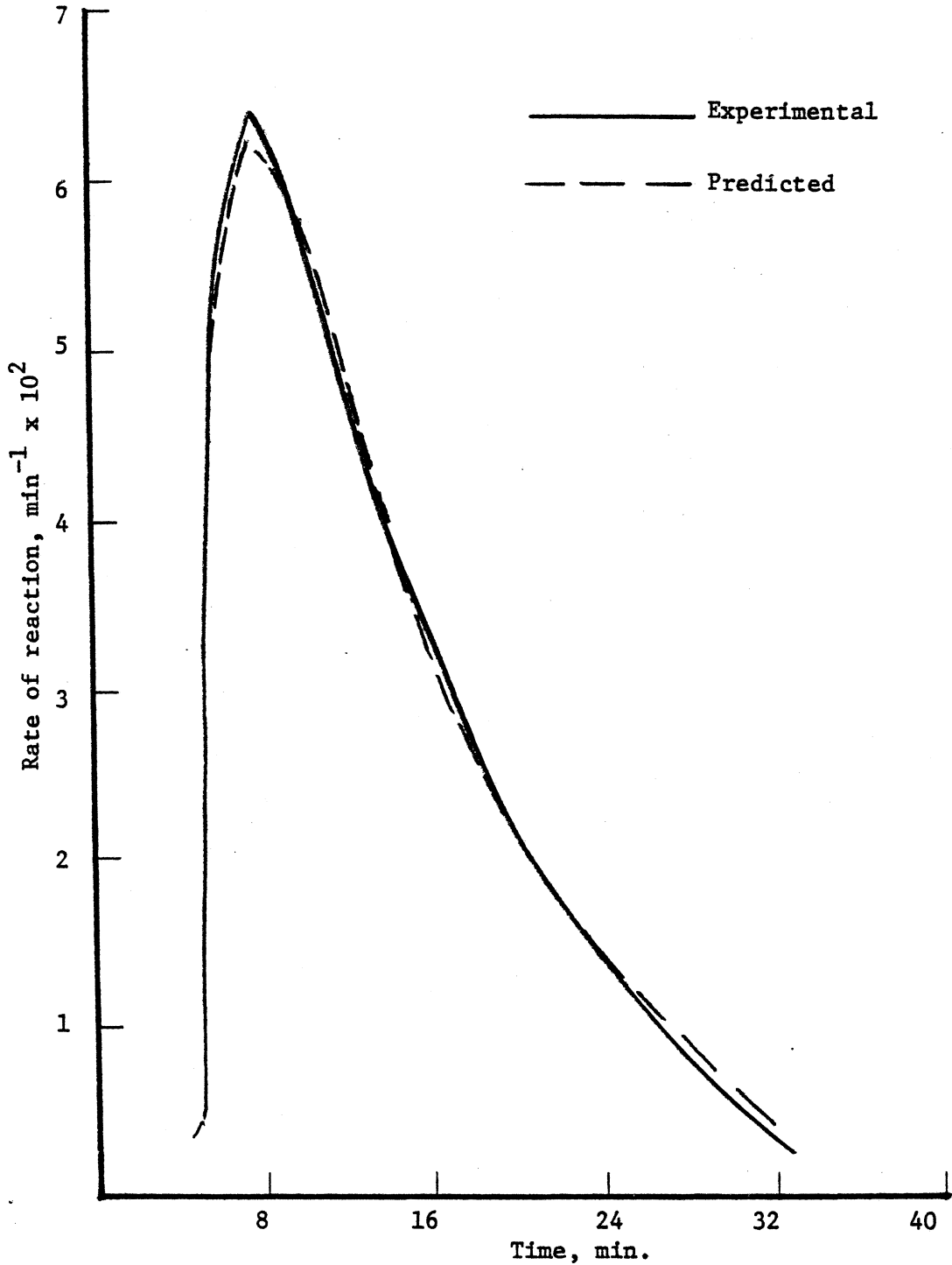


Figure 27. Comparison between experimental and predicted rate of cure at 93°C.

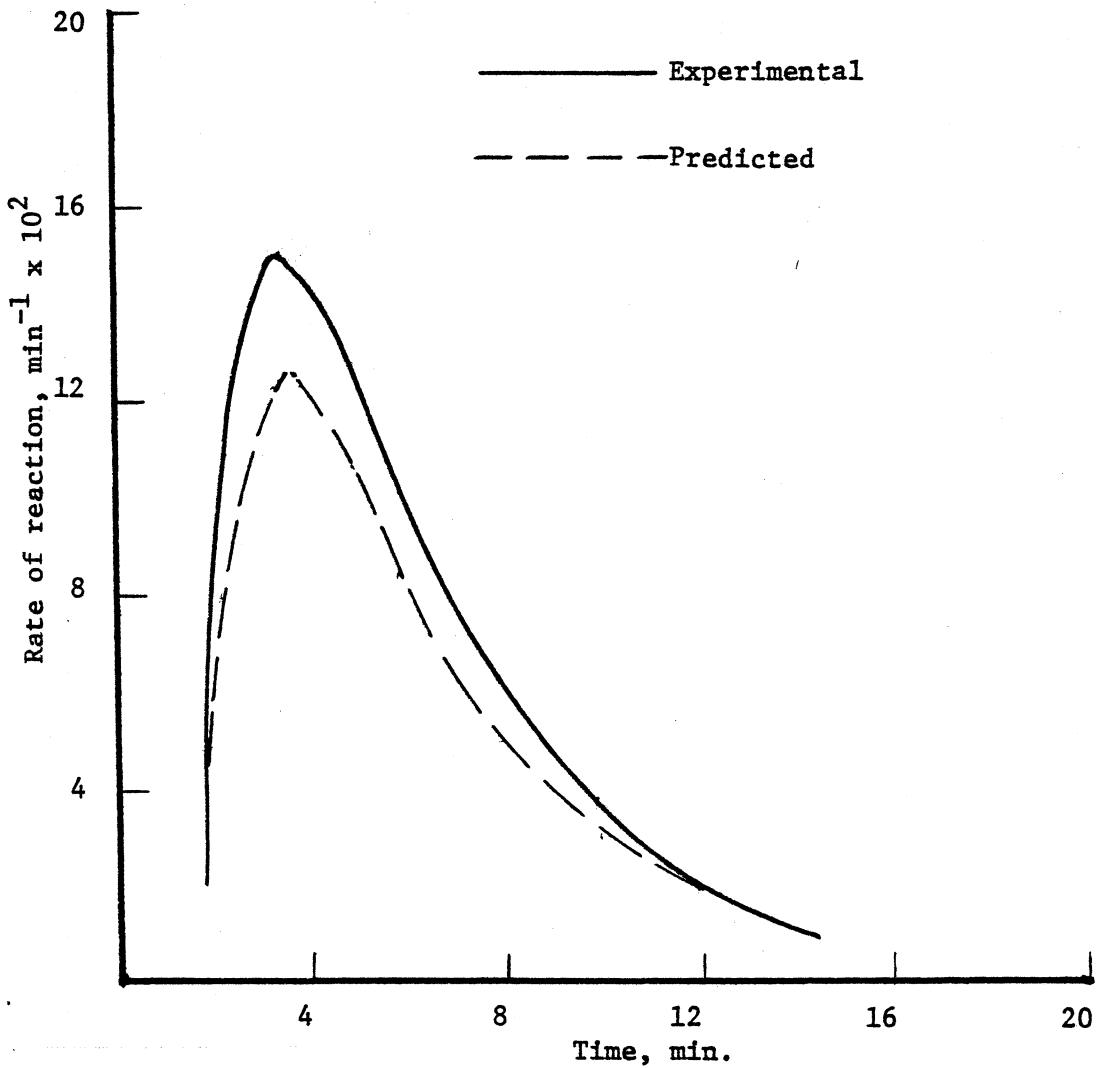


Figure 28. Comparison between experimental and predicted rate of cure at 105°C .

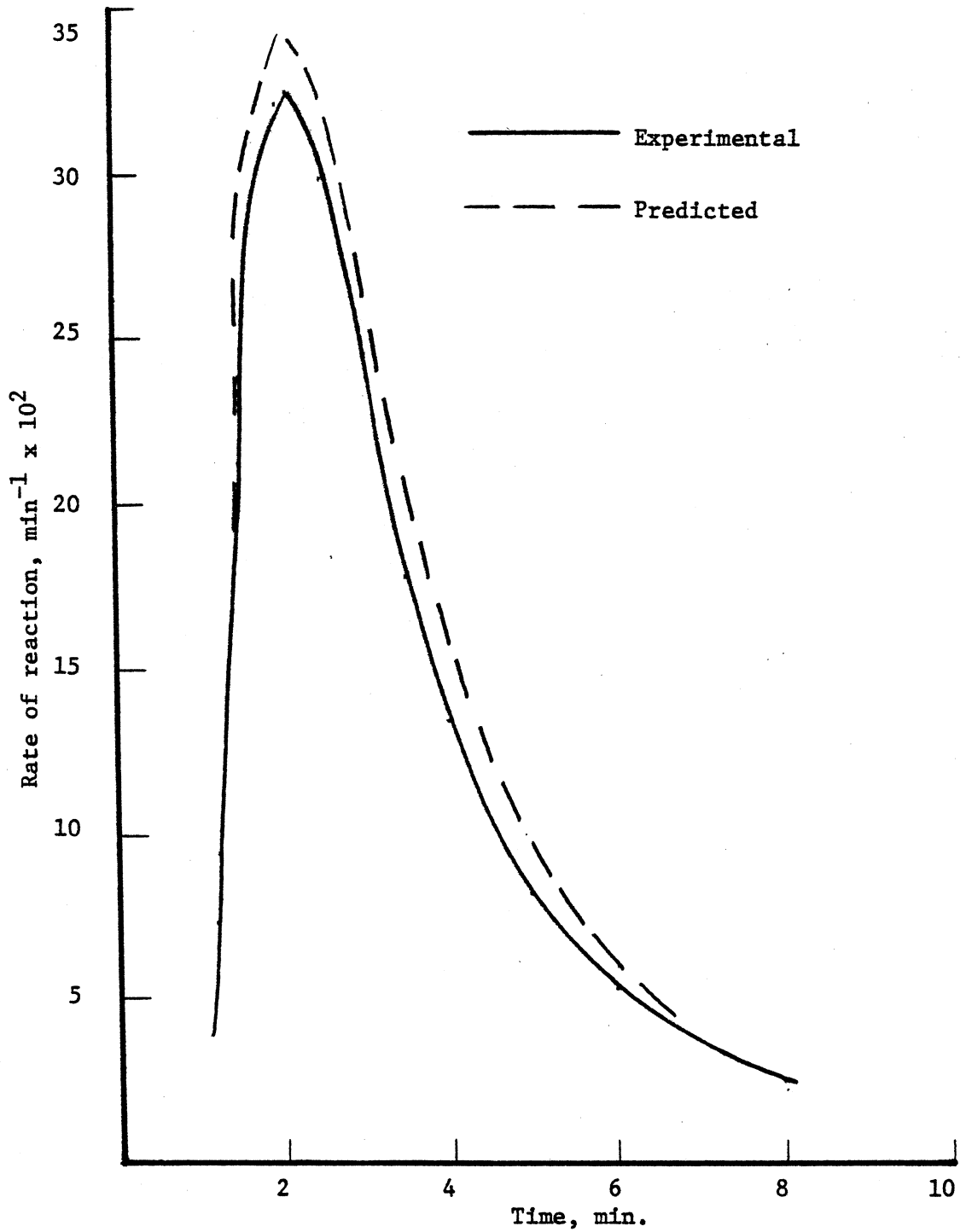


Figure 29. Comparison between experimental and predicted rate of cure at 122°C.

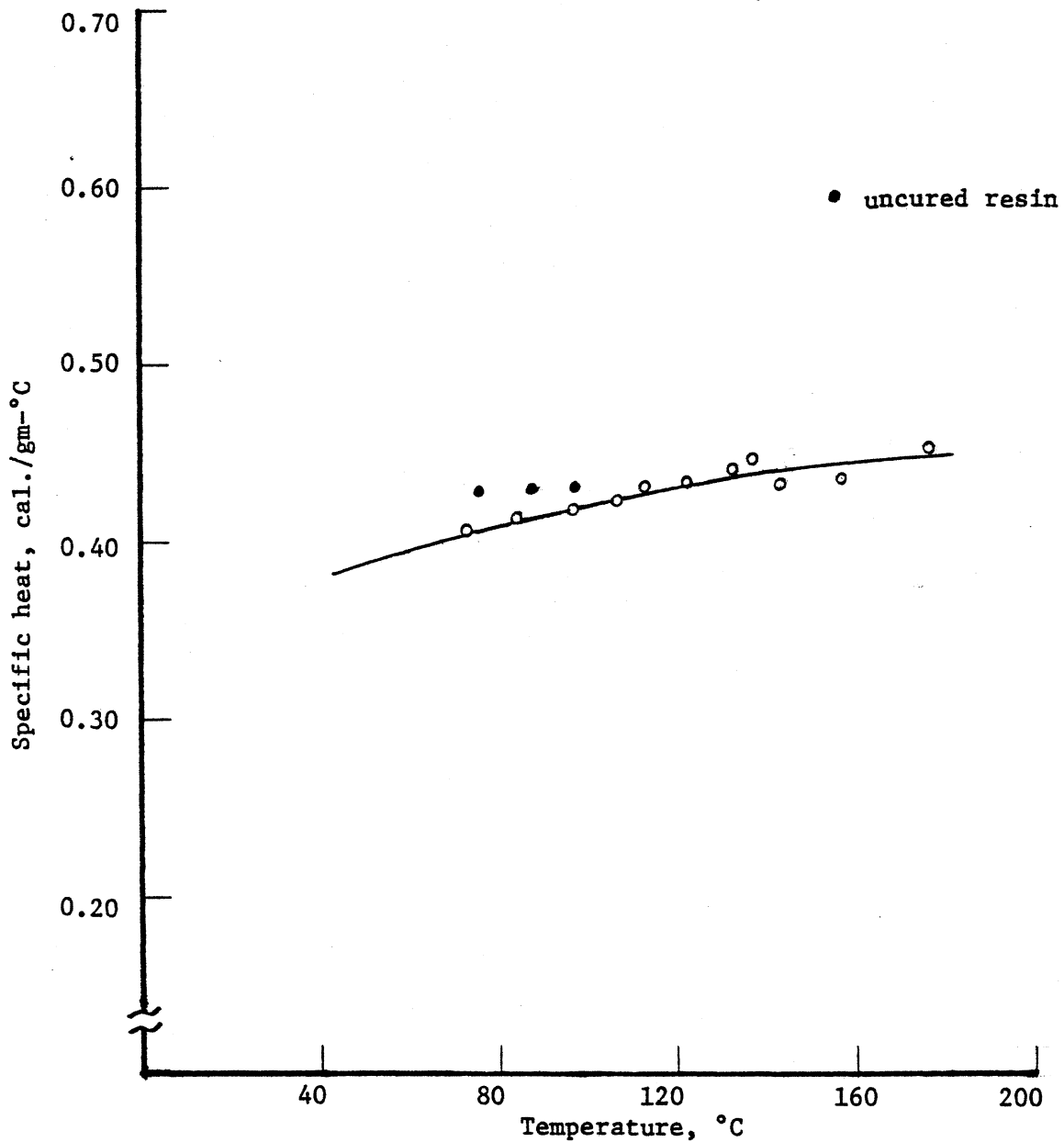


Figure 30. Specific heat of cured polyester.

range used here. This was attributable to the highly crosslinked structure of these materials. Crosslinking reduces the probability of low frequency vibrations of the polymer chains, as well as the probability of further structural change (50).

On the other hand, DSC heating curves showed a sharp exothermic transition at 210°C. That was due to the thermal degradation of these materials above this temperature which has also been confirmed by the TGA data.

The specific heat of uncured resin was observed by heating an uncatalyzed polyester sample in the DSC cell, and it was found to be 0.43 cal/g°C over the temperature range 70-100°C. The samples began to cure due to thermal copolymerization when heated above 100°C.

In order to evaluate the variation of specific heat during the polymerization reaction, a mathematical procedure (17) was followed. Following is a description of this procedure:

During the scanning of an uncured sample, the experimentally measured rate of heat input to the sample, \dot{Q}_S , represents a combination of the heat of reaction and the heat required to raise the sample temperature according to the following heat balance

$$C_p(P,T) \frac{dT}{dt} = \dot{Q}_S(T) - \dot{Q}_R(P,T) \quad [27]$$

where C_p is the specific heat of the sample and is a function of temperature, T , and degree of cure, P . Similarly, the instantaneous rate of heat generation by reaction, \dot{Q}_R , depends on T and P .

Since the heating rate, $\frac{dT}{dt}$, was constant during the scanning of a sample, the above equation could be applied to determine the variation of specific heat with degree of polymerization. Values of the rate of heat generation were obtained from the isothermal data.

Values of specific heat by this method of calculation could be determined only over a small temperature range because of the lack of isothermal data over wider temperature ranges. The predicted values of specific heat using Equation [27] at 100° and 122°C were almost in the same order of magnitude as the values that were predicted for the cured resin at those temperatures.

Thermomechanical Analysis

In order to check the variation of density of the polyester with temperature, cured samples were sent to S. D. Warren Co., for a thermomechanical analysis. Samples were heated from 20°C to 160°C, at 5°C/min, cooled back and then reheated to 160°C again at the same rate to measure the coefficient of linear expansion over this temperature range. From the results that were submitted from the Warren Co., the coefficient of linear expansion was calculated to be about $15.0 \times 10^{-5} \text{ } ^\circ\text{C}^{-1}$ and independent of temperature within the accuracy of these measurements.

Application of Proposed
Mathematical Model

The model was applied to simulating a room temperature polyester casting process. The major input parameters for the computer simulation were the independently measured thermal properties, heat of polymerization, and the constants of the kinetic model. The results of the simulation were checked with the experimentally determined temperature distributions.

Formulation

The model was re-formulated by introducing the following dimensionless quantities:

$$\theta = \frac{T}{T_0}$$

$$X = \frac{y}{h}$$

$$\tau = \frac{\alpha}{h^2} t \quad \text{where } \alpha \text{ was defined as } \alpha = \frac{k_T}{\rho C_p}$$

$$B = \frac{E_a}{RT_0}$$

$$C = 1 - P$$

where C was the fraction of unpolymerized resin.

Variation of specific heat with temperature was defined as

$$\frac{C_p}{C_p^0} = 1 + a(T - T_0) \quad [28]$$

where C_p^0 was the specific heat at T_0 and a was a constant.

Substituting the kinetic model that was developed in this investigation and using the dimensionless quantities, the governing equations [Equations 19 & 20] became

$$\frac{\partial \theta}{\partial \tau} = \frac{1}{[1+aT_0(\theta-1)]} \frac{\partial^2 \theta}{\partial X^2} + \frac{\Delta H_p K' e^{B(1-\frac{1}{\theta})} (1-C)^{0.50} C^{1.50}}{T_0 C_p [1+aT_0(\theta-1)]} \quad [29]$$

$$\frac{\partial C}{\partial \tau} = K' e^{B(1-\frac{1}{\theta})} (1-C)^{0.50} C^{1.50} \quad [30]$$

where

$$K' = \frac{Ah^2}{\alpha} e^{-B}$$

(Definitions of the variables and constants were listed in Table 8.)

It was simply assumed that the rate of heat transfer from the polymer surfaces was proportional to the temperature difference across the mold walls. With this assumption, the boundary conditions took the following form:

Initial Conditions:

$$\theta(X,0) = 1 \quad [31]$$

$$C(X,0) = 1 \quad [32]$$

Boundary Condition 1: (symmetry about X=0)

$$\frac{\partial \theta}{\partial X} (0, \tau) = 0 \quad [33]$$

$$\frac{\partial C}{\partial X} (0, \tau) = 0 \quad [34]$$

TABLE 8
LIST OF VARIABLES USED IN MODEL

Name of Variable	Notation
Temperature, °K	T
Initial polymer temperature, °K	T ₀
Dimensionless temperature	θ
Half slab thickness, cm	h
Space variable, cm	y
Dimensionless space variable	X
Reaction time, sec.	t
Dimensionless time	τ
Activation energy, cal/mol.	E _a
Thermal diffusivity, cm ² /sec	α
Total heat of reaction, cal/g.	ΔH _R
Fraction of polymerized resin	P
Density of resin, gm/cm ³	ρ
Gas constant, 1.987 cal/gmole-°K	R
Thermal conductivity, cal/cm-sec-°K	k _T
Frequency factor, sec ⁻¹	A

Boundary Condition 2: (Mold Wall)

$$\frac{\partial \theta}{\partial X}(1, \tau) = -K[\theta(1, \tau) - \theta_a] \quad [35]$$

where

K was an empirical constant and θ_a was the dimensionless ambient temperature.

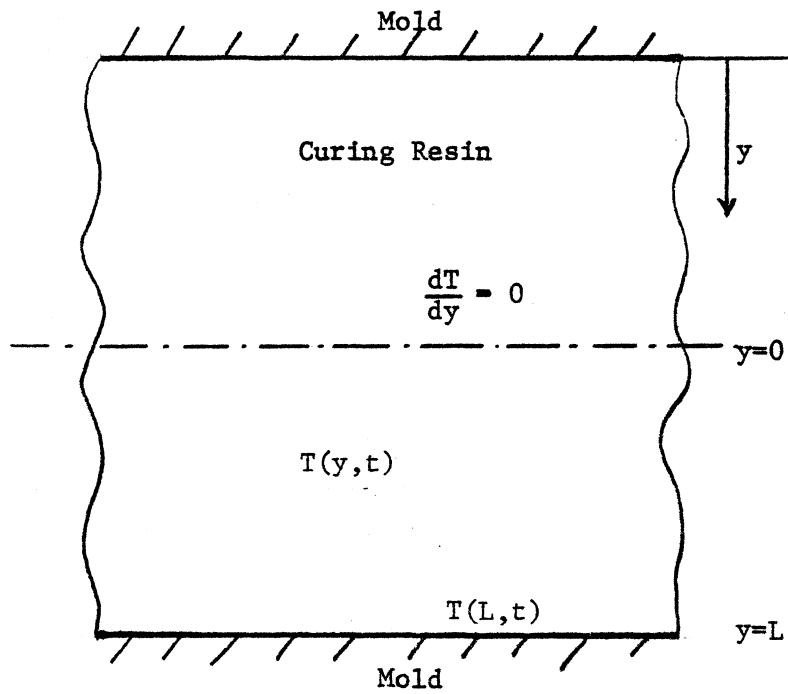
Method of Solution

Equations [29] and [30] were solved simultaneously with the defined boundary conditions by developing a new numerical technique. Since the two differential equations were coupled, an iterative procedure was followed. Basic numerical scheme involved the utilizations of a Crank Nicholson implicit finite difference method for the solution of the heat conduction equation (which was a parabolic type of partial differential equation) and Euler's method for the solution of the reaction rate equation. Further details of these methods were explained in Carnahan's "Applied Numerical Methods" (51).

The coordinate system for the problem is illustrated in Figure 31.

For the finite difference solution, the interval $0 \leq X \leq L$ was subdivided by a grid whose points were spaced ΔX apart, and temperatures at all grid points were computed at time intervals of $\Delta \tau$. The Crank Nicholson implicit finite-difference approximation of Equation [29] was

$$-\frac{\lambda}{2}\theta_{i+1}^* + (F_i + \lambda)\theta_i^* - \frac{\lambda}{2}\theta_{i-1}^* = \frac{\lambda}{2}\theta_{i+1} + (F_i - \lambda)\theta_i + \frac{\lambda}{2}\theta_{i-1} + \phi_i \quad [36]$$



T_a = ambient temperature

Figure 31. Coordinate system of casting.

where

$$\lambda = \frac{\Delta\tau}{(\Delta X)^2}$$

$$F_i = 1 + aT_o(\theta_i - 1)$$

and

$$\theta_i = \Delta\tau K \frac{\Delta HR}{C_p T_o F_i} \left[1 - \frac{C_i^* + C_i}{2} \right]^{0.50} \left[\frac{C_i^* + C_i}{2} \right]^{1.50} \exp B \left[1 - \frac{2}{\theta_i^* + \theta_i} \right]$$

The star denoted a value at the end of a time-step and the subscript i designated the grid point with X coordinate $i\Delta X$.

By applying Equation [36] to the grid points $i = 2, \dots, M$ and to the boundary conditions at $i = 1$, and at $i = M + 1$, the following tridiagonal system was obtained:

$$\begin{aligned} (F_1 + \lambda)\theta_1^* - \lambda\theta_2^* &= (F_1 - \lambda)\theta_1 + \lambda\theta_2 + \phi_1 \\ \frac{\lambda}{2}\theta_{i-1}^* + (F_i + \lambda)\theta_i^* - \frac{\lambda}{2}\theta_{i+1}^* &= \frac{\lambda}{2}\theta_{i-1} + (F_i - \lambda)\theta_i + \frac{\lambda}{2}\theta_{i+1} + \phi_i \\ -\lambda\theta_M^* + [F_{M+1} + \lambda(1 + K\Delta X)]\theta_{M+1}^* &= \lambda\theta_M + [F_{M+1} - \lambda(1 + K\Delta X)]\theta_{M+1} \\ &\quad + 2K\lambda\Delta X\theta_a + \phi_{M+1} \end{aligned} \quad [37]$$

The tridiagonal system of equations thus obtained was solved simultaneously with the reaction rate equation. The reaction rate equation (in Euler integration form) was

$$C_i^* = C_i + \frac{\Delta\tau}{2} Q_i \left[(1 - C_i)^{0.50} C_i^{1.50} \right] \quad [38]$$

where

$$Q_i = K' \exp B \left[1 - \frac{2}{\theta_i^* + \theta_i} \right]$$

The subroutine TRIDAG (51) was used to solve the system in Equation [37]. The flow diagram of the iteration technique is shown in Figure 32.

The complete computer program which was written in FORTRAN for the above calculations is enclosed in Appendix A.

Using a constant time increment throughout the complete polymerization reaction created some stability problems. The best accuracy was obtained by varying the time increments to keep the average concentration changes approximately constant. It was necessary to use lower values of the time increment where the reaction became very fast.

Twenty equal increments were used in $0 \leq X \leq 1$ ($M = 20$).

Solution

The computer output of the simulation contained the temperatures and concentrations (here extent of reaction) at twenty locations in the curing mass from its center line to its surface at each time increment. An example of the computer output is shown in Appendix A.

A common zero time basis was selected in order to make a comparison of the experimental and model-predicted temperature distributions. The time at which the thermocouple readings showed the first indication of a temperature rise in the curing polymer mass was selected as the

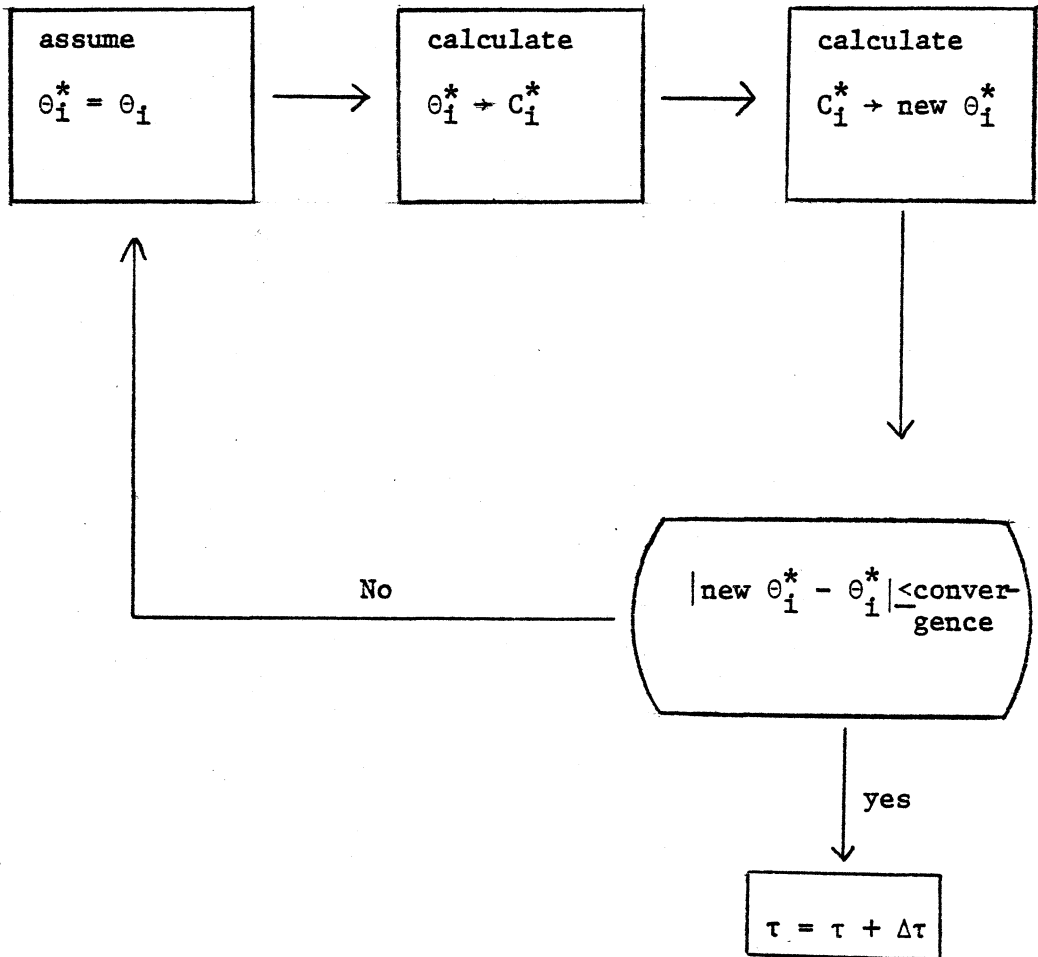


Figure 32. Flow diagram of the iteration procedure.

common "zero" time basis, and the computer simulation was initiated using a uniform pouring temperature corresponding to these initial thermocouple readings at this time. As discussed earlier, the mixing and filling times were neglected since the total cure time was about 23.3 min and the mixing and filling time was only 110 sec.

Simulated reaction exotherms at different locations within the polymer mass and temperature profiles at different times are shown in Figures 33 and 34. The agreement between the model-predicted and experimental results (Figures 35-38) seemed to be quite satisfactory almost over the entire reaction time interval. An exact match of the experimental and computed profiles was not expected because of both experimental and computer round-off errors. Also, k_T/ρ in the thermal diffusivity term was assumed to be constant throughout the reaction. On the other hand, the variation of heat capacity with temperature was included in the simulation.

A more accurate numerical solution could be obtained if the exact variations of thermal properties with the extent of reaction would have been determined. However, the final solution did not change significantly at all when tested with different values of these properties. The accuracy of the simulation seemed more dependent upon the values of the kinetic parameters.

To study the effect of heat conduction during curing, the model was also solved for an adiabatic boundary condition at the walls of the mold. Thus, the conduction term in the energy equation was dropped, and the following equation resulted:

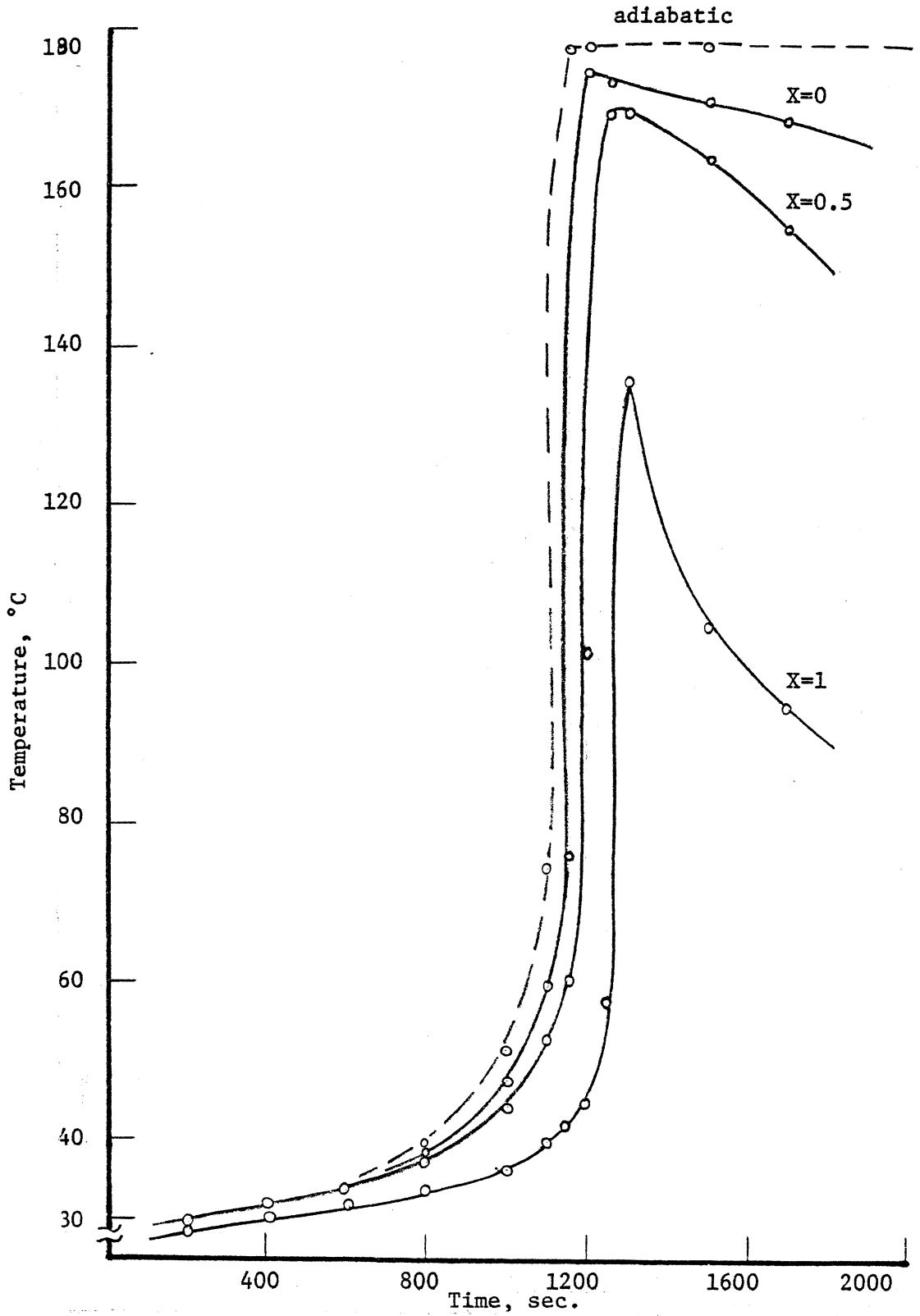


Figure 33. Calculated temperatures at different locations in curing polymer.

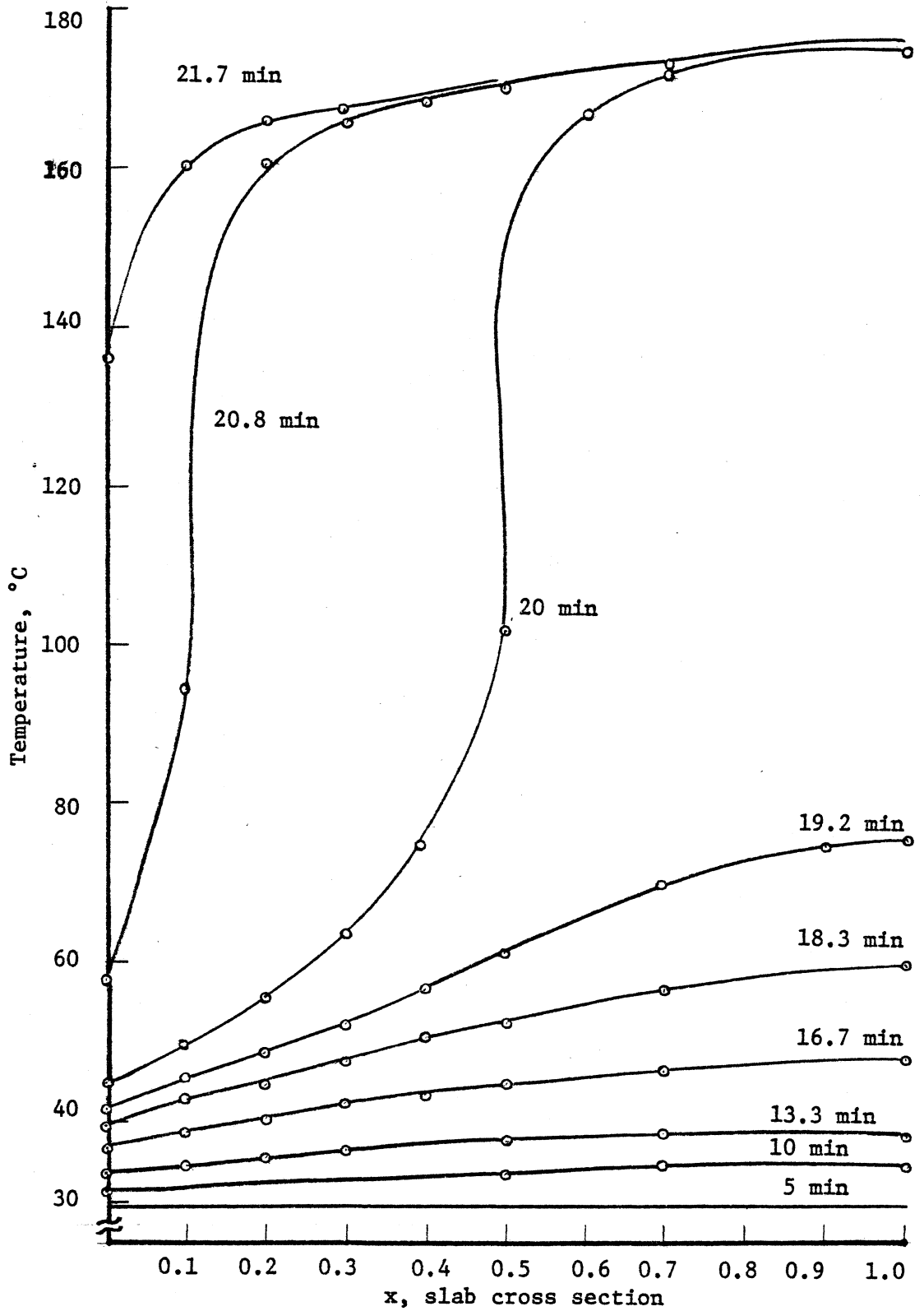


Figure 34. Calculated temperature profiles (here $x=1$ represents center of slab)

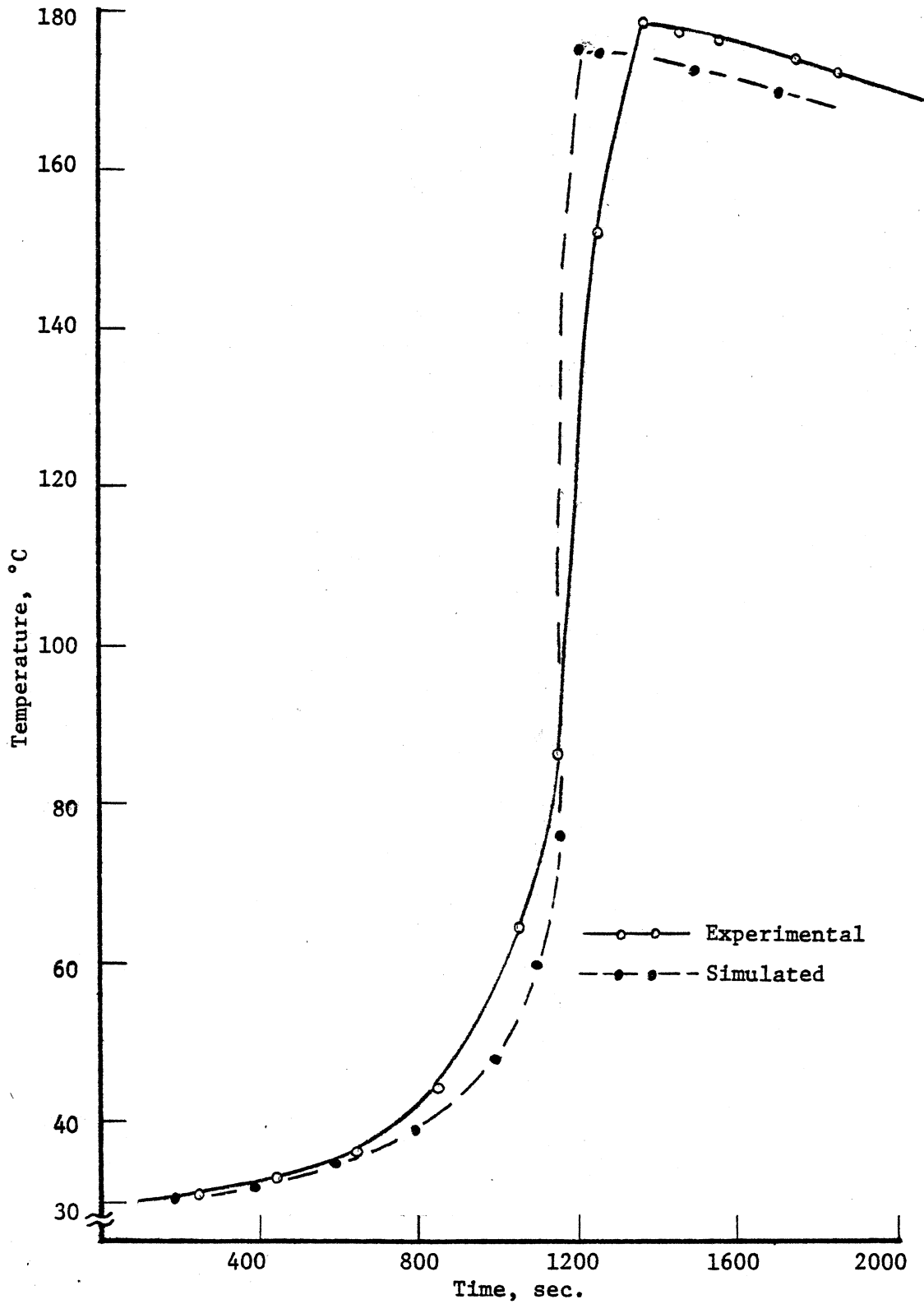


Figure 35. Comparison of experimental and calculated temperatures at the center of curing polymer.

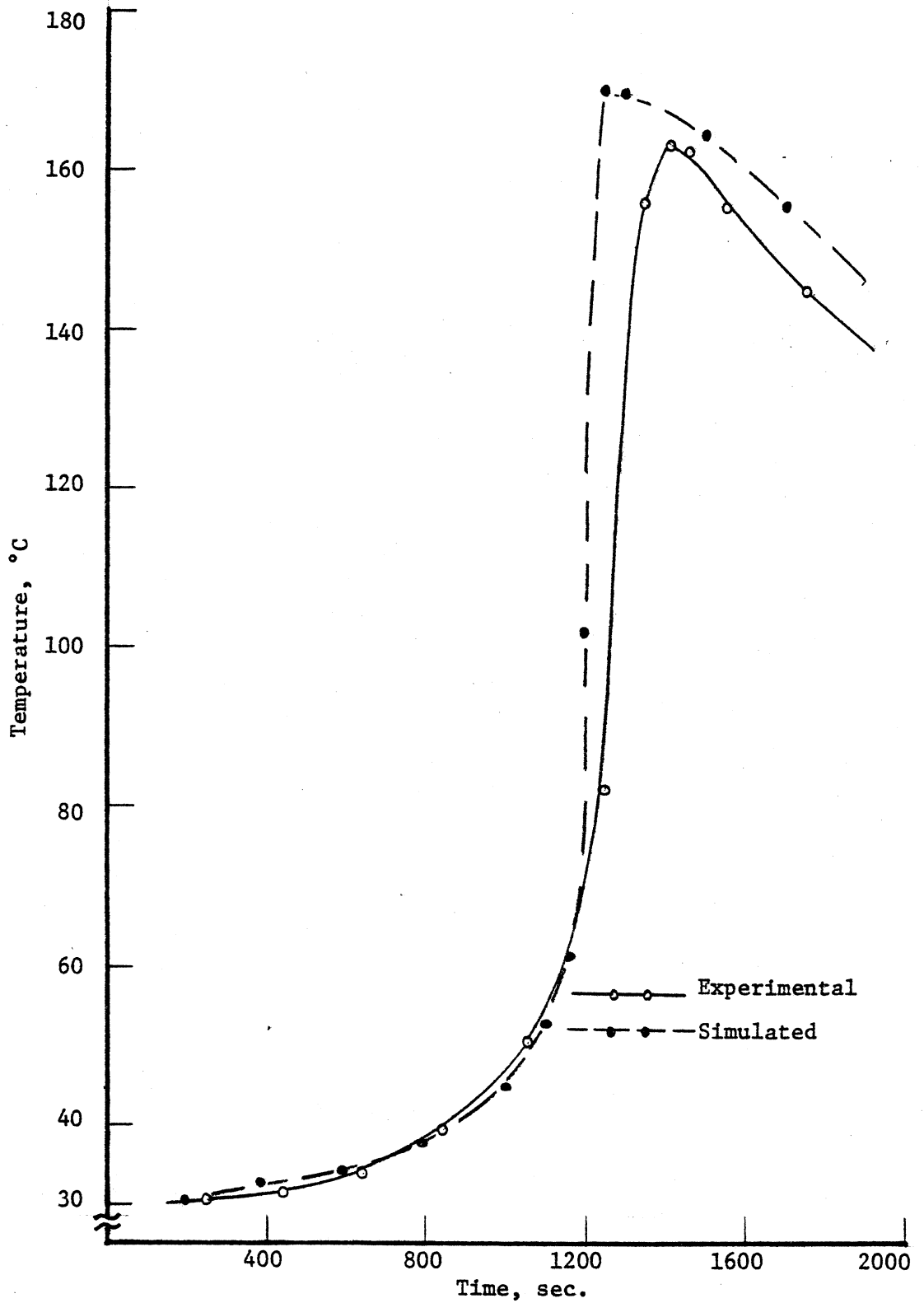


Figure 36. Comparison of experimental and calculated temperatures at $x = 0.5$.

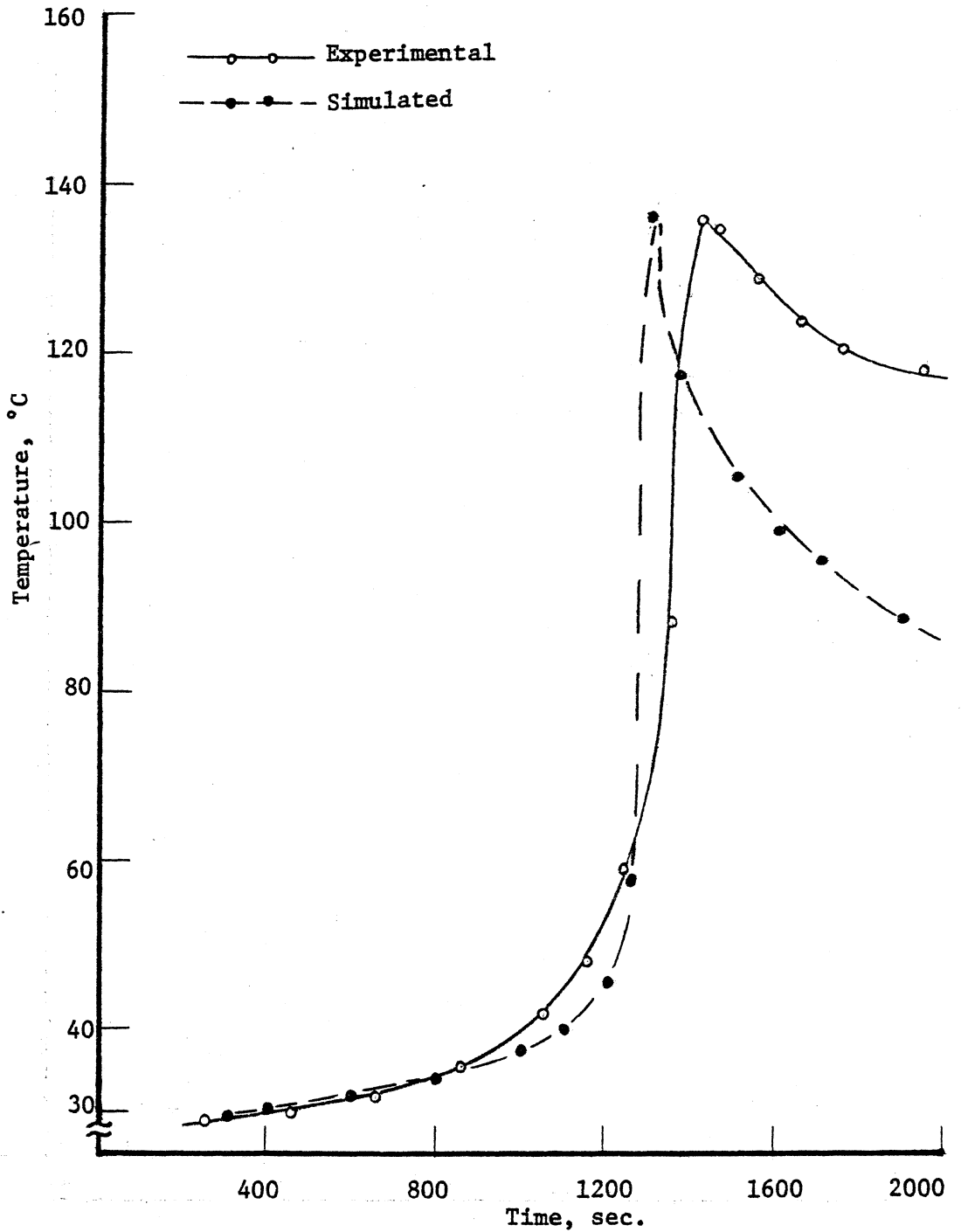


Figure 37. Comparison of experimental and calculated temperatures at the surface of curing polymer.

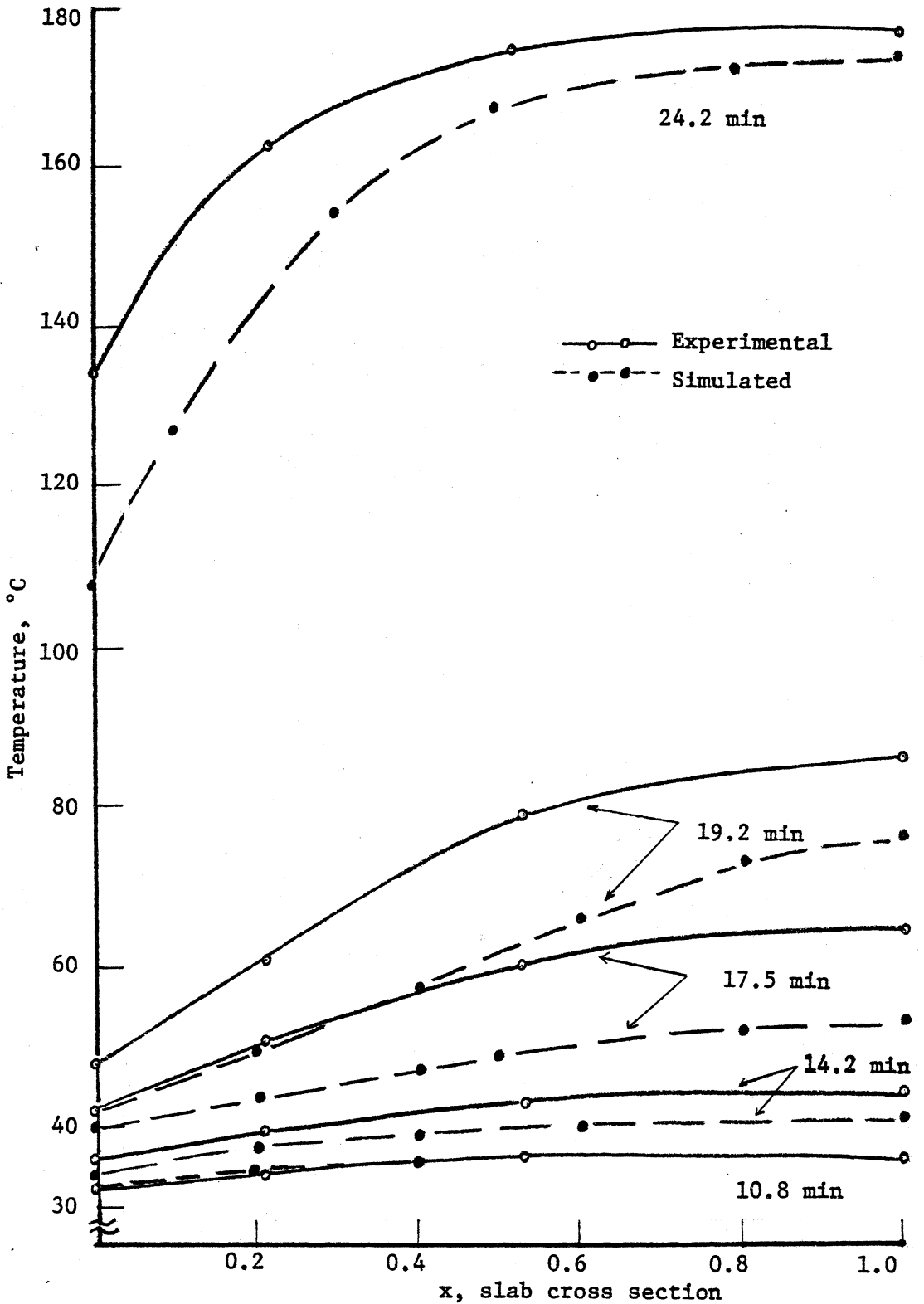


Figure 38. Comparison of experimental and calculated temperature profiles (here $x=1.0$ represents center of slab)

$$\frac{\partial T}{\partial t} = \frac{\Delta H_R}{C_p} A e^{-E_a/RT} (1 - C)^{0.50} C^{1.50} \quad [39]$$

The predicted temperature rise in the curing polymer mass for this case is shown in Figure 33. It is significant to note that, when heat conduction is included, the center of the slab had nearly an adiabatic rise. Only very near to the mold walls was the reaction exotherms reduced to less than the adiabatic rise. This was of course due to the increased effect of the heat transfer rate near the mold walls. Also, because of the poor conductivity of silicone rubber, the heat loss from the mold walls was not too large. This was clear from the near adiabatic character of the curing over a large section of the polymer mass.

Variation of the extent of polymerization with time at different locations within the polymer mass, and the concentration profiles at different times during the reaction are shown in Figures 39 and 40. It can be easily seen that the reaction was faster at the center and slowed down near the walls. That is, it took more time for the polymer near the surface to be cured. This is an important problem in cyclic processes like thermoset injection molding which involves significant capital equipment. In those processes, it is advantageous to cure the surface of the part rapidly and follow with a post-cure. Therefore, it may be desirable to apply a constant heat flux through the mold walls to control the rate of heat transfer from these walls. Although the proposed curing model was applied to a specific casting

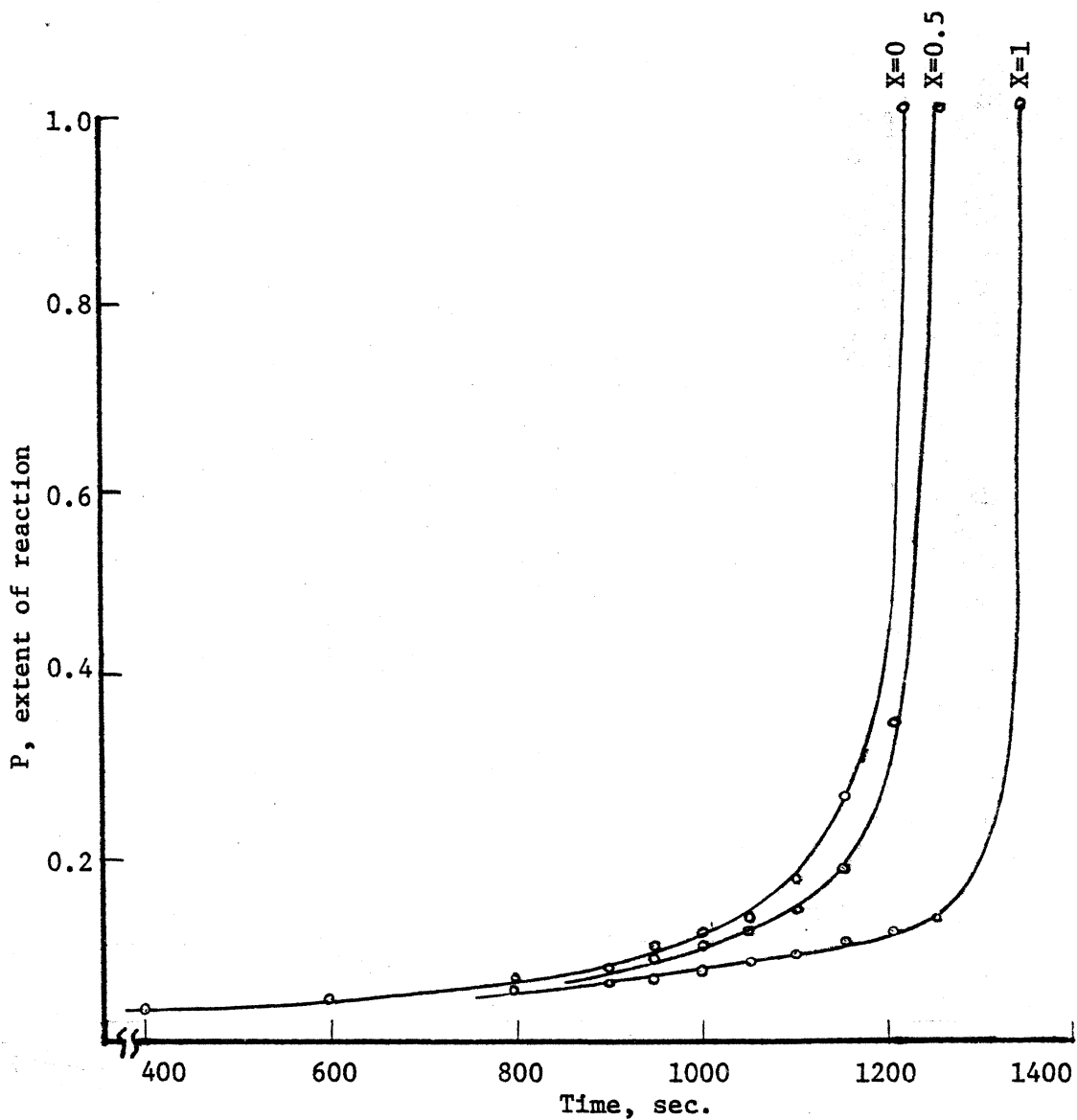


Figure 39. Calculated extent of polymerization at different locations as function of time in curing polymer.

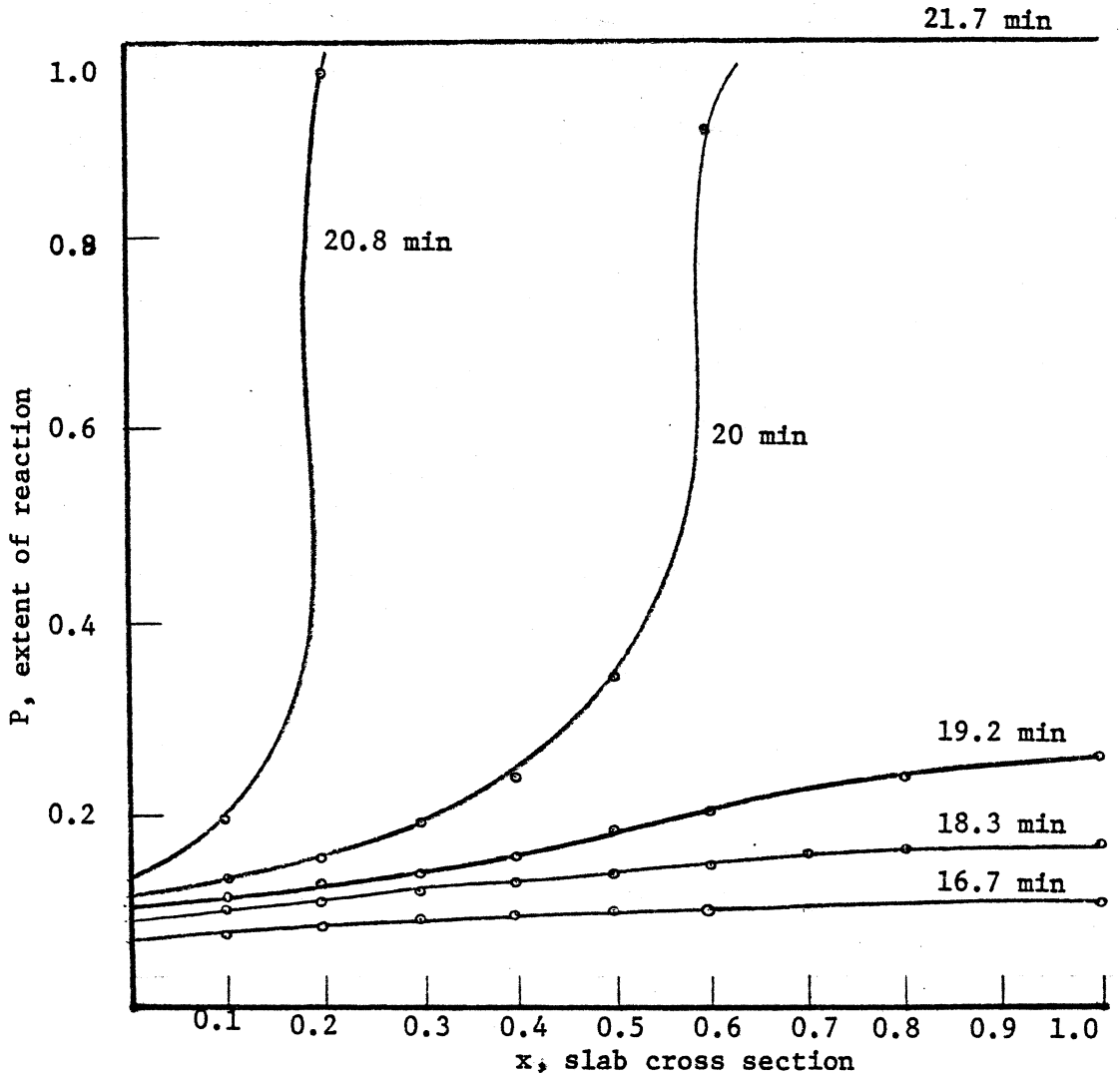


Figure 40. Calculated profiles of extent of polymerization (here $x=1.0$ represents center of slab).

operation in this investigation, the model can be utilized in simulation of most of the reaction molding operations which involve different process conditions.

From the temperature and concentration profiles, and with the known network structure-property relationships, it is possible to calculate certain physical properties like gel point, molecular weight, sol fraction, and modulus changes with position and time within the curing mass.

VI. CONCLUSIONS AND RECOMMENDATIONS

The processing of thermoset polyesters involve problems of transient heat conduction coupled with an exothermic chemical reaction. Therefore, a mathematical curing model was proposed and developed by applying the principles of heat transfer and chemical kinetics. This investigation represents the first comprehensive study of this problem.

Conclusions

1. Both the isothermal and the scanning techniques of Differential Scanning Calorimetry were used to obtain the heats of reaction and a kinetic expression for the polymerization reaction. The ultimate heat of cure was determined as 73.9 ± 0.5 cal/g for the polyester-styrene system that was studied here. Isothermal heats of reaction were predicted at different cure temperatures, and a substantial increase in heat generation was observed with increasing temperature. Using isothermal reaction data, a kinetic model of the polymerization reaction was proposed as

$$\frac{dP}{dt} = (2.60 \times 10^{-9} \text{ min}^{-1}) e^{17.04/RT} P^{0.50} (1 - P)^{1.50}$$

where P represents the fraction of the original double bonds that were reacted in the system. Results from this model revealed excellent agreement with the experimental data over the entire conversion.

2. Variation of the thermal properties (thermal conductivity, specific heat) of the cured products with temperature was determined successfully over the temperature range of interest. They all generally increased with increasing temperature.

3. An accurate and a fast measurement of temperature changes in the curing polymer mass during a casting operation was accomplished by developing a new real-time computing technique.

4. It has been shown that the implicit finite difference approximations to the differential equations describing conductive heat transfer provide an accurate method of determining temperature profiles. In order to simultaneously solve the heat transfer equation with the rate of reaction equation, a computer program was written. The program calculated the temperature and the concentration changes with position and time in the curing mass rather accurately.

5. A satisfactory agreement was obtained between temperature measurements within the curing casting and the computer simulation using independently determined heat of reaction, thermal conductivity, and specific heat.

6. Photographs of the birefringent patterns indicated the existence of residual stresses in the molded pieces as a result of the temperature gradients developed in the piece during cure.

7. The curing model developed here can be utilized in characterizing the curing process, predicting curing performance, and establishing guidelines for better design of the curing operation.

With the proper changes in the input parameters and boundary conditions, the model can be generally utilized in the simulation of processes with most thermoset plastics.

Recommendations

1. Studies on the network structure-property relations of those materials are needed. Results of such studies can be incorporated with the curing model that was developed here to achieve the desired ultimate properties of the cured articles.

2. So far, there has been no systematic study reported in the literature to relate the basic kinetics, thermal, and rheological parameters of thermosets to their behavior during injection molding behavior. This investigation presented information on the kinetics and thermal behavior of thermoset polyesters. In addition to these studies, determination of the rheological parameters such as shear viscosity and shear rate as a function of degree of cure would be a fruitful study to achieve a complete characterization of these plastics for analysis of their moldability.

3. Accurate measurements of the thermal properties as a function of degree of cure could not be achieved because of experimental difficulties resulting from the reactive nature of these materials. This remains as an important task for future investigators in this field. The accuracy of the numerical simulation could be improved with the inclusion of the variation of thermal properties with degree of cure.

4. The model can be easily modified for the cases where the mold has different geometries.

VII. BIBLIOGRAPHY

1. B. Parkyn, F. Lamb, and B. V. Clifton, Polyesters, Vol. 2, Elsevier, New York (1967).
2. J. R. Lawrence, Polyester Resins, Reinhold, New York (1967).
3. W. H. Carothers, J. Am. Chem. Soc., 51, 2560 (1929).
4. T. F. Bradley, E. L. Kropa, and W. B. Johnston, Ind. Eng. Chem., 29, 1270 (1937).
5. D. Campbell, D., et al., "Fiber Glass Reinforced Plastics in the Polyester Laminating Field," p. 1-2, FRP Associates (1953).
6. I. Skeist, SPI-R. P. Div. Preprint, Vol. 12, 15-A (1957).
7. D. K. Hamann, Angew. Chem., 71, 596 (1959).
8. G. M. Burnett, Mechanism of Polymer Reactions, Interscience, New York, 1954, p. 344.
9. M. Gordon and B. M. Grievson, J. Polymer Sci., 17, 107 (1955).
10. S. S. Oleesky and J. G. Mohr, Handbook of Reinforced Plastics, pp. 13-55, Reinhold, New York (1964).
11. B. Golding, Polymers and Resins, D. Van Nostrand Co., Princeton, N. J.
12. R. V. Milby, Plastics Technology, McGraw-Hill, New York (1973).
13. P. J. Flory, Principles of Polymer Chemistry, Chap. IV, Cornell University Press, Ithaca, New York (1953).
14. J. K. Kochi, Free Radicals, Wiley-Interscience, New York (1973), p. 55.
15. G. V. Schulz and G. Harborth, Makromol. Chem., 1, 106 (1947).
16. E. Trommsdorff, H. Köhle, and P. Lagally, Makromol. Chem., 1, 169 (1947).
17. M. R. Kamal and S. Sourour, Polymer Eng. Sci., 13, 59 (1973).

18. A. C. Filson, Plastics, 27, No. 293, 1 (1962).
19. B. Alt, Kunststoffe, 52, 7, 394 (1962).
20. G. S. Learmonth, F. M. Tomlinson, and J. Czerski, J. Appl. Polym. Sci., 12, 403 (1968).
21. A. F. Lewis and J. K. Gillham, SPE Trans, 3, 201 (1963).
22. M. F. Drumm, C. W. Dodge, and L. E. Nielson, Ind. Eng. Chem., 48, 76 (1956).
23. J. H. L. Henson, A. J. Lovett, and G. S. Learmonth, J. Appl. Polym. Sci., 11, 2543 (1967).
24. L. C. Rubens and R. E. Stochdopole, J. Appl. Polym. Sci., 9, 1487 (1965).
25. W. Burlant and J. Hinsch, J. Polym. Sci., Part A, 2, 2135 (1964).
26. P. E. Slade, Jr. and L. T. Jenkins, Thermal Characterization Techniques, Marcel Dekker, Inc., New York (1970).
27. Baxter, R. A., in Thermal Analysis, R. F. Schwenker and P. D. Garn, eds., Academic, New York, 1969, p. 65.
28. D. J. David, J. Thermal Anal., 3, 247 (1971).
29. J. K. Gillham and C. C. Mentzer, J. Appl. Polym. Sci., 17, 1143 (1973).
30. H. J. Borchardt and F. Daniels, J. Am. Chem. Soc., 79, 41 (1957).
31. R. A. Fava, Polymer, 9, 137 (1968).
32. O. R. Abolafia, SPE AnTech, 15, 610 (1969).
33. R. B. Prime, Analytical Chemistry, 2, 201 (1970).
34. S. Y. Choi, SPE J., 26, 51 (1970).
35. K. Horie, I. Mita, and H. Kambe, J. Polym. Sci., Part A-1, 8, 2839 (1970).
36. M. R. Kamal, S. Sourour, and M. Ryan, SPE Tech. Papers, 19, 187 (1973).
37. D. J. Prepelka and J. L. Wharton, J. Cell. Plast., 11, 87 (1975).

38. T. E. Stonecypher, E. L. Allen, D. E. Mastin, and D. A. Willoughby, Chem. Eng. Progr. Symposium Series, 62, 7 (1966).
39. E. Broyer and C. W. Macosko, AIChEJ., 22, 268 (1976).
40. D. A. Hills, Heat Transfer and Vulcanization of Rubber, Chap. 5,, Elsevier, London, England (1971).
41. W. Engelmaier and M. B. Roller, Insulation/Circuits, 21, 4, 43 (1975).
42. J. Schröder, Rev. Sci. Inst., 34, 615 (1963).
43. "DSC Instruction Manual," E. I. du Pont de Nemours and Co., Inc., 1965.
44. R. B. Bird, W. E. Stewart, and E. L. Lightfoot, Transport Phenomena, pp. 554-564, Wiley, New York (1960).
45. J. Crank and G. S. Park, ed., Diffusion in Polymers, pp. 85-100, Academic Press, London, England (1968).
46. M. Jakob, Heat Transfer, Wiley, New York (1949).
47. D. E. Kline, J. Polym. Sci., 50, 441 (1961).
48. R. P. Krehling and D. E. Kline, J. Appl. Polym. Sci., 13, 2411 (1969).
49. S. Sourour and M. R. Kamal, Polym. Eng. Sci., 16, 480 (1976).
50. R. W. Warfield, M. C. Petree, and P. Donovan, J. Appl. Chem., 10, 429 (1960).
51. B. Carnahan, H. A. Luther, and J. D. Wilkes, Applied Numerical Methods, pp. 429-473, Wiley, New York (1969).
52. H. Kubota, J. Appl. Polym. Sci., 19, 2279 (1975).

APPENDICES

APPENDIX A

This section includes the computer program that was written in FORTRAN to solve the partial differential equations in the model. Examples of the computer outputs were also presented.

```
C SIMULATION PROGRAM FOR CASTING PROCESS OF
C THERMOSET POLYESTERS
C BY Y.SELAMI PUSATCIOGLU.....JULY 1977
C PROGRAM CALCULATES THE TEMPERATURE PROFILE
C BY USING "CRANK AND NICHOLSON" IMPLICIT FINITE DIFFERENCE
C METHOD,AND THE CONCENTRATION PROFILE BY USING EULER METHOD.
C UNSTEADY-STATE HEAT TRANSFER AND RATE OF REACTION EQUATIONS
C ARE SOLVED SIMULTANEOUSLY USING AN ITERATION TECHNIQUE.
C FOLLOWING ARE THE DEFINITIONS OF VARIABLES AND CONSTANTS:
C T(I),TP(I):VECTORS OF TEMPERATURES
C C(I),CP(I):VECTORS OF CONCENTRATIONS
C HERE CONCENTRATION IS DEFINED AS THE FRACTION OF
C UNSATURATION
C AL :THERMAL DIFFUSIVITY,CM**2/SEC
C RHO :DENSITY OF RESIN,GM/CM**3
C CPI :SPECIFIC HEAT AT 25 DEG.C,CAL/GM-DEG.C
C EA :ACTIVATION ENERGY,CAL/GM.MOL
C AA :FREQUENCY FACTOR,1/SEC
C TO :INITIAL POLYMER TEMPERATURE,DEG C
C TAMB :AMBIENT TEMPERATURE
C CAO :INITIAL CONCENTRATION OF RESIN,GM/CM**3
C H :POLYMER THICKNESS,CM
C CAP :RATE OF HEAT LOSS(AN EMPRICAL CONSTANT)
C M :NUMBER OF SPACE INCREMENTS
C DT :TIME STEP
C DX :SPACE INCREMENT
C PRINT :NO.OF TIME INTERVALS
C CONV :CONVERGENCE
C A1 :CONSTANT COEFFICIENT OF SPECIFIC HEAT EQUATION
C A2,A3 :CONSTANTS OF THE HEAT OF REACTION EQUATION
C AB,AC :AVERAGE CONCENTRATIONS
C PU,PR :FACTORS TO INCREASE OR TO REDUCE THE TIME STEP
```

```

C FOLLOWING IS THE FORTRAN PROGRAM (USING PDP 11/40)
0001 DIMENSION T(50),TP(50),C(50),CP(50),TPN(50)
0002 DIMENSION AX(50),BX(50),CX(50),D(50),Q(50)
0003 DIMENSION F(50),HR(50)
0004 PHI(I)=DDK*(CP(I)**1.50)*((1.-CP(I))**.50)*EXP(B*
1 (1.-2./(T(I)+TP(I))))
0005 WRITE(5,5000)
C OPTION TO GET OUTPUT.....SCREEN-PRINTER-DISK
0006 5000 FORMAT(' INPUT DEVICE:(TTO,DKO,TI,ETC) ',#)
0007 READ(5,5001) ICHAR,IUNIT
0008 5001 FORMAT(A2,I10)
0009 CALL ASNLUN(6,ICHR,IUNIT,IDS)
0010 1 FORMAT(4F15.7,E10.0)
0011 READ(5,1)AL,RHO,CPI,EA,AA
0012 READ(5,88)TO,TAMB,CAO,H,CAP
0013 88 FORMAT(5F12.5)
0014 READ(5,20)M,DT,DX,PRINT,CONV
0015 20 FORMAT(I5,4F12.5)
0016 READ(5,102)A1,A2,A3,TC,TL,SEL,SELO
0017 102 FORMAT(7F10.6)
0018 READ(5,556)AB,PU,AC,PR
0019 556 FORMAT(4F10.6)
0020 MP=M+1
C INITIAL AND BOUNDARY CONDITIONS
0021 DO 10 I=1,MP
0022 C(I)=.99
0023 T(I)=1.
0024 10 TP(I)=1.
0025 PRT1=0.
0026 KK=0
0027 TIM=0.
0028 TQ=AL/(H*H)
0029 NP=2
0030 PRINT=PRINT*TQ
0031 33 DT=DT*PU
0032 3 RL=DT/(DX*DX)
0033 B=EA/(1.987*TO)
0034 PK=(AA*H*H/AL)*EXP(-B)
0035 DTK=DT*PK
0036 DTAD=CAO/(RHO*TO*CPI)
0037 DDK=DT*PK*DTAD
0038 CATA=2.*RL*CAP*DX*TAMB/TO
0039 WRITE(6,21)
0040 WRITE(6,17)B,PK,DTK,DTAD,DDK,CATA
0041 21 FORMAT(1X,'B,PK,DTK,DTAD,DDK,CATA')
0042 TEM1=-RL/2.
0043 15 NC=0
C NC IS THE ITERATION COUNTER
0044 13 NC=NC+1
0045 IF(NC.GT,20) GO TO 99

```

```

0047      DO 11 I=1,MP
          C      VARIATION OF SPECIFIC HEAT WITH TEMPERATURE
0048      F(I)=1.-A1*TO*(((T(I)+TP(I))/2.)-1.)
          C      VARIATION OF HEAT OF REACTION WITH TEMPERATURE
0049      HR(I)=A2*(((T(I)+TP(I))/2.)*TO)-A3
0050      GO TO 200
          C      SET UP TRIDIAGONALS
0051      200  AX(I)=TEM1
0052      BX(I)=F(I)+RL
0053      CX(I)=TEM1
0054      AX(MP)=-RL
0055      BX(MP)=F(MP)+RL*(1.+CAP*DX)
0056      CX(1)=-RL
0057      Q(I)=DTK*EXP(B*(1.-2./(T(I)+TP(I))))
0058      11  CP(I)=-(((1.-C(I))**.50)*(C(I))*1.50))*Q(I)/2.+C(I)
          C      DECISION TO CHANGE TIME STEP
0059      CC1=CP(1)-C(1)
0060      CC2=CP(MP)-C(MP)
0061      DD=ABS(CC1+CC2)
0062      IF(DD.GT.AB) GO TO 33
0064      IF(DD.LT.AC) GO TO 129
0066      GO TO 166
0067      129  DT=DT*FR
0068      GO TO 3
          C      CALCULATES RHS FOR TRIDAG
0069      166  DO 12 I=2,M
0070      12  D(I)=RL*(T(I+1)+T(I-1))/2.+T(I)*(F(I)-RL)+PHI(I)*HR(I)
0071      D(1)=(F(1)-RL)*T(1)+RL*T(2)+PHI(1)*HR(1)
0072      D(MP)=RL*T(M)+(F(MP)-RL*(1.+CAP*DX))*T(MP)+CATA
          1 +PHI(MP)*HR(MP)
0073      CALL TRIDAG(1,MP,AX,BX,CX,D,TPN)
          C      NOW HAVE A NEW VECTOR OF TEMPERATURES,TPN
          C      CHECK FOR CONVERGENCE
0074      KS=0
0075      DO 14 I=1,MP
0076      SSQ=ABS(TPN(I)-TP(I))
0077      TP(I)=TPN(I)
0078      IF(SSQ.GT.CONV) KS=1
0080      14  CONTINUE
0081      IF(KS.EQ.1) GO TO 13
0083      DO 16 I=1,MP
0084      Q(I)=DTK*EXP(B*(1.-2./(T(I)+TP(I))))
0085      C(I)=-(((1.-CP(I))**.50)*(CP(I))*1.50))*Q(I)/2.+CP(I)
0086      16  T(I)=TP(I)
0087      TIM=TIM+DT
0088      IF(TIM.LT.PRT1) GO TO 15

```

```

0090      PRT1=PRT1+PRINT
0091      TIM1=TIM/TQ
0092      IF(TIM1.GT.2000.)GO TO 177
0094      WRITE(6,18)TIM1
0095  18   FORMAT(1X,'TIME=',F10.3,' SECONDS')
0096      DO 30 I=1,MP
0097      TN(I)=T(I)*TQ
0098  30   CP(I)=C(I)
0099      WRITE(6,31)
0100      WRITE(6,17)(TN(I),I=1,MP,NP)
0101      WRITE(6,32)
0102      WRITE(6,17)(CP(I),I=1,MP,NP)
0103  17   FORMAT(6F12.4)
0104  31   FORMAT(1X,'TEMPERATURES')
0105  32   FORMAT(1X,'CONCENTRATIONS')
0106      IF(TIM1.GT.TC) GO TO 555
0108      IF(TN(MP).GT.TL) GO TO 558
0110      GO TO 15
0111  555  CAP=SEL
0112      GO TO 3
0113  558  CAP=SELD
0114      GO TO 3
0115  99   KK=KK+1
0116      IF(KK.GT.10)STOP
0118      DT=DT/3.
0119      WRITE(6,98)DT
0120  98   FORMAT(1X,'NEW DT =',G12.4)
0121      GO TO 3
0122  177  STOP
0123      END

```

```

C      TRIDIAGONAL SOLUTIONS FROM CARNAHAN,ET AL.,P.446
0001      SUBROUTINE TRIDAG(IF,L,A,B,C,D,V)
0002      DIMENSION A(1),B(1),C(1),D(1),V(1),BETA(102),GAMMA(102)
0003      BETA(IF)=B(IF)
0004      GAMMA(IF)=D(IF)/BETA(IF)
0005      IFP1=IF+1
0006      DO 1 I=IFP1,L
0007      BETA(I)=B(I)-A(I)*C(I-1)/BETA(I-1)
0008  1     GAMMA(I)=(D(I)-A(I)*GAMMA(I-1))/BETA(I)
0009      V(L)=GAMMA(L)
0010      LAST=L-IF
0011      DO 2 K=1,LAST
0012      I=L-K
0013  2     V(I)=GAMMA(I)-C(I)*V(I+1)/BETA(I)
0014      RETURN
0015      END

```

INPUT DATA

AL =0.0011
 RHO=1.16
 CFI=0.33
 EA =16080.
 AA =1.2E8
 A1 =-0.00333
 AB =0.3
 PR =1.43

TO =301.5
 TAMB=301.5
 CA0 =1.16
 H =1.8
 CAF =2.65
 A2 =0.0
 AC =0.00002

M =20
 DT =0.001
 DX =0.05
 PRINT=50
 CONV =0.01
 A3 =-74.0
 PU =0.75

B,PK,DTK,DTAD,DDK,CATA
 26.8411 0.7787 0.0006 0.0101 0.0000 0.0795
 TIME= 2.209 SECONDS
 TEMPERATURES
 301.5129 301.5129 301.5129 301.5129 301.5129 301.5129
 301.5129 301.5129 301.5129 301.5129 301.5125
 CONCENTRATIONS
 0.9899 0.9899 0.9899 0.9899 0.9899 0.9899
 0.9899 0.9899 0.9899 0.9899 0.9899
 TIME= 50.809 SECONDS
 TEMPERATURES
 301.8100 301.8100 301.8099 301.8098 301.8098 301.8098
 301.8096 301.8084 301.8036 301.7880 301.7457
 CONCENTRATIONS
 0.9886 0.9886 0.9886 0.9886 0.9886 0.9886
 0.9886 0.9886 0.9886 0.9886 0.9886
 TIME= 101.618 SECONDS
 TEMPERATURES
 302.1488 302.1488 302.1488 302.1487 302.1483 302.1471
 302.1434 302.1338 302.1115 302.0640 301.9715
 CONCENTRATIONS
 0.9871 0.9871 0.9871 0.9871 0.9871 0.9871
 0.9871 0.9871 0.9871 0.9871 0.9871

TIME= 150.218 SECONDS

TEMPERATURES

302.5024	302.5024	302.5021	302.5013	302.4991	302.4939
302.4823	302.4584	302.4122	302.3287	302.1863	

CONCENTRATIONS

0.9855	0.9855	0.9855	0.9855	0.9855	0.9855
0.9855	0.9855	0.9855	0.9855	0.9856	

TIME= 201.027 SECONDS

TEMPERATURES

302.9055	302.9052	302.9040	302.9011	302.8949	302.8821
302.8578	302.8137	302.7377	302.6125	302.4157	

CONCENTRATIONS

0.9837	0.9837	0.9837	0.9837	0.9837	0.9837
0.9837	0.9837	0.9837	0.9838	0.9838	

TIME= 251.836 SECONDS

TEMPERATURES

303.3459	303.3450	303.3419	303.3351	303.3222	303.2985
303.2573	303.1885	303.0782	302.9076	302.6537	

CONCENTRATIONS

0.9817	0.9817	0.9817	0.9817	0.9817	0.9817
0.9817	0.9818	0.9818	0.9819	0.9820	

TIME= 300.436 SECONDS

TEMPERATURES

303.8047	303.8029	303.7970	303.7848	303.7629	303.7257
303.6646	303.5681	303.4211	303.2037	302.8921	

CONCENTRATIONS

0.9796	0.9796	0.9797	0.9797	0.9797	0.9797
0.9797	0.9797	0.9798	0.9799	0.9800	

TIME= 351.245 SECONDS

TEMPERATURES

304.3278	304.3247	304.3145	304.2947	304.2608	304.2058
304.1202	303.9909	303.8012	303.5306	303.1549	

CONCENTRATIONS

0.9773	0.9773	0.9773	0.9773	0.9773	0.9773
0.9773	0.9774	0.9775	0.9777	0.9779	

TIME= 402.054 SECONDS

TEMPERATURES

304.8999	304.8950	304.8794	304.8498	304.8010	304.7250
304.6108	304.4441	304.2072	303.8788	303.4343	

CONCENTRATIONS

0.9746	0.9746	0.9746	0.9746	0.9747	0.9747
0.9748	0.9749	0.9750	0.9752	0.9756	

TIME= 450.655 SECONDS

TEMPERATURES

305.4986	305.4917	305.4696	305.4287	305.3628	305.2631
305.1173	304.9104	304.6235	304.2349	303.7198	

CONCENTRATIONS

0.9718	0.9718	0.9718	0.9719	0.9719	0.9720
0.9721	0.9722	0.9724	0.9727	0.9732	

TIME= 501.464 SECONDS

TEMPERATURES

306.1862	306.1765	306.1461	306.0909	306.0040	305.8753
305.6920	305.4375	305.0927	304.6353	304.0405	

CONCENTRATIONS

0.9686	0.9686	0.9686	0.9687	0.9687	0.9688
0.9690	0.9692	0.9695	0.9699	0.9705	

TIME= 550.065 SECONDS

TEMPERATURES

306.9113	306.8986	306.8587	306.7873	306.6767	306.5160
306.2913	305.9857	305.5791	305.0492	304.3716	

CONCENTRATIONS

0.9651	0.9652	0.9652	0.9652	0.9653	0.9655
0.9657	0.9660	0.9664	0.9670	0.9678	

TIME= 600.874 SECONDS

TEMPERATURES

307.7525	307.7358	307.6843	307.5926	307.4528	307.2531
306.9789	306.6124	306.1335	305.5198	304.7476	

CONCENTRATIONS

0.9611	0.9611	0.9612	0.9612	0.9614	0.9616
0.9619	0.9623	0.9629	0.9637	0.9647	

TIME= 651.683 SECONDS

TEMPERATURES

308.6945 308.6732 308.6074 308.4917 308.3174 308.0719

307.7401 307.3039 306.7430 306.0358 305.1593

CONCENTRATIONS

0.9565 0.9565 0.9566 0.9567 0.9569 0.9573

0.9577 0.9583 0.9591 0.9601 0.9614

TIME= 700.284 SECONDS

TEMPERATURES

309.7100 309.6833 309.6012 309.4578 309.2439 308.9468

308.5508 308.0378 307.3877 306.5799 305.5928

CONCENTRATIONS

0.9515 0.9515 0.9517 0.9518 0.9521 0.9526

0.9532 0.9540 0.9550 0.9564 0.9580

TIME= 751.093 SECONDS

TEMPERATURES

310.9199 310.8862 310.7831 310.6046 310.3408 309.9791

309.5035 308.8965 308.1390 307.2118 306.0956

CONCENTRATIONS

0.9455 0.9455 0.9457 0.9460 0.9464 0.9470

0.9479 0.9490 0.9503 0.9521 0.9542

TIME= 801.903 SECONDS

TEMPERATURES

312.3224 312.2799 312.1504 311.9278 311.6025 311.1616

310.5900 309.8710 308.9876 307.9227 306.6601

CONCENTRATIONS

0.9384 0.9385 0.9388 0.9392 0.9398 0.9407

0.9418 0.9433 0.9451 0.9474 0.9500

TIME= 850.503 SECONDS

TEMPERATURES

313.8995 313.8463 313.6846 313.4084 313.0085 312.4730

311.7882 310.9398 309.9131 308.6945 307.2716

CONCENTRATIONS

0.9304 0.9305 0.9309 0.9315 0.9324 0.9336

0.9351 0.9371 0.9395 0.9424 0.9456

TIME= 901.312 SECONDS

TEMPERATURES

315.8842	315.8160	315.6091	315.2588	314.7570	314.0941
313.2592	312.2422	311.0331	309.6233	308.0057	

CONCENTRATIONS

0.9202	0.9204	0.9209	0.9218	0.9231	0.9248
0.9270	0.9297	0.9328	0.9365	0.9406	

TIME= 952.122 SECONDS

TEMPERATURES

318.3625	318.2728	318.0022	317.5478	316.9050	316.0689
315.0348	313.7992	312.3597	310.7154	308.8660	

CONCENTRATIONS

0.9074	0.9077	0.9084	0.9098	0.9117	0.9142
0.9173	0.9209	0.9252	0.9299	0.9351	

TIME= 1000.722 SECONDS

TEMPERATURES

321.4469	321.3257	320.9623	320.3585	319.5173	318.4432
317.1428	315.6241	313.8961	311.9680	309.8485	

CONCENTRATIONS

0.8912	0.8916	0.8929	0.8949	0.8978	0.9015
0.9058	0.9109	0.9165	0.9227	0.9291	

TIME= 1051.532 SECONDS

TEMPERATURES

325.9645	325.7859	325.2555	324.3877	323.2053	321.7364
320.0114	318.0605	315.9120	313.5892	311.1125	

CONCENTRATIONS

0.8673	0.8680	0.8701	0.8736	0.8782	0.8840
0.8906	0.8979	0.9057	0.9138	0.9221	

TIME= 1100.132 SECONDS

TEMPERATURES

332.8606	332.5620	331.6874	330.2951	328.4668	326.2922
323.8554	321.2269	318.4610	315.5970	312.6637	

CONCENTRATIONS

0.8301	0.8315	0.8356	0.8421	0.8504	0.8601
0.8706	0.8816	0.8926	0.9036	0.9142	

TIME= 1150.941 SECONDS

TEMPERATURES

348.9536	348.1524	345.9084	342.6134	338.7089	334.5500
330.3639	326.2704	322.3192	318.5242	314.8899	

CONCENTRATIONS

0.7404	0.7451	0.7579	0.7761	0.7969	0.8180
0.8383	0.8571	0.8743	0.8900	0.9042	

TIME= 1201.751 SECONDS

TEMPERATURES

447.9292	447.6772	446.8331	445.0920	440.1277	374.5596
348.4808	337.0260	329.3282	323.3385	318.4108	

CONCENTRATIONS

0.0031	0.0034	0.0050	0.0113	0.0882	0.6568
0.7617	0.8117	0.8454	0.8708	0.8912	

B,PK,DTK,DTAD,DDK,CATA

26.8411	0.7787	0.0006	0.0101	0.0000	0.1020
---------	--------	--------	--------	--------	--------

TIME= 1250.351 SECONDS

TEMPERATURES

447.8273	447.6084	446.9576	445.8995	444.4922	442.8295
440.9562	438.8932	433.8345	368.1288	331.0689	

CONCENTRATIONS

0.0003	0.0003	0.0003	0.0004	0.0006	0.0009
0.0017	0.0044	0.0226	0.8079	0.8717	

B,PK,DTK,DTAD,DDK,CATA

26.8411	0.7787	0.0006	0.0101	0.0000	0.1020
---------	--------	--------	--------	--------	--------

B,PK,DTK,DTAD,DDK,CATA

26.8411	0.7787	0.0004	0.0101	0.0000	0.0765
---------	--------	--------	--------	--------	--------

B,PK,DTK,DTAD,DDK,CATA

26.8411	0.7787	0.0003	0.0101	0.0000	0.0574
---------	--------	--------	--------	--------	--------

TIME= 1300.609 SECONDS

TEMPERATURES

447.3611	447.1536	446.5425	445.5620	444.2715	442.7646
441.2399	440.1466	439.3625	433.4597	408.9767	

CONCENTRATIONS

0.0001	0.0001	0.0001	0.0001	0.0002	0.0002
0.0003	0.0005	0.0007	0.0011	0.0027	

B,PK,DTK,DTAD,DDK,CATA						
26.8411	0.7787	0.0003	0.0101	0.0000	0.0574	
B,PK,DTK,DTAD,DDK,CATA						
26.8411	0.7787	0.0005	0.0101	0.0000	0.0820	
B,PK,DTK,DTAD,DDK,CATA						
26.8411	0.7787	0.0007	0.0101	0.0000	0.1173	
B,PK,DTK,DTAD,DDK,CATA						
26.8411	0.7787	0.0010	0.0101	0.0000	0.1678	
B,PK,DTK,DTAD,DDK,CATA						
26.8411	0.7787	0.0014	0.0101	0.0000	0.2399	
TIME=	1354.581	SECONDS				
TEMPERATURES						
446.8721	446.6795	446.1147	445.2193	444.0606	442.6802	
440.8609	437.5504	430.1911	415.0935	389.8466		
CONCENTRATIONS						
0.0000	0.0000	0.0000	0.0001	0.0001	0.0001	
0.0001	0.0002	0.0002	0.0004	0.0017		
B,PK,DTK,DTAD,DDK,CATA						
26.8411	0.7787	0.0014	0.0101	0.0000	0.2399	
B,PK,DTK,DTAD,DDK,CATA						
26.8411	0.7787	0.0020	0.0101	0.0000	0.3431	
B,PK,DTK,DTAD,DDK,CATA						
26.8411	0.7787	0.0028	0.0101	0.0000	0.4906	
TIME=	1408.516	SECONDS				
TEMPERATURES						
446.4168	446.2389	445.7115	444.8370	443.5476	441.5564	
438.1285	431.8980	421.0178	403.8693	380.0705		
CONCENTRATIONS						
0.0000	0.0000	0.0000	0.0000	0.0000	0.0000	
0.0001	0.0001	0.0001	0.0003	0.0014		
B,PK,DTK,DTAD,DDK,CATA						
26.8411	0.7787	0.0028	0.0101	0.0000	0.3607	
B,PK,DTK,DTAD,DDK,CATA						
26.8411	0.7787	0.0040	0.0101	0.0000	0.5159	

TIME= 1454.099 SECONDS

TEMPERATURES

446.0468	445.8657	445.3051	444.2884	442.5993	439.7654
434.9674	427.1239	415.3678	399.7523	381.1547	

CONCENTRATIONS

0.0000	0.0000	0.0000	0.0000	0.0000	0.0000
0.0000	0.0001	0.0001	0.0003	0.0012	

B,PK,DTK,DTAD,DDK,CATA

26.8411	0.7787	0.0040	0.0101	0.0000	0.5159
---------	--------	--------	--------	--------	--------

B,PK,DTK,DTAD,DDK,CATA

26.8411	0.7787	0.0057	0.0101	0.0001	0.7377
---------	--------	--------	--------	--------	--------

TIME= 1506.217 SECONDS

TEMPERATURES

445.5814	445.3635	444.6635	443.3232	441.0255	437.2603
431.3652	422.6892	410.8252	395.7589	377.8567	

CONCENTRATIONS

0.0000	0.0000	0.0000	0.0000	0.0000	0.0000
0.0000	0.0000	0.0001	0.0002	0.0011	

B,PK,DTK,DTAD,DDK,CATA

26.8411	0.7787	0.0057	0.0101	0.0001	0.7377
---------	--------	--------	--------	--------	--------

B,PK,DTK,DTAD,DDK,CATA

26.8411	0.7787	0.0082	0.0101	0.0001	1.0549
---------	--------	--------	--------	--------	--------

TIME= 1580.745 SECONDS

TEMPERATURES

444.6886	444.3721	443.3573	441.4480	438.3212	433.5565
426.7030	417.3787	405.3740	390.7198	373.6929	

CONCENTRATIONS

0.0000	0.0000	0.0000	0.0000	0.0000	0.0000
0.0000	0.0000	0.0001	0.0002	0.0010	

B,PK,DTK,DTAD,DDK,CATA

26.8411	0.7787	0.0082	0.0101	0.0001	1.0549
---------	--------	--------	--------	--------	--------

TIME= 1611.816 SECONDS

TEMPERATURES

444.2090	443.8456	442.6903	440.5515	437.1261	432.0366
424.8950	415.3871	403.3543	388.8459	372.1304	

CONCENTRATIONS

0.0000	0.0000	0.0000	0.0000	0.0000	0.0000
0.0000	0.0000	0.0001	0.0002	0.0009	
B,FK,DTK,DTAD,DDK,CATA					
26.8411	0.7787	0.0082	0.0101	0.0001	1.0549
B,FK,DTK,DTAD,DDK,CATA					
26.8411	0.7787	0.0117	0.0101	0.0001	1.5085
TIME= 1656.248 SECONDS					

TEMPERATURES

443.4072	442.9785	441.6314	439.1906	435.3884	429.9048
422.4273	412.7182	400.6773	386.3822	370.0905	

CONCENTRATIONS

0.0000	0.0000	0.0000	0.0000	0.0000	0.0000
0.0000	0.0000	0.0001	0.0002	0.0009	
B,FK,DTK,DTAD,DDK,CATA					
26.8411	0.7787	0.0117	0.0101	0.0001	1.5085
TIME= 1700.680 SECONDS					

TEMPERATURES

442.4748	441.9857	440.4646	437.7571	433.6327	427.8250
420.0837	410.2317	398.2141	384.1274	368.2211	

CONCENTRATIONS

0.0000	0.0000	0.0000	0.0000	0.0000	0.0000
0.0000	0.0000	0.0001	0.0002	0.0008	
B,FK,DTK,DTAD,DDK,CATA					
26.8411	0.7787	0.0117	0.0101	0.0001	1.5085
B,FK,DTK,DTAD,DDK,CATA					
26.8411	0.7787	0.0168	0.0101	0.0002	2.1571
TIME= 1764.218 SECONDS					

TEMPERATURES

440.9364	440.3728	438.6386	435.6109	431.1104	424.9374
416.9155	406.9364	394.9950	381.2091	365.8157	

CONCENTRATIONS

0.0000	0.0000	0.0000	0.0000	0.0000	0.0000
0.0000	0.0000	0.0001	0.0002	0.0008	

B,PK,DTK,DTAD,DDK,CATA						
26.8411	0.7787	0.0168	0.0101	0.0002	2.1571	
TIME= 1827.756 SECONDS						
TEMPERATURES						
439.1955	438.5721	436.6683	433.3902	428.6039	422.1659	
413.9587	403.9258	392.0972	378.6030	363.6694		
CONCENTRATIONS						
0.0000	0.0000	0.0000	0.0000	0.0000	0.0000	
0.0000	0.0000	0.0001	0.0001	0.0007		
B,PK,DTK,DTAD,DDK,CATA						
26.8411	0.7787	0.0168	0.0101	0.0002	2.1571	
B,PK,DTK,DTAD,DDK,CATA						
26.8411	0.7787	0.0240	0.0101	0.0002	3.0847	
TIME= 1918.615 SECONDS						
TEMPERATURES						
436.4231	435.7361	433.6539	430.1175	425.0462	418.3606	
410.0080	399.9869	388.3640	375.2812	360.9489		
CONCENTRATIONS						
0.0000	0.0000	0.0000	0.0000	0.0000	0.0000	
0.0000	0.0000	0.0000	0.0001	0.0007		

B,PK,DTK,DTAD,DDK,CATA						
26.8411	0.7787	0.0006	0.0101	0.0000	0.0000	
TIME=	2.209 SECONDS					
TEMPERATURES						Adiabatic
301.5129	301.5129	301.5129	301.5129	301.5129	301.5129	solution
301.5129	301.5129	301.5129	301.5129	301.5129	301.5129	
CONCENTRATIONS						
0.9899	0.9899	0.9899	0.9899	0.9899	0.9899	
0.9899	0.9899	0.9899	0.9899	0.9899	0.9899	
TIME=	50.809 SECONDS					
TEMPERATURES						
301.8100	301.8100	301.8099	301.8098	301.8098	301.8098	
301.8098	301.8098	301.8098	301.8098	301.8099	301.8098	
CONCENTRATIONS						
0.9886	0.9886	0.9886	0.9886	0.9886	0.9886	
0.9886	0.9886	0.9886	0.9886	0.9886	0.9886	
TIME=	101.618 SECONDS					
TEMPERATURES						
302.1488	302.1488	302.1489	302.1489	302.1489	302.1489	
302.1489	302.1489	302.1489	302.1489	302.1489	302.1489	
CONCENTRATIONS						
0.9871	0.9871	0.9871	0.9871	0.9871	0.9871	
0.9871	0.9871	0.9871	0.9871	0.9871	0.9871	
TIME=	150.218 SECONDS					
TEMPERATURES						
302.5026	302.5026	302.5026	302.5027	302.5027	302.5027	
302.5027	302.5027	302.5027	302.5027	302.5026	302.5026	
CONCENTRATIONS						
0.9855	0.9855	0.9855	0.9855	0.9855	0.9855	
0.9855	0.9855	0.9855	0.9855	0.9855	0.9855	
TIME=	201.027 SECONDS					
TEMPERATURES						
302.9063	302.9063	302.9063	302.9064	302.9064	302.9064	
302.9064	302.9064	302.9064	302.9064	302.9064	302.9064	

CONCENTRATIONS

0.9837	0.9837	0.9837	0.9837	0.9837	0.9837
0.9837	0.9837	0.9837	0.9837	0.9837	

TIME= 251.836 SECONDS

TEMPERATURES

303.3487	303.3487	303.3487	303.3487	303.3487	303.3487
303.3487	303.3487	303.3487	303.3487	303.3487	

CONCENTRATIONS

0.9817	0.9817	0.9817	0.9817	0.9817	0.9817
0.9817	0.9817	0.9817	0.9817	0.9817	

TIME= 300.436 SECONDS

TEMPERATURES

303.8120	303.8120	303.8120	303.8120	303.8120	303.8120
303.8120	303.8120	303.8120	303.8120	303.8120	

CONCENTRATIONS

0.9796	0.9796	0.9796	0.9796	0.9796	0.9796
0.9796	0.9796	0.9796	0.9796	0.9796	

TIME= 351.245 SECONDS

TEMPERATURES

304.3437	304.3437	304.3436	304.3437	304.3437	304.3437
304.3437	304.3437	304.3437	304.3437	304.3438	

CONCENTRATIONS

0.9773	0.9773	0.9773	0.9773	0.9773	0.9773
0.9773	0.9773	0.9773	0.9773	0.9773	

TIME= 402.054 SECONDS

TEMPERATURES

304.9302	304.9302	304.9302	304.9303	304.9303	304.9303
304.9303	304.9303	304.9303	304.9303	304.9303	

CONCENTRATIONS

0.9746	0.9746	0.9746	0.9746	0.9746	0.9746
0.9746	0.9746	0.9746	0.9746	0.9746	

TIME= 450.655 SECONDS

TEMPERATURES

305.5503	305.5503	305.5503	305.5503	305.5503	305.5502
305.5502	305.5502	305.5502	305.5502	305.5502	

CONCENTRATIONS

0.9718	0.9718	0.9718	0.9718	0.9718	0.9718
0.9718	0.9718	0.9718	0.9718	0.9718	

TIME= 501.464 SECONDS

TEMPERATURES

306.2698	306.2699	306.2699	306.2698	306.2698	306.2698
306.2698	306.2698	306.2698	306.2698	306.2698	

CONCENTRATIONS

0.9686	0.9686	0.9686	0.9686	0.9686	0.9686
0.9686	0.9686	0.9686	0.9686	0.9686	

TIME= 550.065 SECONDS

TEMPERATURES

307.0381	307.0381	307.0381	307.0381	307.0381	307.0381
307.0381	307.0381	307.0381	307.0381	307.0381	

CONCENTRATIONS

0.9651	0.9651	0.9651	0.9651	0.9651	0.9651
0.9651	0.9651	0.9651	0.9651	0.9651	

TIME= 600.874 SECONDS

TEMPERATURES

307.9409	307.9409	307.9409	307.9409	307.9409	307.9409
307.9409	307.9409	307.9409	307.9409	307.9409	

CONCENTRATIONS

0.9610	0.9610	0.9610	0.9610	0.9610	0.9610
0.9610	0.9610	0.9610	0.9610	0.9610	

TIME= 651.683 SECONDS

TEMPERATURES

308.9673	308.9673	308.9673	308.9673	308.9672	308.9671
308.9671	308.9671	308.9671	308.9671	308.9671	

CONCENTRATIONS

0.9563	0.9563	0.9563	0.9563	0.9563	0.9563
0.9563	0.9563	0.9563	0.9563	0.9563	

TIME= 700.284 SECONDS

TEMPERATURES

310.0919	310.0919	310.0919	310.0919	310.0919	310.0919
310.0919	310.0919	310.0919	310.0919	310.0919	

CONCENTRATIONS

0.9511 0.9511 0.9511 0.9511 0.9511 0.9511
 0.9511 0.9511 0.9511 0.9511 0.9511

TIME= 751.093 SECONDS

TEMPERATURES

311.4567 311.4567 311.4567 311.4567 311.4567 311.4567
 311.4567 311.4567 311.4567 311.4567 311.4567

CONCENTRATIONS

0.9448 0.9448 0.9448 0.9448 0.9448 0.9448
 0.9448 0.9448 0.9448 0.9448 0.9448

TIME= 801.903 SECONDS

TEMPERATURES

313.0746 313.0746 313.0746 313.0746 313.0746 313.0746
 313.0746 313.0746 313.0746 313.0746 313.0746

CONCENTRATIONS

0.9374 0.9374 0.9374 0.9374 0.9374 0.9374
 0.9374 0.9374 0.9374 0.9374 0.9374

TIME= 850.503 SECONDS

TEMPERATURES

314.9437 314.9437 314.9436 314.9436 314.9436 314.9436
 314.9436 314.9436 314.9436 314.9436 314.9436

CONCENTRATIONS

0.9287 0.9287 0.9287 0.9287 0.9287 0.9287
 0.9287 0.9287 0.9287 0.9287 0.9287

TIME= 901.312 SECONDS

TEMPERATURES

317.3798 317.3797 317.3796 317.3796 317.3795 317.3795
 317.3795 317.3795 317.3795 317.3795 317.3795

CONCENTRATIONS

0.9173 0.9173 0.9173 0.9173 0.9173 0.9173
 0.9173 0.9173 0.9173 0.9173 0.9173

B,PK,DTK,DTAD,DDK,CATA

26.8411 0.7787 0.0006 0.0101 0.0000 0.0000

TIME= 952.122 SECONDS

TEMPERATURES

320.5777	320.5778	320.5778	320.5778	320.5777	320.5776
320.5776	320.5775	320.5775	320.5776	320.5776	

CONCENTRATIONS

0.9021	0.9021	0.9021	0.9021	0.9021	0.9021
0.9021	0.9021	0.9021	0.9021	0.9021	

B,PK,DTK,DTAD,DDK,CATA

26.8411	0.7787	0.0006	0.0101	0.0000	0.0000
---------	--------	--------	--------	--------	--------

TIME= 1000.722 SECONDS

TEMPERATURES

324.8695	324.8695	324.8695	324.8695	324.8693	324.8693
324.8693	324.8691	324.8690	324.8690	324.8690	

CONCENTRATIONS

0.8816	0.8816	0.8816	0.8816	0.8816	0.8816
0.8816	0.8816	0.8816	0.8816	0.8816	

B,PK,DTK,DTAD,DDK,CATA

26.8411	0.7787	0.0006	0.0101	0.0000	0.0000
---------	--------	--------	--------	--------	--------

TIME= 1051.532 SECONDS

TEMPERATURES

332.0827	332.0827	332.0826	332.0826	332.0825	332.0823
332.0822	332.0822	332.0821	332.0820	332.0820	

CONCENTRATIONS

0.8464	0.8464	0.8464	0.8464	0.8464	0.8464
0.8464	0.8464	0.8464	0.8464	0.8464	

B,PK,DTK,DTAD,DDK,CATA

26.8411	0.7787	0.0006	0.0101	0.0000	0.0000
---------	--------	--------	--------	--------	--------

TIME= 1100.132 SECONDS

TEMPERATURES

347.5419	347.5419	347.5418	347.5416	347.5414	347.5412
347.5408	347.5405	347.5402	347.5400	347.5399	

CONCENTRATIONS

0.7677	0.7677	0.7677	0.7677	0.7677	0.7677
0.7677	0.7677	0.7677	0.7677	0.7677	

B,PK,DTK,DTAD,DDK,CATA						
26.8411	0.7787	0.0006	0.0101	0.0000	0.0000	
TIME=	1150.941	SECONDS				
TEMPERATURES						
450.8959	450.8959	450.8959	450.8958	450.8957	450.8956	
450.8954	450.8954	450.8953	450.8952	450.8952		
CONCENTRATIONS						
0.0023	0.0023	0.0023	0.0023	0.0023	0.0023	
0.0023	0.0023	0.0023	0.0023	0.0023		
B,PK,DTK,DTAD,DDK,CATA						
26.8411	0.7787	0.0006	0.0101	0.0000	0.0000	
B,PK,DTK,DTAD,DDK,CATA						
26.8411	0.7787	0.0008	0.0101	0.0000	0.0000	
B,PK,DTK,DTAD,DDK,CATA						
26.8411	0.7787	0.0012	0.0101	0.0000	0.0000	
TIME=	1201.541	SECONDS				
TEMPERATURES						
451.1882	451.1883	451.1882	451.1882	451.1882	451.1881	
451.1880	451.1880	451.1879	451.1879	451.1878		
CONCENTRATIONS						
0.0002	0.0002	0.0002	0.0002	0.0002	0.0002	
0.0002	0.0002	0.0002	0.0002	0.0002		
B,PK,DTK,DTAD,DDK,CATA						
26.8411	0.7787	0.0012	0.0101	0.0000	0.0000	
B,PK,DTK,DTAD,DDK,CATA						
26.8411	0.7787	0.0017	0.0101	0.0000	0.0000	
B,PK,DTK,DTAD,DDK,CATA						
26.8411	0.7787	0.0024	0.0101	0.0000	0.0000	
B,PK,DTK,DTAD,DDK,CATA						
26.8411	0.7787	0.0035	0.0101	0.0000	0.0000	
B,PK,DTK,DTAD,DDK,CATA						
26.8411	0.7787	0.0050	0.0101	0.0001	0.0000	
TIME=	1260.315	SECONDS				
TEMPERATURES						
451.2071	451.2071	451.2071	451.2070	451.2069	451.2069	
451.2068	451.2068	451.2067	451.2067	451.2067		

CONCENTRATIONS

0.0001	0.0001	0.0001	0.0001	0.0001	0.0001
0.0001	0.0001	0.0001	0.0001	0.0001	
B,PK,DTK,DTAD,DDK,CATA					
26.8411	0.7787	0.0050	0.0101	0.0001	0.0000
B,PK,DTK,DTAD,DDK,CATA					
26.8411	0.7787	0.0071	0.0101	0.0001	0.0000
B,PK,DTK,DTAD,DDK,CATA					
26.8411	0.7787	0.0102	0.0101	0.0001	0.0000
B,PK,DTK,DTAD,DDK,CATA					
26.8411	0.7787	0.0146	0.0101	0.0001	0.0000

TIME= 1342.565 SECONDS

TEMPERATURES

451.2114	451.2114	451.2114	451.2113	451.2113	451.2114
451.2112	451.2112	451.2111	451.2111	451.2111	

CONCENTRATIONS

0.0000	0.0000	0.0000	0.0000	0.0000	0.0000
0.0000	0.0000	0.0000	0.0000	0.0000	
B,PK,DTK,DTAD,DDK,CATA					
26.8411	0.7787	0.0146	0.0101	0.0001	0.0000
B,PK,DTK,DTAD,DDK,CATA					
26.8411	0.7787	0.0209	0.0101	0.0002	0.0000
B,PK,DTK,DTAD,DDK,CATA					
26.8411	0.7787	0.0299	0.0101	0.0003	0.0000
B,PK,DTK,DTAD,DDK,CATA					
26.8411	0.7787	0.0427	0.0101	0.0004	0.0000

TIME= 1504.093 SECONDS

TEMPERATURES

451.2120	451.2120	451.2120	451.2122	451.2122	451.2121
451.2121	451.2119	451.2118	451.2117	451.2116	

CONCENTRATIONS

0.0000	0.0000	0.0000	0.0000	0.0000	0.0000
0.0000	0.0000	0.0000	0.0000	0.0000	

APPENDIX B

This section presents the original outputs of the DSC studies.

SAMPLE: POLYESTER	SIZE 20.98 mg	ATM. air 760 MM	RUN NO. 2b
	REF. empty	T	DATE 4/14/77
ORIGIN:	PROG. MODE Isothermal	SCALE 100 °C IN.	OPERATOR Selami
	RATE 5 °C MIN. START °C	SHIFT - IN.	BASE LINE SLOPE
		ΔT	
		0.5 °C IN.	

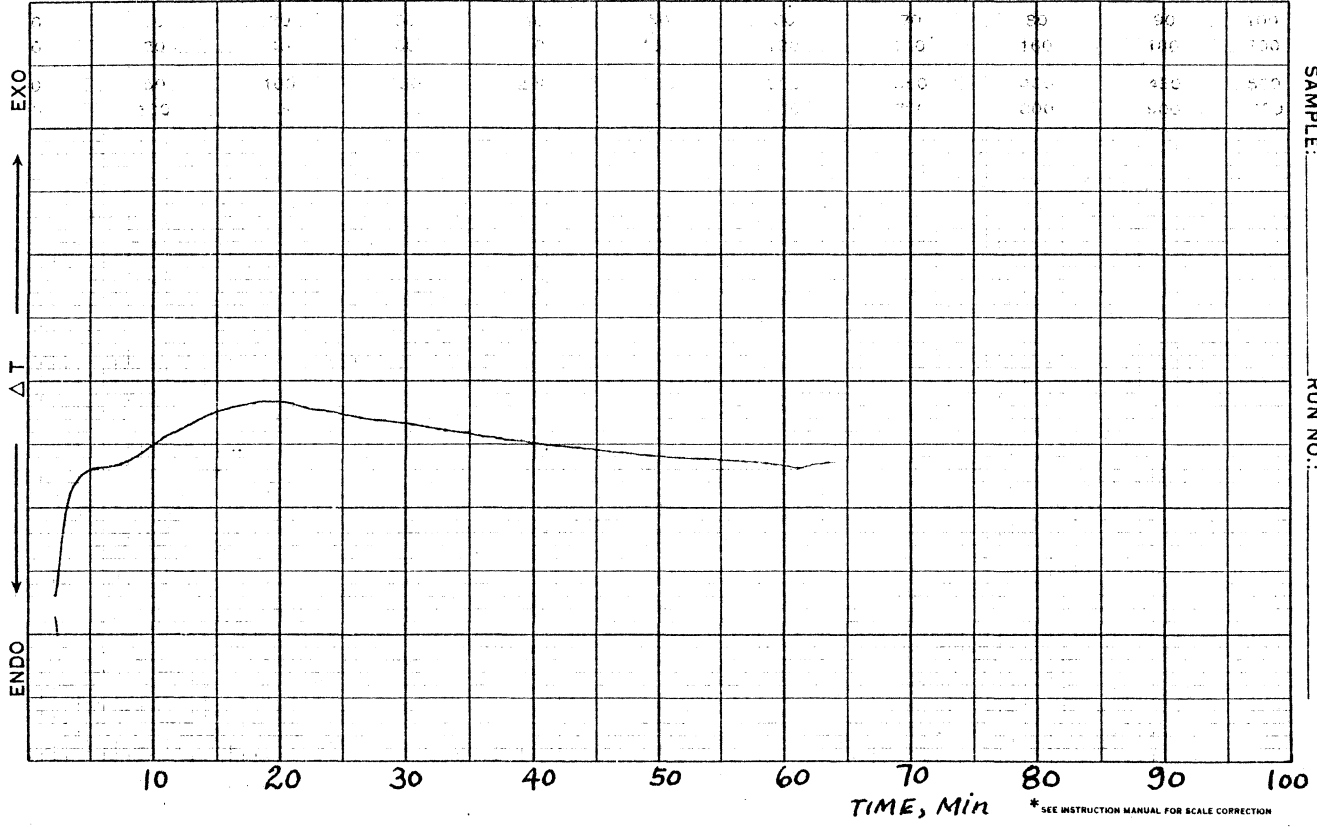


Figure 41. Isothermal curing at 82°C.

SAMPLE: POLYESTER	SIZE 20.98 mg	ATM. air 760 MM	RUN NO. 2b
ORIGIN:	REF. empty	T	DATE 4/14/77
	PROG. MODE Heat	SCALE 50 $\frac{^{\circ}\text{C}}{\text{IN}}$	OPERATOR Selami
	RATE 10 $\frac{^{\circ}\text{C}}{\text{MIN}}$, START $^{\circ}\text{C}$	SHIFT - IN.	BASE LINE SLOPE

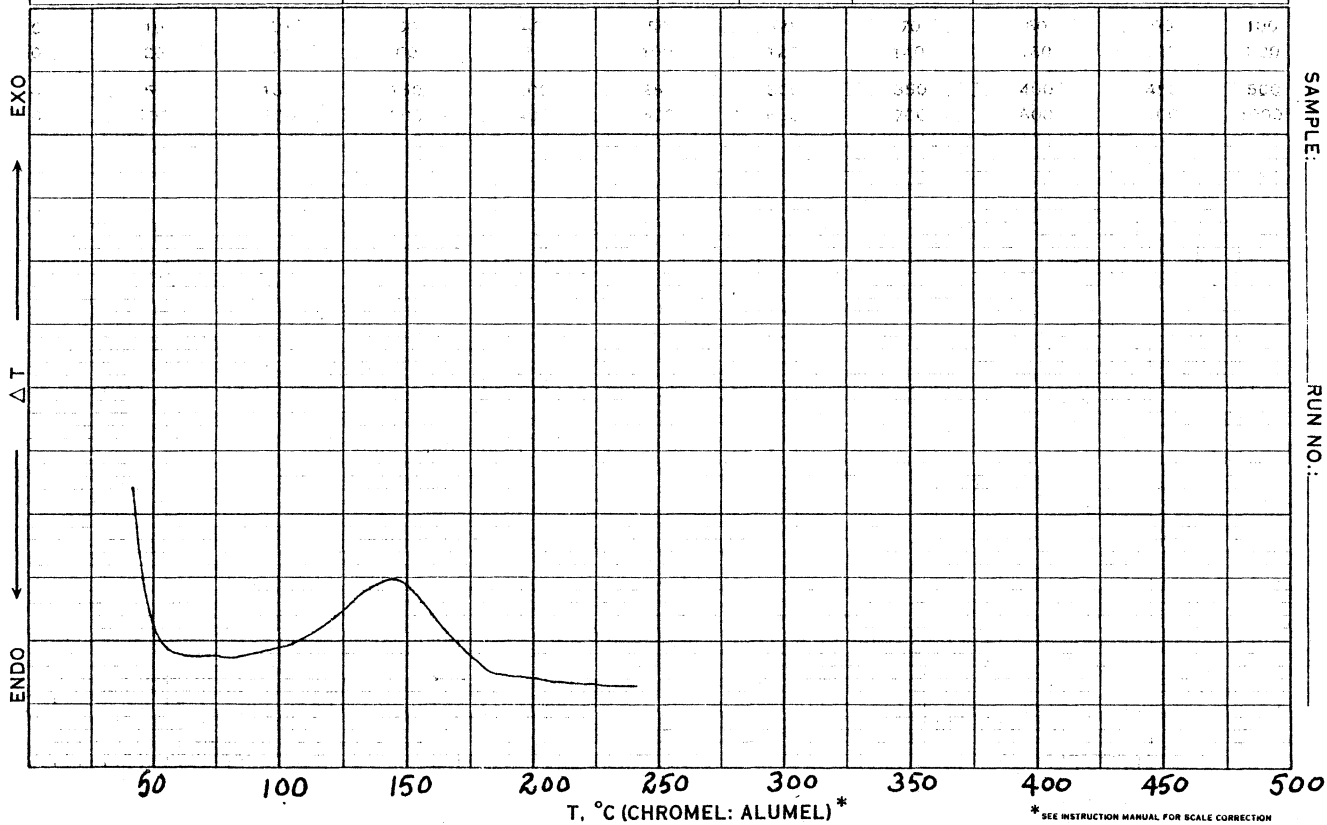


Figure 42. Rescanning of sample previously cured at 82°C.

SAMPLE:	SIZE 24.36 mg	ATM. air 760 MM	RUN NO. 3
POLYESTER	REF. empty	T	DATE 4/14/77
ORIGIN:	PROG. MODE Isothermal	SCALE 50 $\frac{^{\circ}\text{C}}{\text{IN}}$	OPERATOR Selami
	RATE 5 $\frac{^{\circ}\text{C}}{\text{MIN}}$, START $^{\circ}\text{C}$	SHIFT - IN.	BASE LINE SLOPE

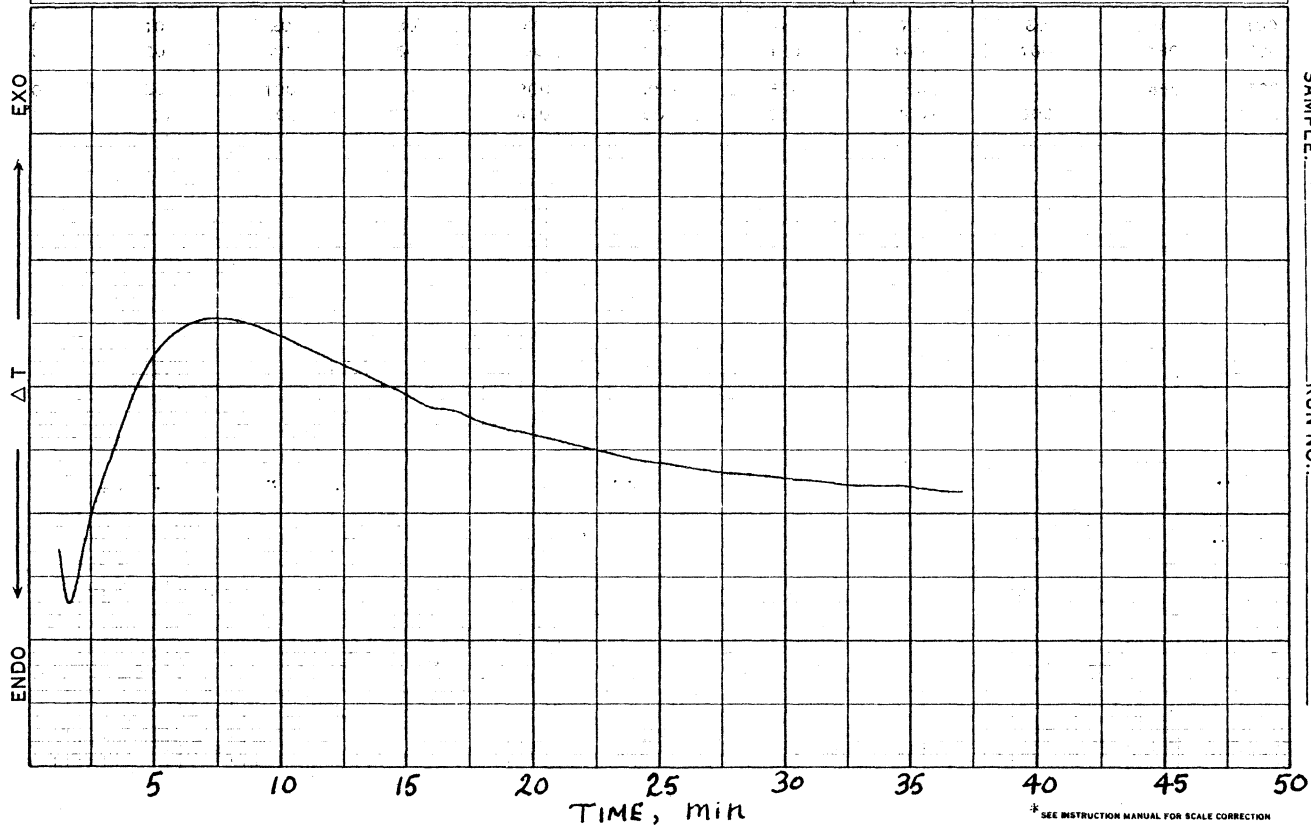


Figure 43. Isothermal curing at 93°C.

SAMPLE: Polyester	SIZE 24.36 mg	ATM. air 760 MM	RUN NO. 3
	REF. empty	T	ΔT
ORIGIN:	PROG. MODE Heat	SCALE 50 $\frac{^{\circ}\text{C}}{\text{IN}}$	DATE 4/14/77
	RATE 10 $\frac{^{\circ}\text{C}}{\text{MIN}}$, START $^{\circ}\text{C}$	SHIFT - IN.	OPERATOR SELAMI
			BASE LINE SLOPE

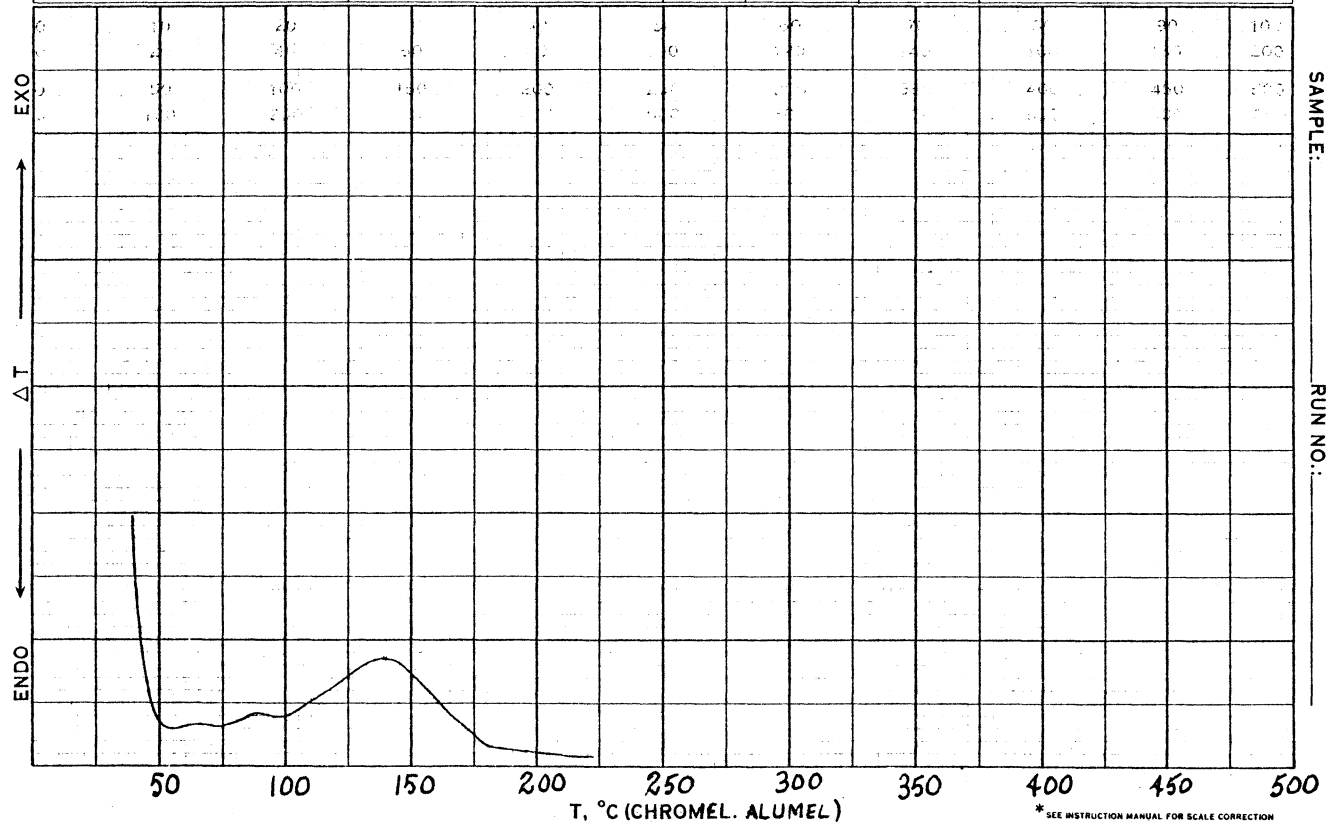


Figure 44. Rescanning of sample previously cured at 93°C.

SAMPLE: POLYESTER	SIZE 24.83mg	ATM. air 760 MM	RUN NO. 4
	REF. Empty	T	ΔT
ORIGIN:	PROG. MODE Isothermal	SCALE 20 $\frac{^{\circ}\text{C}}{\text{IN}}$	DATE 4/15/77
	RATE 5 $\frac{^{\circ}\text{C}}{\text{MIN}}$, START $^{\circ}\text{C}$	SHIFT - IN.	OPERATOR Selami
			BASE LINE SLOPE

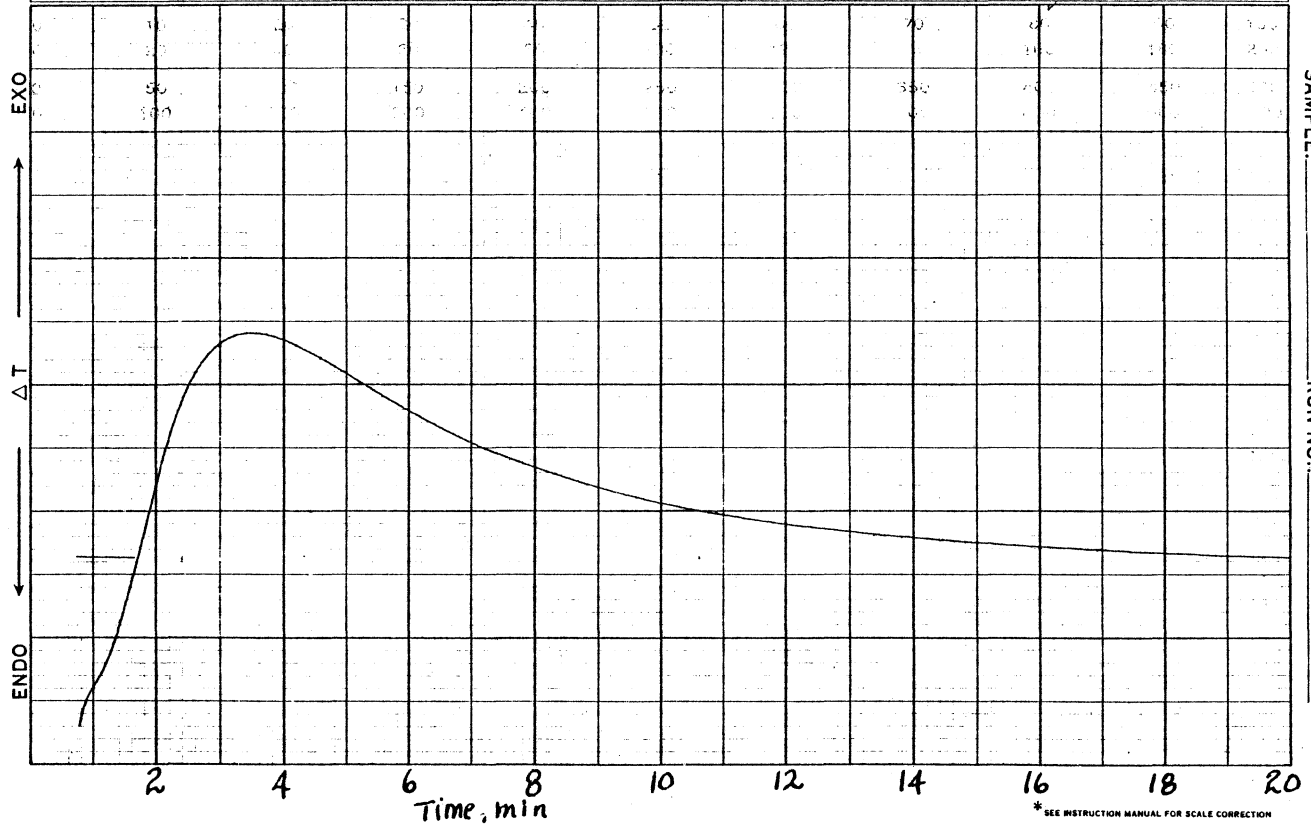


Figure 45. Isothermal curing at 105°C.

SAMPLE: <i>Polyester</i>	SIZE <i>24.83 mg</i>	ATM. <i>air</i> <i>760</i> MM	RUN NO. <i>4</i>
	REF. <i>empty</i>	T	ΔT
ORIGIN:	PROG. MODE <i>Heat</i>	SCALE <i>50</i> $\frac{^{\circ}\text{C}}{\text{IN}}$	DATE <i>4/15/77</i>
	RATE <i>10</i> $\frac{^{\circ}\text{C}}{\text{MIN}}$, START $^{\circ}\text{C}$	SHIFT <i>-</i> IN.	OPERATOR <i>Selami</i>
			BASE LINE SLOPE

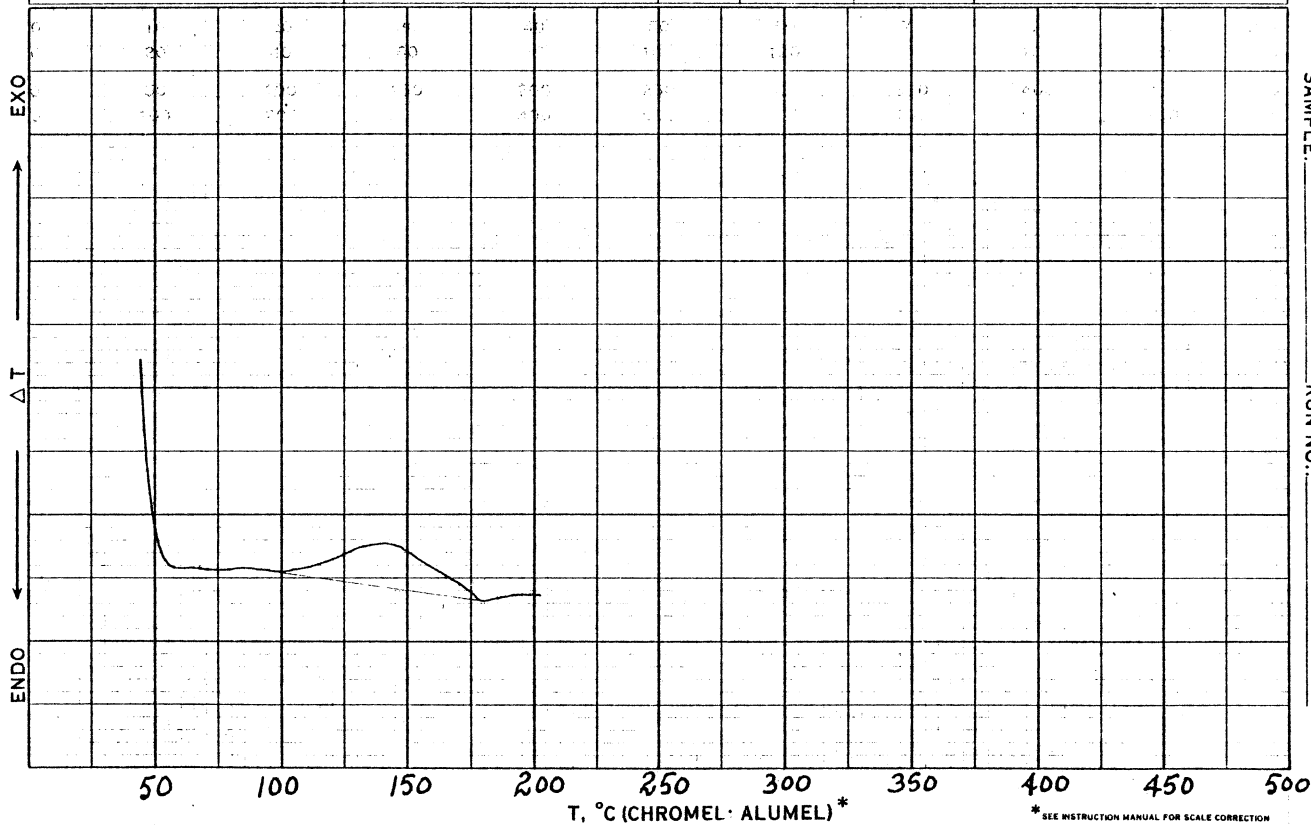


Figure 46. Rescanning of sample previously cured at 105°C.

SAMPLE: UNSATURATED POLYESTER	SIZE <i>20.15 mg</i>	ATM. <i>air</i> 760 MM	RUN NO. <i>5</i>
	REF. <i>Empty</i>	T	ΔT
	PROG. MODE <i>Isothermal</i>	SCALE <i>10</i> $\frac{^{\circ}\text{C}}{\text{IN}}$	<i>2</i> $\frac{^{\circ}\text{C}}{\text{IN}}$
ORIGIN:	RATE <i>5</i> $\frac{^{\circ}\text{C}}{\text{MIN}}$ START $^{\circ}\text{C}$	SHIFT - IN. - IN.	OPERATOR <i>Selami</i>
			BASE LINE SLOPE

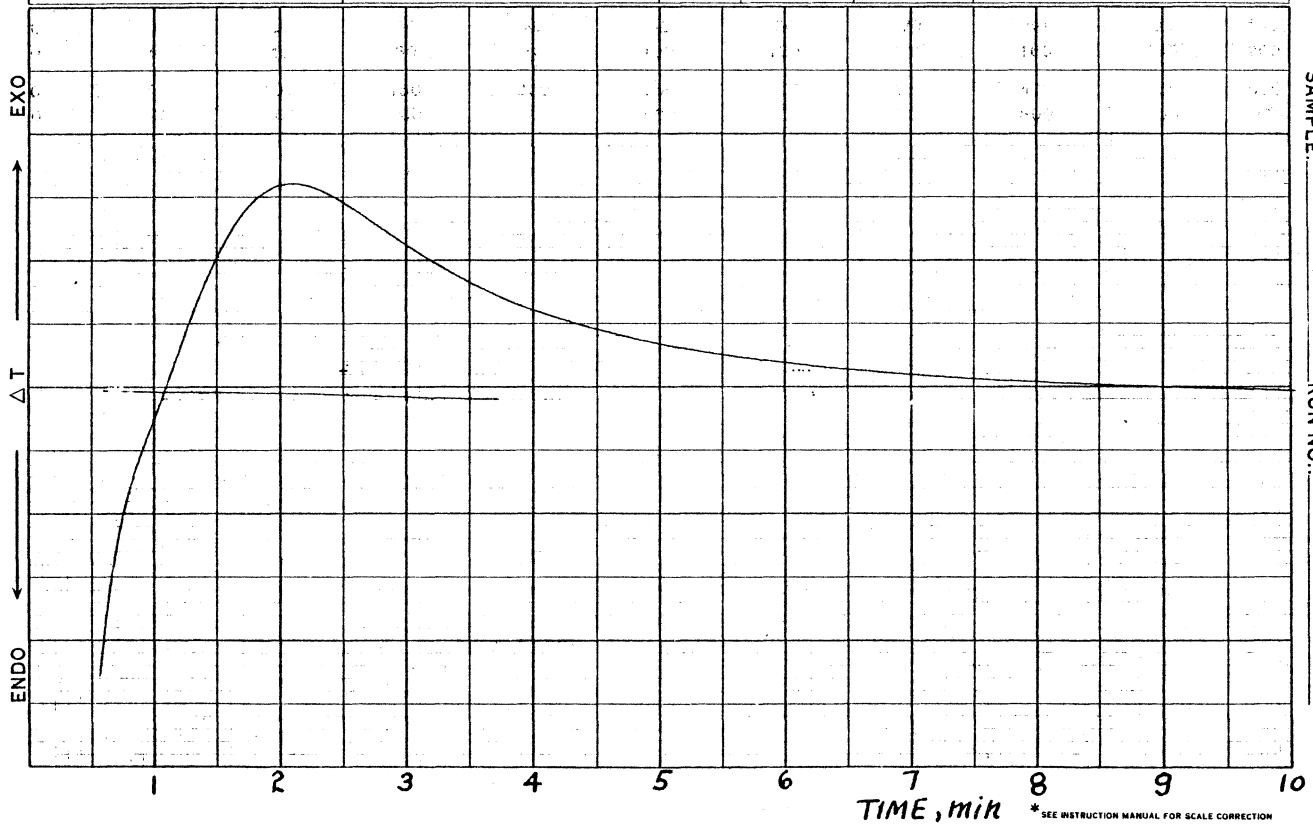


Figure 47. Isothermal curing at 122°C.

SAMPLE: Polyester	SIZE 20.15 mg	ATM. air 760 MM	RUN NO. 5
	REF. empty	T	ΔT
ORIGIN:	PROG. MODE Heat	SCALE 50 $\frac{^{\circ}\text{C}}{\text{IN}}$	DATE 4/15/77
	RATE 10 $\frac{^{\circ}\text{C}}{\text{MIN}}$, START $^{\circ}\text{C}$	SHIFT - IN.	OPERATOR Selami
			BASE LINE SLOPE

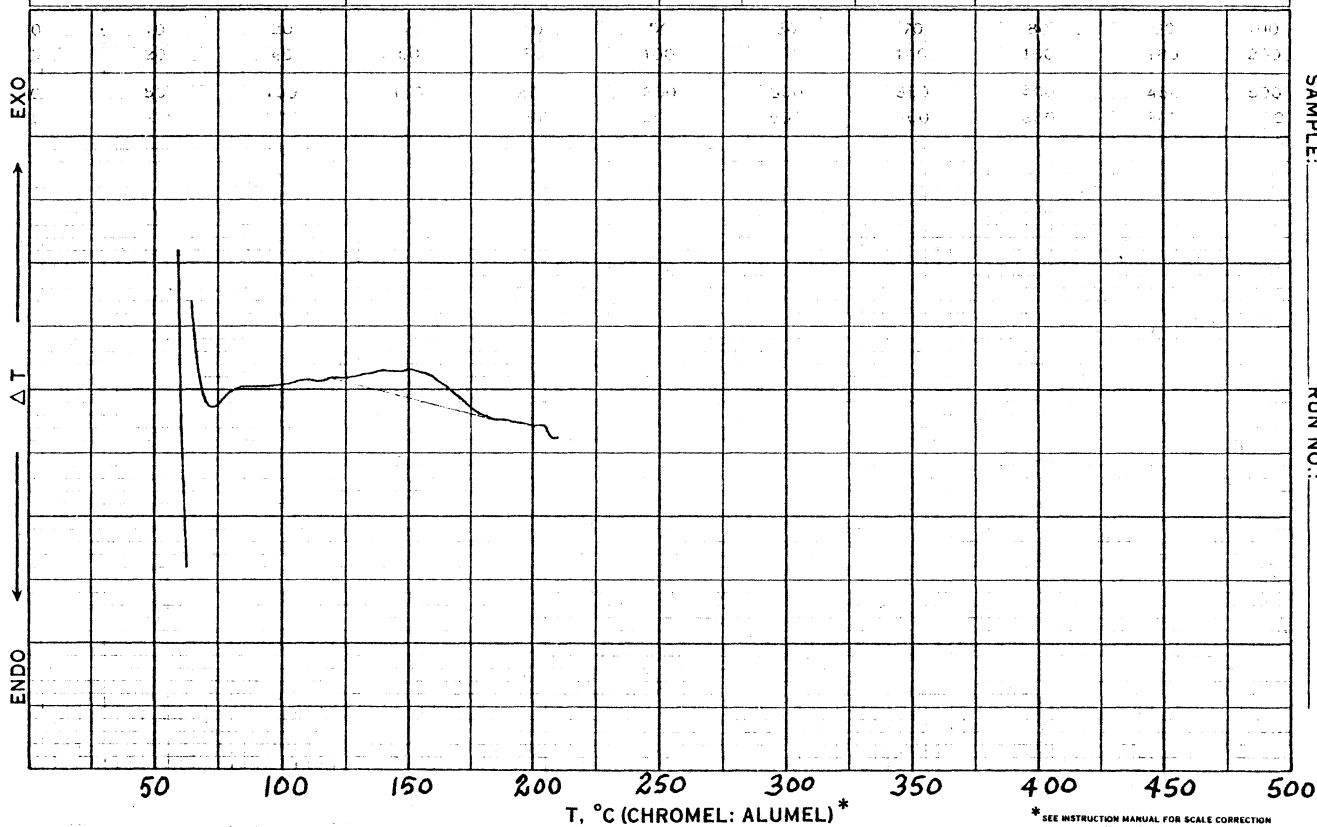


Figure 48. Rescanning of sample previously cured at 122°C.

SAMPLE: POLYESTER	SIZE 16.85 mg	ATM. air 760 MM	RUN NO. 3
	REF. empty	T	ΔT
ORIGIN:	PROG. MODE Heat	SCALE 50 $\frac{^{\circ}\text{C}}{\text{IN}}$	DATE 4/15/77
	RATE 10 $\frac{^{\circ}\text{C}}{\text{MIN}}$, START. $^{\circ}\text{C}$	SHIFT - IN.	OPERATOR Selami
			BASE LINE SLOPE

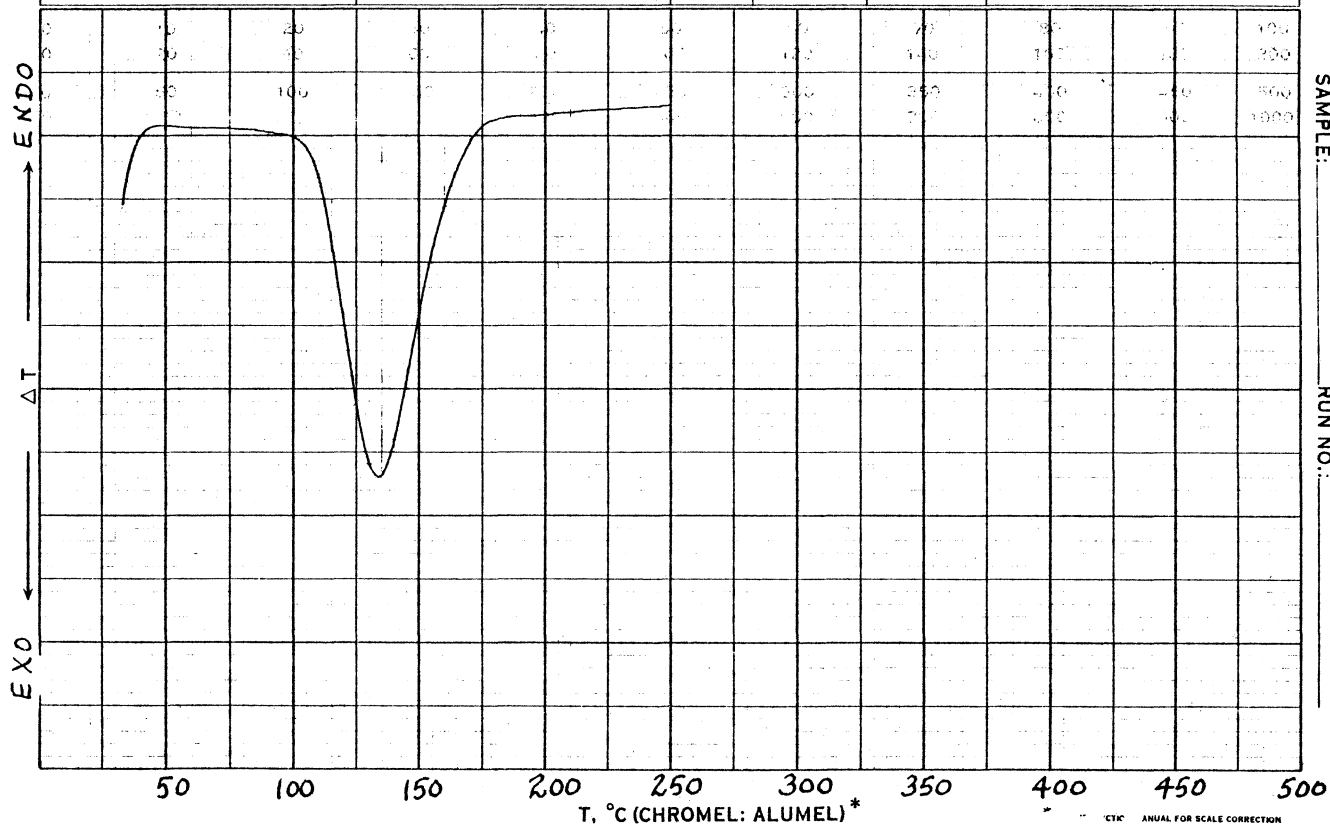


Figure 49. Scanning of a fresh sample.

SAMPLE: I Tin II Cured Polyester	SIZE I: 29.72 II: 5.82 mg	ATM. air 760 MM	RUN NO.
	REF. empty	T	DATE 8/18/77
ORIGIN:	PROG. MODE Heat/Hold	SCALE 20 $\frac{^{\circ}\text{C}}{\text{IN}}$	OPERATOR SELAMI
	RATE 20 $\frac{^{\circ}\text{C}}{\text{MIN}}$ START $^{\circ}\text{C}$	SHIFT - IN. - IN.	BASE LINE SLOPE

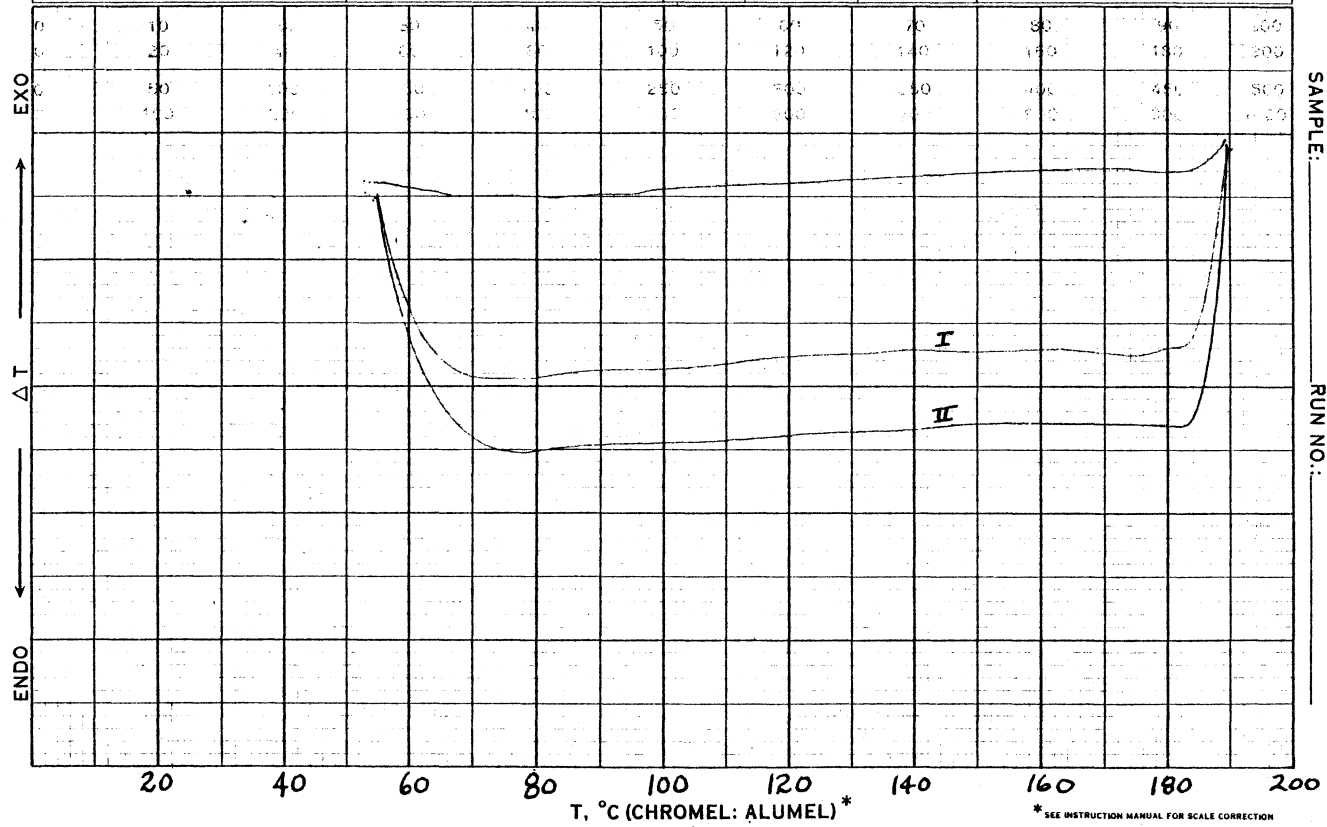


Figure 50. Determination of specific heat of polyester.

SAMPLE: <i>Cured Polyester</i>	SIZE _____	ATM. <i>air</i> <i>760</i> MM	RUN NO. _____
ORIGIN:	REF. <i>empty</i>	T _____	DATE <i>5/27/77</i>
	PROG. MODE <i>Heat</i>	SCALE <i>50</i> °C IN. <i>0.5</i> °C IN.	OPERATOR <i>Selami</i>
	RATE <i>10</i> °C MIN. START _____ °C	SHIFT <i>-</i> IN. <i>-</i> IN.	BASE LINE SLOPE _____

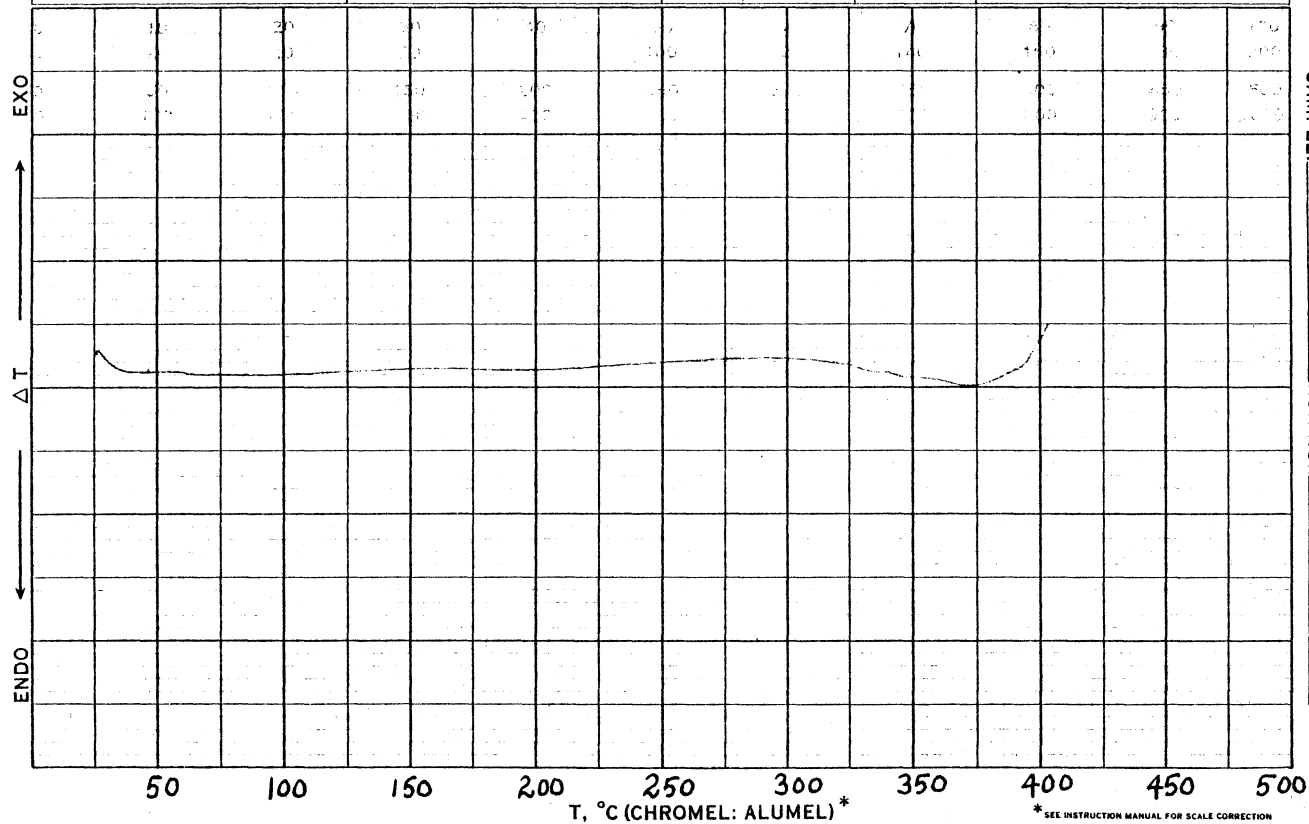


Figure 51. DSC thermogram of cured polyester.

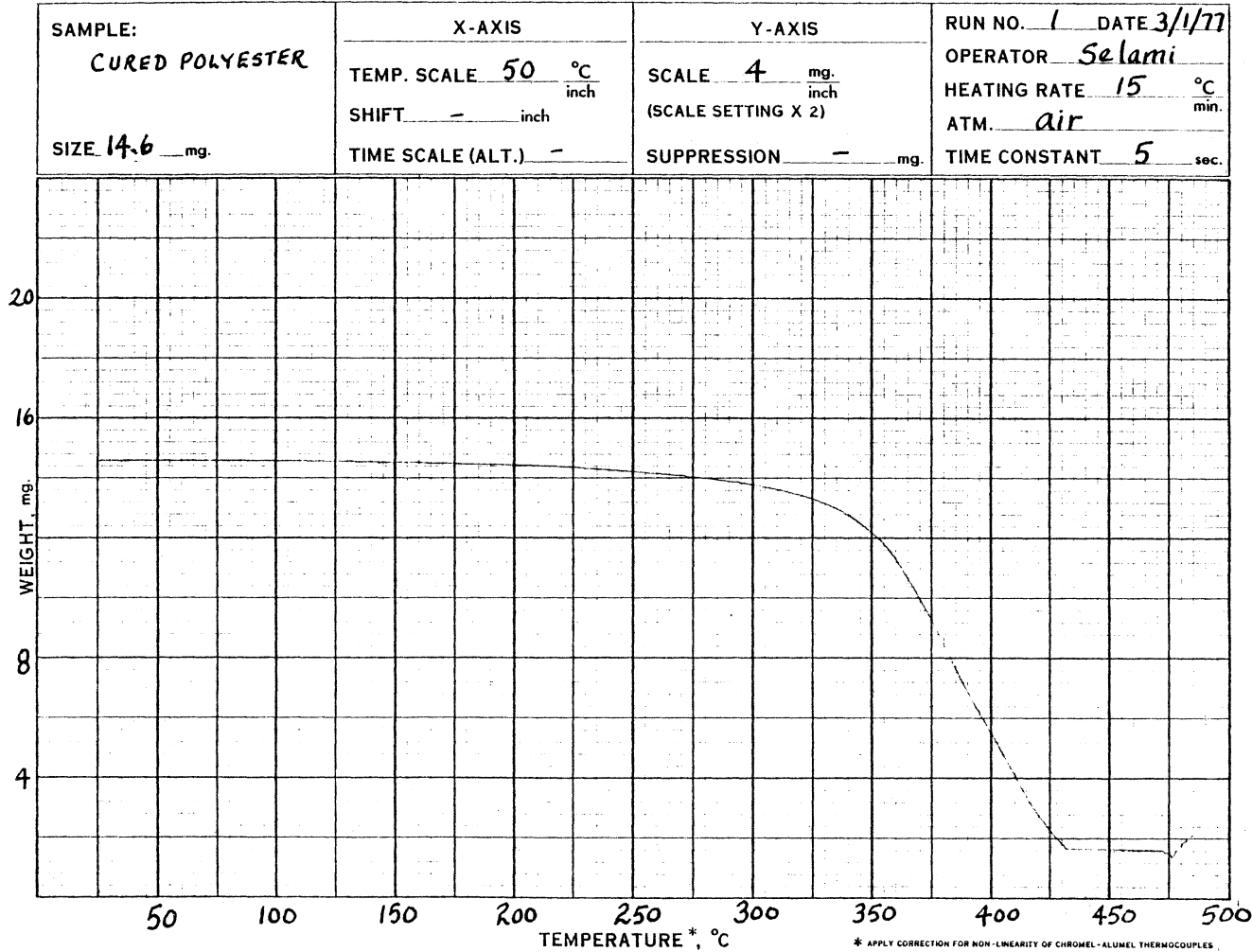


Figure 52. TGA thermogram of cured polyester.

APPENDIX C

This section includes the sample calculations.

Heat of ReactionIsothermal

$$Q_T = E_T \frac{\Delta T_s t_s}{M}$$

$$T = 82^\circ\text{C}$$

$$E_T = 123.6 \text{ mcal}/^\circ\text{C-min}$$

$$A = 1.43 \text{ in}^2$$

$$\Delta T_s = 0.5^\circ\text{C/in}$$

$$t_s = 10 \text{ min/in}$$

$$M = 20.98 \text{ mg}$$

$$Q_{82^\circ\text{C}} = \frac{(123.6)(1.43)(0.5)(10)}{20.98} = 42.12 \text{ cal/g}$$

Scanning

$$Q_S = \frac{E_T \Delta T_s T_s}{Ma}$$

$$E_{129^\circ\text{C}} = 125.0 \text{ mcal}/^\circ\text{C-min}$$

$$A = 1.32 \text{ in}^2$$

$$\Delta T_s = 2^\circ\text{C/in}$$

$$T_s = 50^\circ\text{C/in}$$

$$M = 22.53 \text{ mg}$$

$$a = 10^\circ\text{C/min}$$

$$Q_S = \frac{(125.0)(1.32)(2)(50)}{(22.53)(10)} = 73.24 \text{ cal/g}$$

Specific Heat

$$(C_p)_T = \frac{(\Delta T_x + \Delta T_{\text{blank}})E_T}{Ma}$$

$$T = 117^\circ\text{C}$$

$$(\Delta T_x + \Delta T_{\text{blank}}) = 0.1657^\circ\text{C}$$

$$E_{117^\circ\text{C}} = 124.6 \text{ mcal/}^\circ\text{C-min}$$

$$M = 4.87 \text{ mg}$$

$$a = 10^\circ\text{C/min}$$

$$(C_p)_{117^\circ\text{C}} = \frac{(0.1657)(124.6)}{(4.87)(10)} = 0.42 \text{ cal/g-}^\circ\text{C}$$

Definitions of the variables used in the above equations are given in Table 9.

Thermal Conductivity

Cured Polyester

$$k_T = \frac{4H}{R\pi D^2}$$

$$T = 93.5^\circ\text{C}$$

$$R = 0.106t - 6.114$$

$$t = 994 \text{ sec}$$

$$H = 0.1247 \text{ cm}$$

$$D = 1.7968 \text{ cm}$$

TABLE 9
LIST OF VARIABLES USED IN DSC CALCULATIONS

Name of Variable	Notation
Calibration coefficient, mcal/°C-min	E_T
Peak area, sq. in.	A
Y-axis sensivity, °C/in	ΔT_S
X-axis sensivity (scanning), °C/in	T_S
Sample mass, mg	M
Heating rate, °C/min	a
X-axis sensivity (isothermal), min/in	t_S
Absolute differential temperature for sample, °C	ΔT_X
Absolute differential temperature under no sample conditions, °C	ΔT_{blank}

$$k_{93.5^{\circ}\text{C}} = \frac{(4)(0.1247)}{(99.25)(\pi)(1.7968)^2} = 4.96 \times 10^{-4} \text{ cal/cm-sec-}^{\circ}\text{C}$$

Partially Polymerized Resin

$$\frac{1}{R_S} = \frac{1}{R_M} + \frac{1}{R_K}$$

R_S = Total resistance of sample

R_M = Resistance of embedded material (Resin)

R_K = Resistance of polyester ring

T = 70.6°C

R = $0.039t - 27.059$

Total Time = 6700 sec (for 1 ml of condensate)

R_S = $235.2 \text{ sec}^{\circ}\text{C/cal}$ (Total resistance of the sample system)

$K_T(\text{ring})$ = $4.8 \times 10^{-4} \text{ cal/sec-cm-}^{\circ}\text{C}$

$H(\text{ring})$ = 0.280 cm

$ID(\text{ring})$ = 1.28 cm

$OD(\text{ring})$ = 1.79 cm

$$R_K = \frac{(4)(0.280)}{(4.8 \times 10^{-4})(\pi) [(1.79)^2 - (1.28)^2]} = 476.4 \text{ sec}^{\circ}\text{C/cal}$$

$$\frac{1}{R_M} = \frac{1}{R_S} - \frac{1}{R_K}$$

$$\therefore R_M = 464.9 \text{ sec}^{\circ}\text{C/cal.}$$

Since the bottom surface of the ring was formed by a cured polyester sheet (in some cases a teflon sheet was used), the resistance of that surface was also considered.

$$R_{\text{bottom}} = \frac{(4)(0.0914)}{(4.8 \times 10^{-4})(\pi)(1.28)^2} = 148.0 \text{ sec}^\circ\text{C/cal}$$

$$R(\text{test sample}) = 465.0 - 148.0 = 317.0 \text{ sec}^\circ\text{C/cal}$$

$$\therefore k_T = \frac{(4)(0.1887)}{(317.0)(\pi)(1.2806)^2} = 4.60 \times 10^{-4} \text{ cal/sec-cm}^\circ\text{C}$$

**The vita has been removed from
the scanned document**

A MODEL FOR CASTING POLYESTERS

by

Selami Y. Pusatcioglu

(ABSTRACT)

Control of the rate of heat generation and the resulting temperature variations during the processing of thermosets is very necessary both to achieve the desired ultimate properties of the final product and to conserve energy and time. With this motivation, theoretical and experimental studies on the kinetics and thermal characterization of the curing reaction of thermoset polyesters were accomplished, and a mathematical curing model was proposed for the casting operation of these plastics.

Temperature distribution through the thickness of the polymer mass was obtained by monitoring thermocouples placed at known locations with the aid of PDP-11/40 computer.

Both isothermal and dynamic techniques of differential scanning calorimetry (Du Pont DSC) were used to obtain the heats of reaction and a kinetic expression for the polymerization reaction. The proposed kinetic model can be utilized to obtain the rates of heat generation at different curing temperatures. The overall activation energy of the curing reaction was calculated as 17.0 kcal/mole and the overall reaction rate constant as $2.60 \times 10^9 \exp(-17,000/RT) \text{ min}^{-1}$.

The thermal properties of the polyester were determined as a function of temperature, and also attempts were made to measure these properties as a function of extent of reaction. The specific heat of cured polyester samples was determined over the temperature range 60-180°C. A more or less linear increase in specific heat was observed with increasing temperature between 60° and 120°C where the values were 0.38 and 0.43 cal/g-°C, respectively. Thermal conductivity measurements were accomplished by using a Colora Thermoconductometer, but a new sample system had to be developed for use with this instrument for the measurements of uncured and partially cured samples. A linear increase in conductivity of cured polyester with increasing temperature from a value of 4.5×10^{-4} cal/cm-sec-°C at 40°C to 5.0×10^{-4} cal/cm-sec-°C at 94°C was observed.

Simulation of the curing process was based upon differential equations describing one-dimensional unsteady-state conductive heat transfer through the casting and the rate of the crosslinking reaction. The numerical scheme that was presented predicts the temperature and concentration profiles during the curing process. Agreement between the simulated and experimental temperature profiles was very good.

The proposed model can be readily utilized in characterizing the curing process, predicting curing performance, and establishing guidelines for better design of the casting and other reaction molding operations with most of the thermoset plastics.